Nishikawa *et al.*
Progress in Earth and Planetary Science (2023) 10:1
https://doi.org/10.1186/s40645-022-00528-w

Progress in Earth and Planetary Science

REVIEW

Open Access

A review on slow earthquakes in the Japan Trench

Tomoaki Nishikawa[1*], Satoshi Ide[2] and Takuya Nishimura[1]

Abstract

Slow earthquakes are episodic slow fault slips. They form a fundamental component of interplate deformation processes, along with fast, regular earthquakes. Recent seismological and geodetic observations have revealed detailed slow earthquake activity along the Japan Trench—the subduction zone where the March 11, 2011, moment magnitude (M_w) 9.0 Tohoku-Oki earthquake occurred. In this paper, we review observational, experimental, and simulation studies on slow earthquakes along the Japan Trench and their research history. By compiling the observations of slow earthquakes (e.g., tectonic tremors, very-low-frequency earthquakes, and slow slip events) and related fault slip phenomena (e.g., small repeating earthquakes, earthquake swarms, and foreshocks of large interplate earthquakes), we present an integrated slow earthquake distribution along the Japan Trench. Slow and megathrust earthquakes are spatially complementary in distribution, and slow earthquakes sometimes trigger fast earthquakes in their vicinities. An approximately 200-km-long along-strike gap of seismic slow earthquakes (i.e., tectonic tremors and very-low-frequency earthquakes) corresponds with the huge interplate locked zone of the central Japan Trench. The M_w 9.0 Tohoku-Oki earthquake ruptured this locked zone, but the rupture terminated without propagating deep into the slow-earthquake-genic regions in the northern and southern Japan Trench. Slow earthquakes are involved in both the rupture initiation and termination processes of megathrust earthquakes in the Japan Trench. We then compared the integrated slow earthquake distribution with the crustal structure of the Japan Trench (e.g., interplate sedimentary units, subducting seamounts, petit-spot volcanoes, horst and graben structures, residual gravity, seismic velocity structure, and plate boundary reflection intensity) and described the geological environment of the slow-earthquake-genic regions (e.g., water sources, pressure–temperature conditions, and metamorphism). The integrated slow earthquake distribution enabled us to comprehensively discuss the role of slow earthquakes in the occurrence process of the Tohoku-Oki earthquake. The correspondences of the slow earthquake distribution with the crustal structure and geological environment provide insights into the slow-earthquake-genesis in the Japan Trench and imply that highly overpressured fluids are key to understanding the complex slow earthquake distribution. Furthermore, we propose that detailed monitoring of slow earthquake activity can improve the forecasts of interplate seismicity along the Japan Trench.

Keywords: Japan Trench, Slow earthquake, Tectonic tremor, Very-low-frequency earthquake, Slow slip event, Megathrust earthquake, Tohoku-Oki earthquake, Subduction zone, Crustal structure, Geological environment

1 Introduction

The Japan Trench is a subduction zone located off the Pacific coast of eastern Japan (Fig. 1). In this trench, the Pacific Plate, whose age is approximately 130–140 Ma (Müller et al. 2008), is subducting beneath the Okhotsk Plate at a convergence rate of approximately 9 cm/yr (Bird 2003) (Fig. 1). Many large interplate earthquakes

*Correspondence: nishikawa.tomoaki.2z@kyoto-u.ac.jp

[1] Disaster Prevention Research Institute, Kyoto University, Gokasho, Uji, Kyoto, Japan
Full list of author information is available at the end of the article

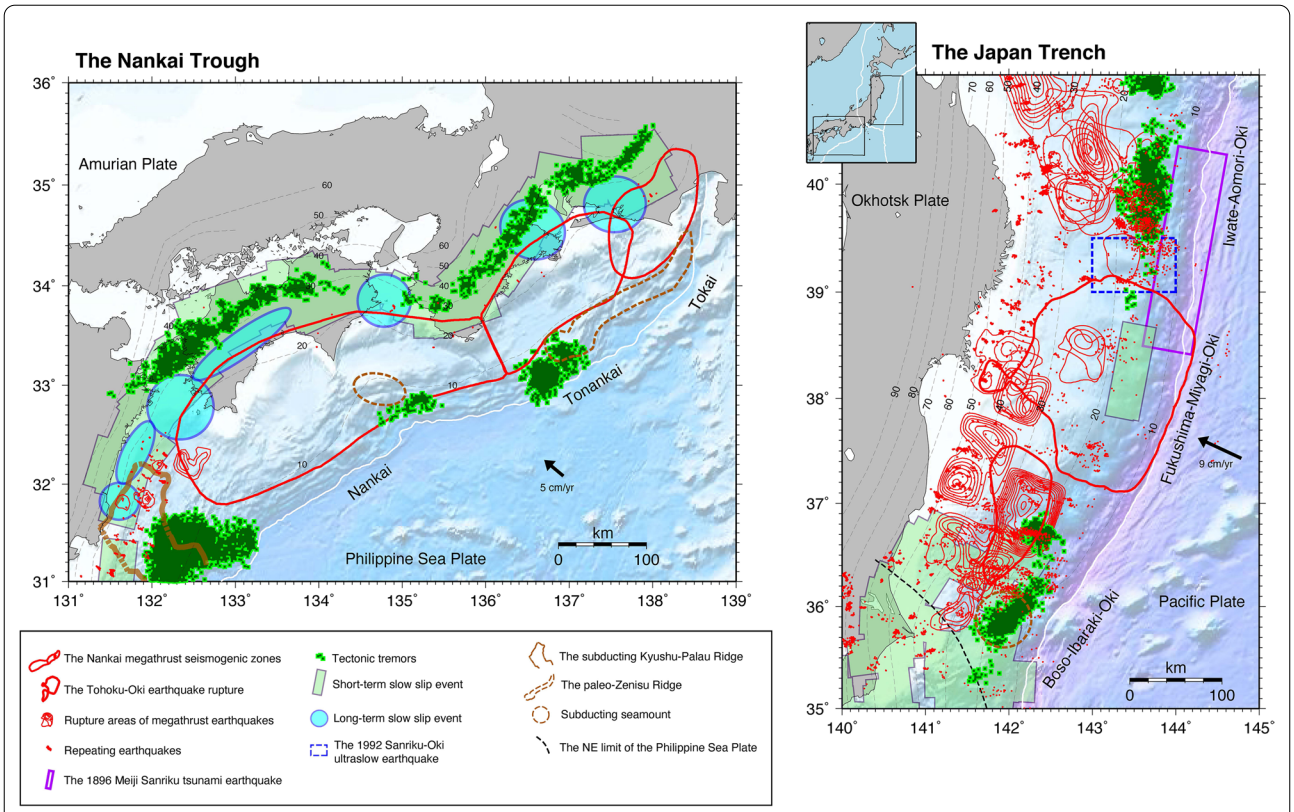

Fig. 1 Distribution of slow and fast earthquakes in the Japan Trench and Nankai Trough. Green and blue symbols semi-schematically show the distribution of slow earthquakes (tectonic tremors, short-term slow slip events, and long-term slow slip events). Red symbols indicate the distribution of fast, regular earthquakes. For an explanation of the other symbols, refer to the legend in the figure. The distribution of slow and fast earthquakes in the Nankai Trough is adapted from Obara and Kato (2016) and Obara (2020). Depth contours of the upper surface of the Pacific and Philippine Sea plates are based on Baba et al. (2002), Nakajima and Hasegawa (2006), Nakajima and Hasegawa (2007), Hirose et al. (2008), Nakajima et al. (2009), and Kita et al. (2010). The slip distributions of the March 11, 2011, Tohoku-Oki earthquake (10 m or larger) and other megathrust earthquakes are from Yagi et al. (1998), Yagi et al. (1999), Nagai et al. (2001), Tanioka and Seno (2001), Murotani et al. (2003), Yamanaka and Kikuchi (2004), Earthquake Research Center (2005), Mochizuki et al. (2008), Research Center for Seismology, Volcanology, and Disaster Mitigation (2008), Iinuma et al. (2012), Ohta et al. (2012), Kubo et al. (2013), and Kubo and Nishikawa (2020). The distribution of small repeating earthquakes is from Uchida and Matsuzawa (2013) and Igarashi (2020). The distribution of tectonic tremors is based on Idehara et al. (2014), Yamashita et al. (2015), Araki et al. (2017), Nishikawa et al. (2019), Yabe et al. (2019), and Yamashita et al. (2021). The distribution of short-term slow slip events is based on Ito et al. (2013), Nishimura et al. (2013), Nishimura (2014), and Nishimura (2021). The source area of the 1992 Sanriku-Oki ultraslow earthquake is from Kawasaki et al. (2001). The locations of subducting ridges and seamounts are based on Kodaira et al. (2000), Park et al. (2004), Mochizuki et al. (2008), and Yamamoto et al. (2013). The northeastern limit of the Philippine Sea Plate is from Uchida et al. (2009a). Seafloor topography is from Smith and Sandwell (1997). The plate motion is based on Bird (2003)

have been observed and actively studied in this subduction zone. In the central (37–39° N) and northern (39–41° N) Japan Trench, moment magnitude (M_w) 7–8 megathrust earthquakes have repeatedly occurred at a depth of 20–50 km (Nagai et al. 2001; Murotani et al. 2003; Yamanaka and Kikuchi 2004; Fig. 1). On March 11, 2011, the M_w 9.0 Tohoku-Oki earthquake ruptured the central and southern parts of the Japan Trench, and it was the largest earthquake ever recorded in Japan (the thick red contours in the Japan Trench in Fig. 1). In the central Japan Trench (37–39° N), the Tohoku-Oki rupture reached the trench axis, and the Japan Trench megathrust slipped more than 50 m (e.g., Lay 2018; Kodaira et al. 2020, 2021), as indicated by the seismic waveforms (Ide et al. 2011), crustal deformation (Iinuma et al. 2012), and bathymetric changes (Fujiwara et al. 2011). In addition to megathrust earthquakes, small interplate earthquakes have been vigorously studied in the Japan Trench. Small repeating earthquakes, in which the same area on the plate interface repeatedly undergoes similar ruptures (e.g., Nadeau and Johnson 1998), have been observed in the Japan Trench (Matsuzawa et al. 2002; Igarashi et al. 2003; Uchida and Matsuzawa 2013; Fig. 1). The regularity and diversity of their rupture patterns have been

investigated in detail (e.g., Okada et al. 2003; Uchida et al. 2007; Okuda and Ide 2018; Ide 2019a; Chang and Ide 2021).

While much has been revealed about fast, regular earthquakes in the Japan Trench, activity of slow earthquakes, another major category of earthquake phenomenon, had remained poorly resolved until recently. Slow earthquakes are a general term for a wide variety of fault slip phenomena of much longer duration than fast, regular earthquakes of comparable seismic moment (Ide et al. 2007a). Slow earthquakes have been observed in many circum-Pacific subduction zones and are actively studied in subduction zones such as the Nankai Trough, a subduction zone located off the Pacific coast of southwest Japan (Fig. 1). In contrast to the Japan Trench, the complex distribution and occurrence patterns of various slow earthquakes were revealed along the Nankai Trough (e.g., Obara 2002; Ito et al. 2007; Obara and Kato 2016). In addition, it is noteworthy that in the Nankai Trough, the young and warm Philippine Sea Plate (approximately 15–25 Ma) is subducting (Müller et al. 2008), in contrast to the Japan Trench, where the old and cold Pacific Plate is subducting. This has been thought to cause striking differences in subduction zone processes (e.g., slow and fast earthquakes, arc volcanism, and metamorphism) between these two subduction zones (e.g., Peacock and Wang 1999; Katayama et al. 2012).

Slow earthquake research in the Japan Trench has accelerated since the 2011 Tohoku-Oki earthquake. A M_w 7.0 short-term slow slip event (SSE) accompanied by an earthquake swarm was observed approximately a month before the Tohoku-Oki earthquake on the shallow plate interface of the central Japan Trench (Kato et al. 2012; Ito et al. 2013; a green rectangle within the Tohoku-Oki earthquake rupture in Fig. 1). Furthermore, detection based on a visual inspection of broadband seismograms (Matsuzawa et al. 2015) and an analysis of repeating earthquakes (Uchida et al. 2016) also provided important insights into activity of slow earthquakes (very-low-frequency earthquakes and SSEs, respectively) in the Japan Trench, although systematic and comprehensive detection of slow earthquakes along the entire Japan Trench remained unachieved.

In 2019, pop-up-type ocean-bottom seismometers installed in the southern part of the Japan Trench (Ohta et al. 2019) and the Seafloor Observation Network for Earthquakes and Tsunamis along the Japan Trench (S-net) (NIED 2019a) finally led to revealing the detailed distribution of tectonic tremors, a type of slow earthquake, along the entire Japan Trench (Ohta et al. 2019; Tanaka et al. 2019; Nishikawa et al. 2019; Fig. 1). The tremor detection was followed by the systematic and comprehensive detection of other types of slow earthquakes (very-low-frequency earthquakes and short-term SSEs) using onshore seismic and geodetic observation networks (Baba et al. 2020; Nishimura 2021). These accumulating research findings are beginning to provide a full picture of the slow earthquake distribution along the Japan Trench (Fig. 1).

Based on the above research advances, we review the studies related to slow earthquakes along the Japan Trench and describe their research history from the first report of a large transient aseismic slip in the Japan Trench (Kawasaki et al. 1995) to the present. By compiling the observations of slow earthquakes (e.g., tectonic tremors, very-low-frequency earthquakes, and slow slip events) and related fault slip phenomena (e.g., small repeating earthquakes, earthquake swarms, and foreshocks of large interplate earthquakes), we present an integrated slow earthquake distribution along the Japan Trench. Based on the slow earthquake distribution, we discuss the occurrence processes of megathrust earthquakes along the Japan Trench, focusing on the role of slow earthquakes. Furthermore, we explore the conditions causing slow earthquakes by comparing the slow earthquake distribution with the crustal structure and geological environment of the Japan Trench.

In addition to the Japan Trench (34–41° N), we also mention slow earthquake activity in the southern end of the Kuril Trench (41–43° N). However, we limit our main discussion to the Japan Trench. Hereafter, we refer to the regions from 39 to 41° N (Iwate-Aomori-Oki), 37–39° N (Fukushima-Miyagi-Oki), 34–37° N (Boso-Ibaraki-Oki) as the northern, central, and southern Japan Trench, respectively. Because this review paper focuses on slow earthquakes along the Japan Trench, readers who are interested in the 2011 Tohoku-Oki earthquake and associated phenomena rather than slow earthquakes are referred to other review papers (Lay 2018; Kodaira et al. 2020, 2021; Uchida and Bürgmann 2021).

An overview of the subsequent sections is described below. Section 2 briefly summarizes basic knowledge about slow earthquakes for readers unfamiliar with the concept to facilitate a better understanding of the subsequent sections (Sects. 3, 4, 5, and 6); readers familiar with slow earthquakes can skip this section. Section 3 reviews observational, experimental, and simulation studies on slow earthquakes along the Japan Trench. Furthermore, we synthesized the results of observational studies of slow earthquakes and summarized what has been revealed so far about the spatiotemporal distribution of slow earthquakes before and after the 2011 Tohoku-Oki earthquake. Section 4 compares the spatial distribution of slow earthquakes along the Japan Trench with that of other fault slip phenomena. Specifically, we compared the slow earthquake distribution with the

distributions of megathrust earthquake ruptures, including the 2011 Tohoku-Oki rupture, interplate coupling, small interplate earthquakes, tsunami earthquakes, and seismicity parameters (the Gutenberg–Richter relationship's b value, tidal response of seismicity, and p value of the Omori–Utsu aftershock law). Section 5 compares the slow earthquake distribution with the crustal structure of the Japan Trench (e.g., interplate sedimentary units, subducting seamounts, petit-spot volcanoes, horst and graben structures, residual gravity, seismic velocity structure, and plate boundary reflection intensity) and describes the geological environments of the slow-earthquake-genic regions (e.g., fluid sources, pressure–temperature conditions, and metamorphism). Section 6 provides the comprehensive discussion. Specifically, we discuss the occurrence process of the Tohoku-Oki earthquake, focusing on the roles that slow earthquakes played. We also discuss the structural and geological origins of the slow earthquake distribution in the Japan Trench. Finally, we discuss how slow earthquake observations could be utilized to improve forecasts of interplate seismicity along the Japan Trench. Section 7 presents the conclusions.

2 Brief introduction to slow earthquakes

This section provides a brief introduction to slow earthquakes at subduction zone plate boundaries, focusing on topics essential to the subsequent sections (Sects. 3, 4, 5, and 6). Several remarkable review papers on slow earthquakes have been published (e.g., Peng and Gomberg 2010; Beroza and Ide 2011; Ide 2014; Saffer and Wallace 2015; Obara and Kato 2016; Bürgmann 2018; Obara 2020; Behr and Bürgmann 2021; Kirkpatrick et al. 2021). We refer readers to these papers for more information. Obara (2020) extensively reviewed the detailed occurrence patterns of various slow earthquakes, which are not included in this section. Obara and Kato (2016) provided a detailed discussion on the relationship between slow earthquakes and megathrust earthquakes. Geological environment and possible physical mechanisms of slow earthquakes have been described in detail by Bürgmann (2018), Behr and Bürgmann (2021), and Kirkpatrick et al. (2021). For details on slow earthquakes on shallow subduction plate interfaces, readers can refer to Saffer and Wallace (2015).

2.1 Types of slow earthquakes

There are five major types of slow earthquakes: low-frequency earthquakes (LFEs), tectonic tremors, very-low-frequency earthquakes (VLFEs), short-term SSEs, and long-term SSEs (Fig. 2).

Three types of slow earthquakes can be observed by seismometers (Fig. 2a–c), hereafter referred to as "seismic slow earthquakes." The first type of seismic slow earthquake is the LFE (Fig. 2a). LFEs were first discovered by Nishide et al. (2000) at a deeper part (approximately 30 km depth) of the Nankai Trough (see also Katsumata and Kamaya 2003). LFEs are slow earthquakes with the smallest moment magnitudes (approximately M_w 1.5) and characterized by the shortest characteristic time scale (source duration of ~0.3 s) (Ide et al. 2007a, 2007b). They are also characterized by low dominant frequencies (1–10 Hz) compared to fast microearthquakes of comparable seismic moment (e.g., Shelly et al. 2007; Obara 2020).

The second type of seismic slow earthquake is the tectonic tremor (Fig. 2b), which is a seismic event that generates a weak seismic signal lasting more than several tens of seconds without clear P- and S-wave arrivals. The dominant frequency is 1–10 Hz (e.g., Shelly et al. 2007; Obara 2020). Similar to the LFEs, tectonic tremors were first discovered at the deeper part of the Nankai Trough in 2002 (Obara 2002). These tremors were aligned along the 30–40 km deep contours of the plate interface and located downdip of the megathrust seismogenic zones (10–20 km depth) of the Nankai Trough (Obara 2002; Obara and Kato 2016; Fig. 1). Previous reports revealed LFEs to be fault slip phenomena with a low-angle reverse fault mechanism on the plate interface (Shelly et al. 2006; Ide et al. 2007b). Furthermore, Shelly et al. (2007) demonstrated that tectonic tremor is a swarm of LFEs, by detecting many LFE signals embedded in tremor waveforms using a matched filter technique.

The third type of seismic slow earthquake is the VLFE (Fig. 2c), which is a fault slip phenomenon (M_w 3–4) comprised predominantly of seismic waves with periods of tens to hundreds of seconds, with shorter-period waves lacking (e.g., Ito et al. 2007; Obara 2020). VLFEs were first discovered near the trench axis of the Nankai Trough (Ishihara 2003; Obara and Ito 2005). Subsequently, they were found to occur simultaneously with tectonic tremors on the deeper plate interface of the Nankai Trough (approximately 30–40 km depth) (Ito et al. 2007).

There are two types of slow earthquakes observed by geodetic instruments (Fig. 2d and e), hereafter referred to as "geodetic slow earthquakes." The first type of geodetic slow earthquake is the short-term SSE (Fig. 2d), which is an interplate fault slip event that usually lasts from a few days to a month. Short-term SSEs on subduction plate interfaces were discovered in the late 1990s and early 2000s (Sagiya 1997; Hirose et al. 2000; Dragert et al. 2001). Global navigation satellite system (GNSS) observations (Dragert et al. 2001) in the Cascadia subduction zone, a subduction zone located off the west coast of North America, captured a slow transient slip of ~2 cm that occurred on the deeper plate interface (30–40 km

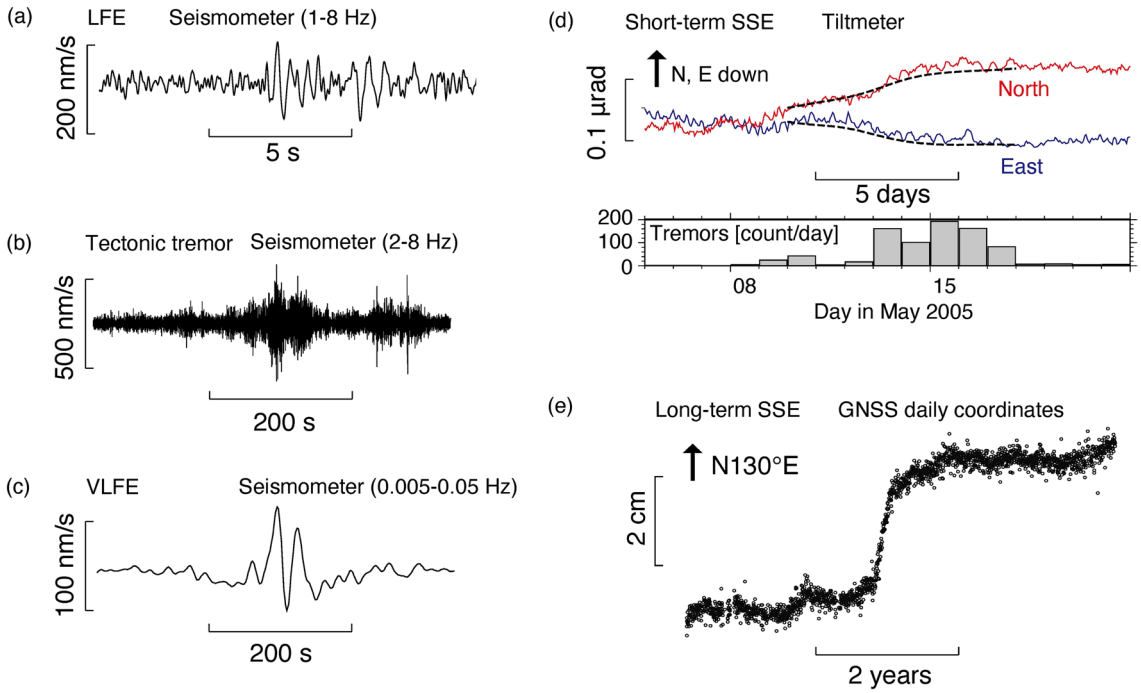

Fig. 2 Observed signals of the slow earthquake family. The slow earthquake family includes **a** low-frequency earthquakes (LFEs) (Shelly et al. 2007), **b** tectonic tremors (Ide et al. 2008), **c** very-low-frequency earthquakes (VLFEs) (Ide et al. 2008), **d** short-term slow slip events (SSEs) (Hirose and Obara 2010), and **e** long-term SSEs (Takagi et al. 2016). In **d** the daily count of concurrent tectonic tremors is presented (Hirose and Obara 2010). The dashed lines in **d** indicate calculated tilt changes due to the short-term SSE (Hirose and Obara 2010). All the above signals of the slow earthquake family were observed on the deeper plate interface (25–40 km depth) of the Nankai Trough. GNSS, global navigation satellite system

depth) in the summer of 1999. Sagiya (1997) and Hirose et al. (2000) also reported similar aseismic transients off the Boso Peninsula and beneath Tokyo Bay, respectively, in the Sagami Trough, eastern Japan. The duration of the short-term SSE in the Cascadia subduction zone was approximately a month (Dragert et al. 2001), and its moment magnitude was M_w 6.7, which is far larger than the moment magnitude of the aforementioned seismic slow earthquakes (Fig. 2a–c). This SSE occurred down-dip of the megathrust seismogenic zone of the Cascadia subduction zone, similar to the deep tectonic tremors in the Nankai Trough (e.g., Obara 2002; Shelly et al. 2006; Obara and Kato 2016). In 2004, short-term SSEs were also discovered on the deeper plate interface (approximately 30–40 km depth) of the Nankai Trough by tiltmeter observations (Obara et al. 2004; Figs. 1 and 2d).

The second type of geodetic slow earthquake is the long-term SSE (Fig. 2e), which is an interplate fault slip event that lasts from several months to years. It was first discovered in 1999 on the deeper plate interface of the Nankai Trough by GNSS observations (Hirose et al. 1999). This event lasted approximately 300 days from March to December 1997 and caused a fault slip of ~ 18 cm, with an estimated magnitude of M_w 6.6. Long-term SSEs on the deeper plate interface of the Nankai Trough are located slightly shallower (approximately 25 km depth) than short-term SSEs (Obara et al. 2004; Takagi et al. 2016; Obara and Kato 2016; Fig. 1). Long-term SSEs are characterized by the largest moment magnitudes (approximately M_w 6.5–7.5) and the longest characteristic time scales (several months to years) in the slow earthquake family.

Note, however, that the distinction between short-term and long-term SSEs is ambiguous. In fact, in the Ryukyu Trench, the southwestern extension of the Nankai Trough, SSEs of medium duration (i.e., a few months) have been observed (Kano et al. 2018b). In the Nankai Trough, different characteristic time scales are often assumed a priori when systematically detecting short-term and long-term SSEs (several days and approximately one year, respectively) (Takagi et al. 2019; Okada et al. 2022). Therefore, the detailed activity of SSEs with time scales intermediate between these two, such as a few months, is less clear. Furthermore, in the Mexico subduction zone, Frank et al. (2018) suggested that a long-term SSE can be decomposed into a cluster of short-term SSEs.

However, it is unclear whether such a decomposition is possible for the long-term SSEs in the Nankai Trough.

Although these five major types of slow earthquakes were first discovered on the deeper plate interfaces of the Nankai Trough and Cascadia subduction zone, they have now been observed in many circum-Pacific subduction zones (e.g., Beroza and Ide 2011; Obara and Kato 2016; Obara 2020). Slow earthquakes may universally occur in subduction zones, regardless of the tectonic characteristics of subduction zones, such as subducting plate age. Furthermore, slow earthquakes can occur under various temperature–pressure conditions (e.g., Peacock 2009; Saffer and Wallace 2015; Behr and Bürgmann 2021; Kirkpatrick et al. 2021). Slow earthquakes are predominantly observed on the plate interface downdip and/or updip of megathrust seismogenic zones (Fig. 1), although the pressure–temperature conditions of the deeper and shallower parts of the plate interface differ considerably. In the Nankai Trough (Fig. 1), for example, slow earthquakes have been observed on both the shallow plate interface less than 10 km deep (100 °C or less to approximately 200 °C) and the deeper plate interface at a depth of 25–40 km (approximately 350–450 °C) (Peacock and Wang 1999; Peacock 2009). They avoid the megathrust seismogenic zones at a depth of 10–25 km (approximately 200–350 °C) (Fig. 1).

2.2 Relationship between slow earthquakes

2.2.1 Simultaneous occurrence of different types of slow and fast earthquakes

Different types of slow earthquakes often occur simultaneously in close proximity. The coincidence of tectonic tremor bursts and short-term SSEs, termed episodic tremor and slip (ETS), was first discovered on the deeper plate interface of the Cascadia subduction zone (Rogers and Dragert 2003). In 2004, ETSs were also discovered in the Nankai Trough (Obara et al. 2004; Fig. 2d). Subsequently, VLFEs were also found to occur during ETS (Ito et al. 2007; Ghosh et al. 2015). Furthermore, long-term SSEs on the deeper plate interface (approximately 25 km depth) of the Nankai Trough are known to activate ETSs on their downdip side (Hirose and Obara 2005). Because of the remarkable correspondence between the short-term SSEs and tectonic tremors at the deeper parts of the Cascadia subduction zone and Nankai Trough, several attempts have been made to estimate the source properties (e.g., source duration, rupture area, and moment) of short-term SSEs too small to be geodetically detected (M_w 5.5 or less) from characteristics of tremor bursts (e.g., Aguiar et al. 2009; Obara 2010; Wech et al. 2010; Gomberg et al. 2016).

The occurrence of ETSs is not limited to the deeper subduction plate interface. On the shallow plate interface (shallower than 10 km depth) of the Nankai Trough, ocean-bottom seismometers and subseafloor borehole pore-fluid pressure measurements observed recurring ETSs (Araki et al. 2017), although shallow ETSs have not been observed in the Cascadia subduction zone (McGuire et al. 2018).

In addition to the Cascadia subduction zone and Nankai Trough, clear ETSs have been observed in the subduction zones of Costa Rica (Walter et al. 2013), Mexico (Rousset et al. 2017), and Alaska (Rousset et al. 2019). However, note that short-term SSEs and tremor bursts do not always occur at exactly the same time. In the Hikurangi Trench, the subduction zone located off the east coast of the North Island of New Zealand, a time lag of 10 days or longer between the occurrence of a short-term SSE and a tremor burst has been observed (Todd et al. 2018; Shaddox and Schwartz 2019; Nishikawa et al. 2021). Furthermore, some short-term SSEs in the Hikurangi Trench lacked detectable tectonic tremors (Todd and Schwartz 2016). However, we cannot rule out the possibility that tectonic tremors of magnitudes below the observational limit occurred. This also holds true for subduction zones where clear ETS has not been reported.

Slow and fast earthquakes can also occur simultaneously. The coincidence of short-term SSEs and swarms of interplate earthquakes ($M_w \leq 5$) has been repeatedly observed off the Boso Peninsula in the Sagami Trough, eastern Japan (Ozawa et al. 2003; Sagiya 2004). These earthquake swarms included repeating earthquakes (Kato et al. 2014; Gardonio et al. 2018). The SSE-induced stress loading is considered to be the triggering mechanism of these earthquake swarms (Fukuda 2018). Similar coincidences of SSEs and fast earthquakes have been observed in the Japan Trench (Ito et al. 2013) and the subduction zones of Mexico (Liu et al. 2007), Hikurangi (Delahaye et al. 2009), Ecuador (Vallée et al. 2013), Peru (Villegas-Lanza et al. 2016), and northern Chile (Socquet et al. 2017). Fast earthquakes that occur concurrently with SSEs are usually interplate earthquakes; however, in the Ecuador and Hikurangi trenches, swarms of intraslab or upper-plate earthquakes accompany short-term SSEs on the plate interface (Collot et al. 2017; Shaddox and Schwartz 2019; Nishikawa et al. 2021). In the Japan, northern Chile, and Mexico trenches, short-term or long-term SSEs were followed by megathrust earthquakes: the 2011 M_w 9.0 Tohoku-Oki (Kato et al. 2012; Ito et al. 2013), 2014 M_w 8.1 Iquique (Ruiz et al. 2014; Socquet et al. 2017), and 2014 M_w 7.3 Papanoa (Radiguet et al. 2016) earthquakes, respectively. The preseismic SSEs of the Tohoku-Oki and Iquique earthquakes were accompanied by swarms of foreshocks. These preseismic SSEs are considered to have triggered the megathrust earthquakes or been involved in their nucleation processes.

SSEs are not the only slow earthquakes that can occur simultaneously with fast earthquakes. In the shallow part of the southern Japan Trench, coincident tectonic tremors and swarms of interplate microearthquakes have been observed (Obana et al. 2021). In the central Hikurangi Trench, tectonic tremors, short-term SSEs, and swarms of intraslab earthquakes occur simultaneously (Romanet and Ide 2019; Nishikawa et al. 2021). Furthermore, a recent study (Yamamoto et al. 2022) reported the simultaneous occurrence of an SSE, VLFEs, and a swarm of interplate microearthquakes on the shallow plate interface of the Nankai Trough off the southeast coast of the Kii Peninsula (the Tonankai region in Fig. 1).

2.2.2 Unified understanding of slow earthquakes

Although slow earthquakes are diverse, efforts have been made to understand them in a unified manner. As described in Sect. 2.1, tectonic tremors are swarms of LFEs (Shelly et al. 2007). Furthermore, Ide et al. (2007a) found that the seismic moment M_0 of slow earthquakes (LFEs, VLFEs, short-term SSEs, and long-term SSEs) is approximately proportional to their source duration T (i.e., $M_0 \propto T$) (blue symbols in Fig. 3a). In contrast, the seismic moment of fast earthquakes is proportional to the cubed source duration (i.e., $M_0 \propto T^3$) (the thick red line in Fig. 3a), and there is a significant gap between the scaling relations of slow and fast earthquakes. Aseismic transients that fall into this gap have been reported in the northern Japan Trench (Kawasaki et al. 1995) and Izu–Bonin subduction zone (Fukao et al. 2021), but are very rare (magenta circles in Fig. 3a).

Based on the moment–duration scaling of slow earthquakes ($M_0 \propto T$), Ide et al. (2007a) interpreted diverse slow earthquakes as the same physical phenomena with different seismic moments. They considered diffusion as a candidate for the process behind slow earthquakes,

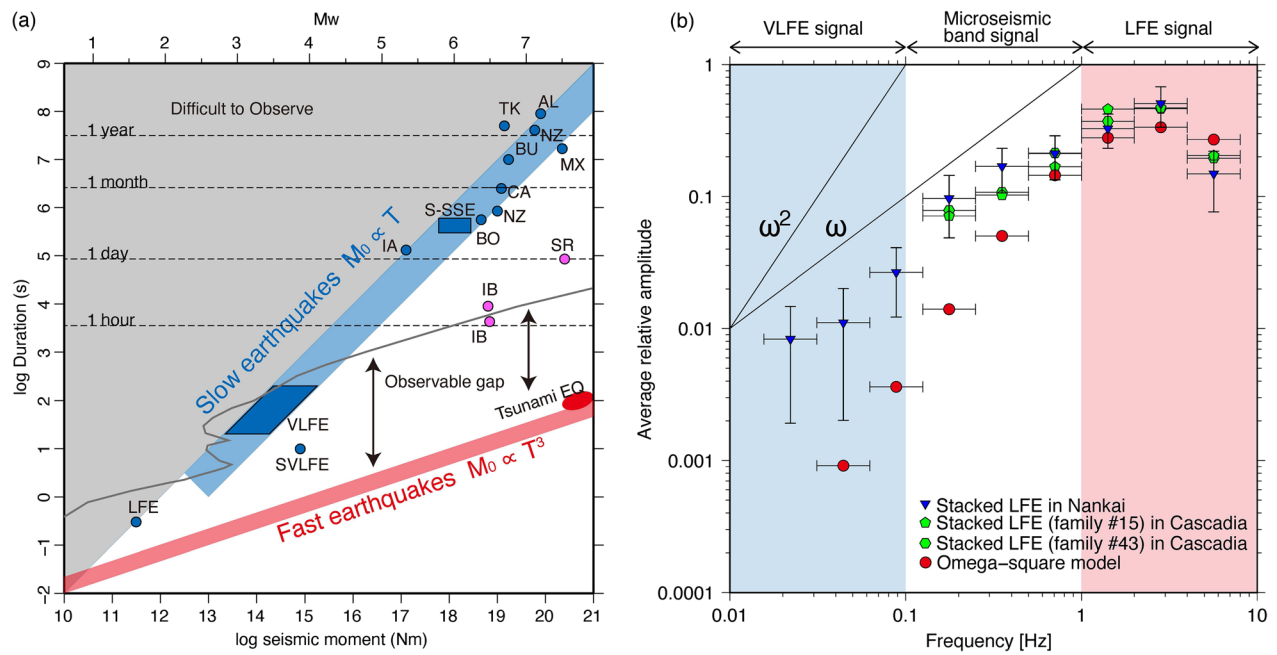

Fig. 3 Slow earthquakes as broadband fault slip phenomena. **a** Moment–duration scaling relations of slow and fast earthquakes. Blue and magenta symbols represent slow earthquakes. LFE, VLFE, SVLFE, and S-SSE indicate LFEs (Ide et al. 2007b), deep VLFEs (Ito et al. 2007; Ide et al. 2008), shallow VLFEs (Ito and Obara 2006), and short-term SSEs (Hirose and Obara 2005) in the Nankai Trough, respectively. Other symbols are as follows: IA, a small short-term SSE near the Kii Peninsula, southwest Japan (Itaba and Ando 2011); BO, a short-term SSE near the Boso Peninsula, eastern Japan (Sagiya 2004); NZ, short- and long-term SSEs in Hikurangi, New Zealand (Wallace et al. 2012); CA, short-term SSEs in Cascadia (Dragert et al. 2004); BU, a long-term SSE in the Bungo Channel, southwest Japan (Hirose and Obara 2005); MX, a long-term SSE in Guerrero, Mexico (Kostoglodov et al. 2003; Yoshioka et al. 2004); TK, a long-term SSE in the Tokai region, central Japan (Miyazaki et al. 2006); AL, a long-term SSE in Alaska (Ohta et al. 2006); IB, aseismic transients in the Izu–Bonin subduction zone (Fukao et al. 2021); and SR, the 1992 Sanriku-Oki ultraslow earthquake in the northern Japan Trench (Kawasaki et al. 1995). The thick red line represents the scaling relationship of fast earthquakes. The red ellipse indicates tsunami earthquakes (Kanamori 1972; Ide et al. 1992). The gray curve represents the approximate observational limit of seismological instruments suggested by the US Geological Survey low-noise model (Peterson 1993). This panel is adapted from Ide (2014). **b** Average maximum amplitude of stacked LFE waveforms for each frequency band. The maximum amplitudes of seismic signals in each frequency band are averaged for each component of each station. Blue inverted triangles represent stacked LFE waveforms in the Nankai Trough (Masuda et al. 2020). Green symbols indicate stacked LFE waveforms in the Cascadia subduction zone (Bostock et al. 2015; Ide 2019b). For comparison, the average maximum amplitude of synthetic waveforms that obey the omega-square model (Aki 1967) with a 2 Hz corner frequency is shown. This panel is adapted from Masuda et al. (2020)

although the specific physical mechanism (e.g., slip phenomena associated with fluid diffusion, stress diffusion, or others) remained unclear. The diffusional aspect of slow earthquakes is evidenced by the parabolic migration patterns of deep tectonic tremors and LFEs in the Nankai Trough on a scale of several tens of kilometers (e.g., Ide 2010; Kato and Nakagawa 2020), although deep tectonic tremors in the Nankai Trough and Cascadia subduction zone show almost constant-velocity (approximately 10 km/day) migration patterns on a larger spatial scale (100 km or larger) (e.g., Ito et al. 2007; Houston et al. 2011; Nakata et al. 2011). Here, parabolic migration means migration with the distance traveled L proportional to the square root of elapsed time t (i.e., $L \propto \sqrt{t}$), which is typical of diffusional phenomena (Ide 2010).

In support of the unified understanding proposed by Ide et al. (2007a), Kaneko et al. (2018) found a continuous seismic signal from the LFE frequency band (1–10 Hz) through the microseismic frequency band (0.1–1 Hz) to the VLFE frequency band (0.01–0.1 Hz) in a seismogram recorded during a tremor burst episode at the shallow part of the Nankai Trough. Furthermore, Masuda et al. (2020) stacked many seismograms recorded in the Nankai Trough relative to the timing of high-frequency LFE signals and found that stacked LFE waveforms have a continuous seismic signal from the LFE frequency band (1–10 Hz) to the VLFE frequency band (0.01–0.1 Hz) (Fig. 2b). These results indicate that tectonic tremors (i.e., swarms of LFEs) and very-low-frequency earthquakes are the high- and low-frequency components, respectively, of a broadband seismic wave emanating from the identical slow fault slip phenomenon. Kaneko et al. (2018) and Masuda et al. (2020) called this slow fault slip phenomenon a broadband slow earthquake.

However, with respect to geodetic slow earthquakes, the unified understanding proposed by Ide et al. (2007a) still remains under debate (e.g., Gomberg et al. 2016; Frank and Brodsky 2019; Michel et al. 2019). For example, Michel et al. (2019) reported that short-term SSEs in the Cascadia subduction zone are likely to have seismic moments proportional to their cubed durations (i.e., $M_0 \propto T^3$). They argue that the moment–duration scaling of SSEs is similar to the fast earthquake scaling (the thick red line in Fig. 3a). Their argument implies that seismic and geodetic slow earthquakes, or even short-term and long-term SSEs, might have different physical origins, and therefore requires different moment–duration scaling relations to describe different types of slow earthquakes. Of note, a single cubic scaling relation cannot explain observations of deep short-term and long-term SSEs in the Nankai Trough, while they are approximately consistent with a single linear scaling relation (Ide et al. 2007a; Okada et al. 2022).

2.3 Fast earthquakes closely related to slow earthquakes

In this section, we briefly introduce repeating earthquakes and earthquake swarms, which are fast earthquakes closely related to slow earthquakes. Repeating earthquakes are a phenomenon in which the same area on the plate interface repeatedly undergoes similar ruptures (e.g., Okada et al. 2003; Uchida et al. 2007; Kim et al. 2016), and are characterized by extremely high waveform similarity (e.g., Nadeau and Johnson 1998; Nadeau and McEvilly 1999; Igarashi et al. 2003) (Fig. 4a). The co-location, high waveform cross-correlations, or high waveform coherence of earthquakes are usually used to identify repeating earthquakes (Uchida 2019; Uchida and Bürgmann 2019, and references therein).

Repeating earthquakes are considered to occur due to stress loading by aseismic slip surrounding their source regions (Nadeau and Johnson 1998; Nadeau and McEvilly 1999; Matsuzawa et al. 2002; Igarashi et al. 2003; Chen and Lapusta 2009). The change in the aseismic slip rate of the surrounding region consequently fluctuates the recurrence interval of repeating earthquakes. Therefore, by examining the activity of repeating earthquakes, we can infer the spatiotemporal evolution of aseismic slip on the plate interface, such as steady slip (e.g., Nadeau and McEvilly 1999; Igarashi et al. 2003), afterslip (i.e., transient aseismic slip following a large earthquake) (e.g., Uchida and Matsuzawa 2013; Uchida et al. 2015), and SSEs (e.g., Nadeau and McEvilly 2004; Uchida et al. 2016). Once we know the occurrence time and seismic moment of a given repeating earthquake sequence and assume that a scaling relation between seismic moment and slip amount is applicable, we can infer the temporal evolution of aseismic slip surrounding the source region of the repeating earthquakes. Several scaling relationships between seismic moment and slip amount of a repeating earthquake have been proposed (e.g., Nadeau and Johnson 1998; Beeler et al. 2001; Khoshmanesh et al. 2015), as summarized and compared in Uchida (2019).

Repeating earthquakes can be used to infer the occurrence of SSEs on the subduction interface. Kato et al. (2012) detected small repeating earthquakes in the central Japan Trench prior to the March 11, 2011, Tohoku-Oki earthquake and calculated the amount of preseismic interplate fault slip. They inferred that an SSE occurred during the month prior to the Tohoku-Oki earthquake at the shallow part (approximately 10–20 km depth) of its source region. Their inference was subsequently supported by seafloor pressure gauge observations (Ito et al. 2013; a green rectangle within the Tohoku-Oki earthquake rupture in Fig. 1). There have been many similar attempts to infer the occurrence of SSEs using repeating earthquakes (e.g., Nadeau and McEvilly 2004; Bouchon et al. 2011; Kato et al. 2014; Uchida et al. 2016; Rolandone

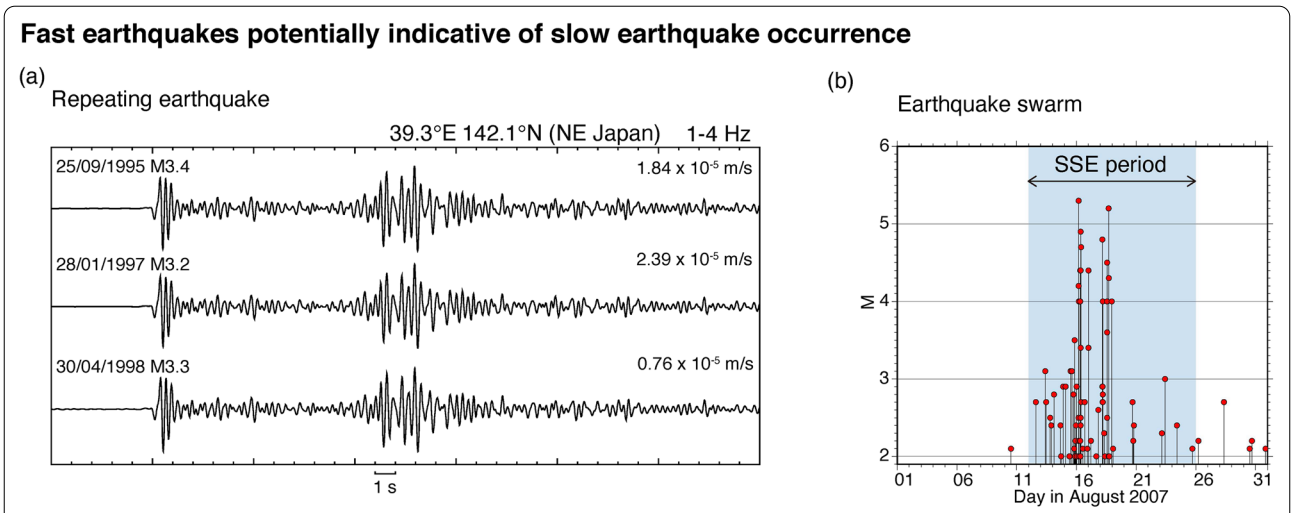

Fig. 4 Fast earthquakes potentially indicative of slow earthquake occurrence. **a** Observed waveforms of repeating earthquakes. These repeating earthquakes were observed off Kamaishi in the northern Japan Trench (Igarashi et al. 2003). **b** Magnitude–time diagram for an earthquake swarm accompanying an SSE. This earthquake swarm was observed during the period of the 2007 SSE off the Boso Peninsula in the Sagami Trough, eastern Japan (Fukuda 2018)

et al. 2018; Nishikawa and Ide 2018). Furthermore, several studies compared geodetically detected SSEs and repeating earthquake activity in detail and found a good correspondence between them (e.g., Shaddox and Schwartz 2019; Uchida et al. 2020; Hughes et al. 2021; Okada et al. 2022). Readers interested in repeating earthquakes can refer to review papers by Uchida (2019) and Uchida and Bürgmann (2019) for more information.

Earthquake swarms are seismic sequences without a distinguishable mainshock (Fig. 4b). They are distinct from regular mainshock–aftershock sequences and do not obey the Omori–Utsu's aftershock law (e.g., Llenos et al. 2009; Holtkamp and Brudzinski 2011; Nishikawa and Ide 2017), which states that aftershock seismicity rates exhibit a power-law decay (e.g., Utsu 1957; Utsu et al. 1995). Earthquake swarms are thought to be triggered by transient aseismic phenomena, such as migration of crustal fluid, magma intrusion, and SSE-induced stress loading (e.g., Toda et al. 2002; Fukuda 2018; Ross et al. 2020). As already described in Sect. 2.2.1, earthquake swarms accompanying SSEs have been observed in many circum-Pacific subduction zones (e.g., Ozawa et al. 2003; Sagiya 2004; Liu et al. 2007; Delahaye et al. 2009; Ito et al. 2013; Vallée et al. 2013; Villegas-Lanza et al. 2016; Socquet et al. 2017; Yamamoto et al. 2022; Fig. 4b). Some of these earthquake swarms accompanying SSEs were followed by megathrust earthquakes (Ito et al. 2013; Socquet et al. 2017), and the earthquake swarms were considered as a swarm of foreshocks retrospectively.

Similar to repeating earthquakes, there have been many attempts to infer the occurrence of SSEs from earthquake swarm activity (e.g., Llenos and McGuire 2011; Okutani and Ide 2011; Marsan et al. 2013; Reverso et al. 2015; Nishikawa and Ide 2018; Rolandone et al. 2018; Nishikawa et al. 2019, 2021). They regarded earthquake swarms in subduction zones as potential indicators of SSEs. For example, Nishikawa et al. (2021) examined earthquake swarm activity and GNSS data along the Hikurangi Trench, New Zealand, and succeeded in detecting small SSEs ($M_w \leq 6$) that had previously been overlooked.

It is generally difficult to detect far offshore SSEs only by onshore geodetic observations. Therefore, repeating earthquakes and earthquake swarms in subduction zones can be useful tools to examine far offshore regions possibly hosting SSEs (Nishikawa et al. 2019).

2.4 Possible physical mechanisms of slow earthquakes

Although in-depth investigations on slow earthquakes, with respect to their distribution and occurrence patterns, have been conducted (Obara and Kato 2016; Obara 2020, and references cited therein), their physical mechanisms remain unclear. Many computational models of slow earthquakes, especially for SSEs, have been proposed. However, no conclusion has been reached as to which model is the most plausible because verification by observations is generally difficult. The proposed models are mostly based on the rate-and-state-dependent friction law (Dieterich 1979). This friction law was derived from rock friction experiments and expresses the shear stress on a frictional surface as a linear combination of the logarithm of the slip rate and the logarithm

of a variable characterizing the state of the frictional surface (state variable). Readers can refer to a review paper by Scholz (1998) for the details of the rate-and-state-dependent friction law. We divide computational models of slow earthquakes into two major groups and briefly introduce them below.

The first group is characterized by a fault patch of homogeneous friction with a mechanism to suppress the slip rate. The mechanisms include a large critical nucleation length (i.e., the minimum slipping patch size required for initiating unstable seismic slip) (e.g., Tse and Rice 1986; Kato 2004; Liu and Rice 2005; Barbot 2019), a friction that exhibits rate-weakening behavior (a decrease in fault strength in response to an increased slip rate) at low slip rates but switches to rate-strengthening behavior (an increase in fault strength in response to an increased slip rate) at high slip rates (e.g., Shibazaki and Iio 2003; Shibazaki and Shimamoto 2007; Wu et al. 2019; Im et al. 2020), and dilatant strengthening (i.e., strengthening of frictional surfaces due to reduction in pore-fluid pressure associated with pore creation induced by fault slip) (e.g., Suzuki and Yamashita 2009; Segall et al. 2010). These slip rate braking mechanisms prevent the acceleration of fault slip to the slip rate of fast earthquakes (approximately 1 m/s) and produce SSEs. A large critical nucleation length (e.g., Tse and Rice 1986; Kato 2004; Liu and Rice 2005; Barbot 2019) can be achieved by a large characteristic slip distance (i.e., a parameter of the rate-and-state-dependent friction describing a slip distance necessary for adjustment of friction to a new steady slip rate), rate-weakening but almost neutral friction, or low effective normal stress (i.e., applied fault-normal stress minus pore-fluid pressure) (e.g., Scholz 1998).

The other group regards slow earthquakes as slow fault slips resulting from heterogeneous friction or rheology (e.g., Nakata et al. 2011; Ando et al. 2012; Skarbek et al. 2012). For example, Skarbek et al. (2012) showed that slow slip naturally occurs on a fault with a heterogeneous distribution of rate-weakening and rate-strengthening frictions without requiring finely tuned frictional parameters. Ando et al. (2012) considered small brittle patches within a viscous flowing matrix and reproduced the coincidence of slow shear deformation and fast shear ruptures similar to ETS (e.g., Rogers and Dragert 2003; Obara et al. 2004; Sect. 2.2.1). This model also reproduced diffusional migration of ETS (e.g., Ide 2010; Kato and Nakagawa 2020) as stress diffusion in the viscous matrix and associated small brittle ruptures. The above models, which consider the heterogeneity of fault materials, are consistent with geological observations of exhumed subduction shear zones that suggest a mixture of brittle fractures and viscous flow in regions hosting ETS (Behr et al. 2018; Ujiie et al. 2018). Furthermore, abundant fine-scale heterogeneity on the slow-earthquake-genic plate interfaces probably requires stochastic modeling rather than continuous deterministic models, as demonstrated by Brownian slow earthquake models (Ide 2008; Ide and Yabe 2019) and a model including stochastic stress fluctuations (Aso et al. 2019). The Brownian slow earthquake models are inspired by observations of tectonic tremors, whose waveforms look like random noise, and they express slow earthquakes as rupture processes that stochastically evolve.

A vast array of previous geophysical and geological observations suggests that areas prone to slow earthquakes are characterized by abundant water and near-lithostatic pore-fluid pressure. Evidence of near-lithostatic pore-fluid pressure includes high Vp/Vs ratios at plate boundaries hosting slow earthquakes (e.g., Kodaira et al. 2004; Shelly et al. 2006), dynamic triggering of tectonic tremors by the passage of surface waves of large distant earthquakes (e.g., Miyazawa and Mori 2005; Rubinstein et al. 2007), significant tidal responses of tectonic tremors (e.g., Nakata et al. 2008; Rubinstein et al. 2008), and abundant veins in an ancient subduction shear zone exhumed from a frictional–viscous transition depth (e.g., Ujiie et al. 2018). For a detailed summary of the evidence of near-lithostatic pore-fluid pressure, refer to Bürgmann (2018), Behr and Bürgmann (2021), and Kirkpatrick et al. (2021). Computational models of slow earthquakes often consider the influence of highly overpressured fluids and assume low effective normal stress on the fault plane. Low effective normal stress stabilizes fault slip and facilitates aseismic slip (e.g., Scholz 1998). However, the process by which the highly overpressured fluids enable the occurrence of various types of slow earthquakes (Sect. 2.1) remains unclear.

3 Studies on slow earthquakes along the Japan Trench

3.1 Brief history of slow earthquake research in the Japan Trench

In this section, we introduce important studies related to slow earthquakes along the Japan Trench in a chronological order, with an aim to help readers understand the history of slow earthquake research in the Japan Trench. The detailed spatiotemporal distribution of slip phenomena discovered by the studies introduced in this section is presented in Sect. 3.2.

3.1.1 Brief history prior to the 2011 Tohoku-Oki earthquake

A large transient aseismic slip was first observed in 1992 at the shallow plate interface (approximately 10–20 km depth) of the northern Japan Trench (39–40° N) by extensometers (Kawasaki et al. 1995; Kawasaki et al. 2001; the blue dashed rectangle in Fig. 1). This transient

aseismic slip was also reported by Miura et al. (1993) and Miura et al. (1994), although these reports were not peer-reviewed journal papers. Kawasaki et al. (1995) named this aseismic slip event the 1992 Sanriku-Oki ultraslow earthquake. This event can be regarded as the first-ever reported SSE at a subduction zone plate boundary. However, the duration of this event was 1 day, and the moment magnitude was approximately M_w 7.3–7.7, making it a strange event—in that it deviates significantly from the linear moment–duration scaling relation of slow earthquakes ($M_0 \propto T$) (Ide et al. 2007a; the magenta circle labeled SR in Fig. 3a). Furthermore, the event occurred immediately after a M_w 6.9 interplate earthquake (the 1992 M_w 6.9 Sanriku-Oki earthquake) and can be interpreted as a huge afterslip. However, this event cannot be considered a typical afterslip (Alwahedi and Hawthorne 2019) because the seismic moment of this event is extremely large, ranging from four to 16 times the seismic moment of the preceding M_w 6.9 earthquake. Similar to the 1992 Sanriku-Oki ultraslow earthquake in the northern Japan Trench, an aseismic slip event with characteristics intermediate between an SSE and an afterslip has been reported in the Peru Trench (Villegas-Lanza et al. 2016). This event also had an extremely large moment, and thus, it cannot be a typical afterslip (10 times or more the seismic moment of the preceding M_w 5.8 earthquake). Villegas-Lanza et al. (2016) interpreted this event as a slow slip "helped" (or triggered) by an earthquake rather than a classical afterslip. Following the classification of Villegas-Lanza et al. (2016), we also regard the 1992 Sanriku-Oki ultraslow earthquake in the northern Japan Trench as a slow slip triggered by an earthquake.

Subsequently, in the late 1990s and 2000s, afterslip following major earthquakes, rather than SSEs, became the focus of much research. A continuous GNSS observation system (GEONET) installed by the Geospatial Information Authority of Japan (GSI) recorded the afterslip following the 1994 M_w 7.7 Sanriku-Oki earthquake (Heki et al. 1997), which ruptured the plate interface (approximately 20–30 km depth) of the northern Japan Trench (40–40.5° N). The afterslip took about a year after the mainshock to release a seismic moment greater than the mainshock. Yagi et al. (2003) found that the coseismic slip of the 1994 M_w 7.7 Sanriku-Oki earthquake and its afterslip were spatially complementary in distribution. In addition, Miura et al. (2006) reported a large afterslip following the 2005 M_w 7.1 Miyagi-Ken-Oki earthquake, which ruptured the deeper part of the central Japan Trench (37.8–38.5° N). This afterslip released a seismic moment comparable to that of the mainshock over a period of approximately one year after the mainshock.

In the 2000s, the GEONET also revealed the interplate slip deficit distribution along the Japan Trench (Ito et al. 2000; Nishimura et al. 2000, 2004; Suwa et al. 2006; Hashimoto et al. 2009; Loveless and Meade 2010). These studies consistently suggested the existence of a huge interplate locked zone in the central Japan Trench (37–39° N). This locked zone was subsequently ruptured by the March 11, 2011, M_w 9.0 Tohoku-Oki earthquake (thick red contours in the Japan Trench in Fig. 1).

In 2002, small repeating earthquakes (e.g., Nadeau and Johnson 1998; Nadeau and McEvilly 1999; Sect. 2.3) were first reported along the Japan Trench (Matsuzawa et al. 2002; small red points in Fig. 1). They were used to estimate the amount of steady (e.g., Igarashi et al. 2003; Igarashi 2010) and transient aseismic slip (e.g., Uchida et al. 2004; Matsuzawa et al. 2004). Igarashi et al. (2003) detected repeating earthquakes by a method based on waveform similarity and estimated the rate of interplate steady slip along the Japan Trench from the recurrence intervals of the repeating earthquakes. Furthermore, they found that few continuous-type small repeating earthquakes (i.e., repeating earthquakes that repeat at almost regular intervals and are not clustered in time) were distributed within the huge locked zone of the central Japan Trench (37–39° N), discovered by the GNSS observations (Ito et al. 2000; Nishimura et al. 2000). This is probably due to the absence of aseismic loading inside the locked region (see Sect. 2.3). Uchida et al. (2004) analyzed repeating earthquake activity prior to interplate large earthquakes in the northern Japan Trench and investigated preseismic changes in the interplate slip rate. They suggested the acceleration of interplate aseismic slip 6 days, 2 days, and 8 months before the 1989 M_w 7.4, 1992 M_w 6.9, and 1994 M_w 7.7 Sanriku-Oki earthquakes, respectively. These preseismic slow slips might have concentrated stress at the source regions of the large earthquakes.

In 2004, Yamanaka and Kikuchi (2004) investigated the slip distribution of M_w 7–8 class megathrust earthquakes from 1931 to 1994 along the northern and central Japan Trench by means of waveform inversion (see thin red contours in the Japan Trench in Fig. 1). They termed large slip areas of megathrust earthquakes asperities. Specifically, they regarded the area where the amount of slip is half the maximum slip or larger as an asperity. They found that in the northern Japan Trench, the asperities of several megathrust earthquakes significantly overlap. That is, the same area on the plate interface has been repeatedly ruptured by the megathrust earthquakes. Furthermore, in the central Japan Trench (38–39° N), the asperity of the 1981 M_w 7.1 earthquake, which is located at approximately 20–30 km depth (thin red contours in the Tohoku-Oki earthquake rupture in Fig. 1), slipped again during the largest foreshock (M_w 7.3) 2 days before the March 11, 2011, M_w 9.0 Tohoku-Oki earthquake

(Ohta et al. 2012). These observations indicate the persistent nature of asperities. Note that there are various definitions of asperity, as summarized in Ide (2014). To avoid ambiguity, we follow Yamanaka and Kikuchi's definition in the subsequent sections.

3.1.2 Brief history after the 2011 Tohoku-Oki earthquake

The M_w 9.0 Tohoku-Oki earthquake occurred on March 11, 2011 (the thick red contours in the Japan Trench in Fig. 1). After the Tohoku-Oki earthquake, aseismic slips that preceded the 2011 Tohoku earthquake were investigated in detail. Seismicity analyses (Ando and Imanishi 2011; Kato et al. 2012) and ocean-bottom pressure gauge observations (Ohta et al. 2012) revealed that afterslip had occurred on the plate interface after the largest foreshock (M_w 7.3) 2 days before the Tohoku-Oki earthquake. Ando and Imanishi (2011) suggested that the afterslip following the largest foreshock had migrated toward the rupture initiation point of the Tohoku-Oki earthquake. Furthermore, a repeating earthquake analysis (Kato et al. 2012), ocean-bottom pressure gauge observations (Ito et al. 2013), and ocean-bottom seismometer observations (Ito et al. 2015; Katakami et al. 2018) suggested that a M_w 7.0 SSE accompanied by a Japan Meteorological Agency magnitude (M_j) 5 class earthquake swarm and tectonic tremors had been occurring on the shallow plate interface (approximately 10–20 km depth) of the central Japan Trench during the month prior to the Tohoku-Oki earthquake (a green rectangle within the Tohoku-Oki earthquake rupture in Fig. 1). The source region of the preseismic slow earthquakes was ruptured by the Tohoku-Oki earthquake and slipped tens of meters (e.g., Ide et al. 2011; Iinuma et al. 2012), indicating that the identical area of the plate interface hosted both aseismic and huge seismic slips. However, we note that the signals of the preseismic slow earthquakes were observed at a small number of ocean-bottom stations (Ito et al. 2013, 2015; Katakami et al. 2018), and there should be large uncertainty in their source locations.

In 2014, GNSS data from the GEONET revealed that aseismic slip had been accelerating on the deeper plate interface (approximately 30–60 km depth) of the central and southern parts (36–39° N) of the Japan Trench in the decade prior to the Tohoku-Oki earthquake (Mavrommatis et al. 2014). A subsequent analysis by Yokota and Koketsu (2015) also supported the acceleration of the aseismic slip from 2002 to the 2011 Tohoku-Oki earthquake and regarded this transient slip as a fault slip phenomenon similar to long-term SSEs on the deeper plate interface of the Nankai Trough (Hirose et al. 1999; Ozawa et al. 2002; Fig. 1). This aseismic transient may have stressed locked parts of the Japan Trench megathrust (Yokota and Koketsu 2015). Furthermore, the decade-long aseismic transient may also have induced slips on the shallow plate interface (10–30 km depth) in the central and southern Japan, partially overlapping with the rupture area of the Tohoku-Oki earthquake, as suggested by repeating earthquake data (Mavrommatis et al. 2015).

In the southern end of the Kuril Trench (41–43° N), which is located just north of the Japan Trench, VLFEs were first observed in 2008 (Asano et al. 2008). In 2015, the F-net broadband seismograph network, which is an onshore seismograph network operated by the National Research Institute for Earth Science and Disaster Resilience (NIED) (NIED 2019b), also observed VLFEs in the Japan Trench (Matsuzawa et al. 2015). VLFEs were detected using a method based on a matched filter technique (Shelly et al. 2007). However, this detection was not sufficient to provide a full picture of the VLFE distribution along the Japan Trench because their template VLFEs were detected by visual inspection and were not spatially complete (Matsuzawa et al. 2015).

In 2016, temporal changes in interplate slip rate estimated from repeating earthquakes (Sect. 2.3) suggested that 1–6 year periodic SSEs are widespread in the Japan Trench (Uchida et al. 2016). Seismicity of M_j 5 or greater was active during the high slip rate periods of the SSEs. Uchida et al. (2016) suggested that the periodic SSEs induce periodic stress perturbations and modulate the activity of medium-to-large earthquakes in the Japan Trench. Furthermore, Nomura et al. (2016) developed a Bayesian statistical method to estimate the detailed space–time distribution of interplate slip rates from the recurrence intervals of repeating earthquakes and confirmed the quasi-periodic slip rate acceleration in the northern Japan Trench.

In 2019, pop-up-type ocean-bottom seismometers (Ohta et al. 2019) and the Seafloor Observation Network for Earthquakes and Tsunamis along the Japan Trench (S-net) (Tanaka et al. 2019; Nishikawa et al. 2019) observed clear signals of tectonic tremors on the shallow plate interface (approximately 10–20 km depth) of the Japan Trench (small green squares in the Japan Trench in Fig. 1). The S-net is an ocean-bottom seismic and pressure observation network that NIED has been operating since 2016 (NIED 2019a). These studies revealed detailed tectonic tremor activity from 2016. The tremors were widely distributed and active on the shallow plate interface of the northern and southern Japan Trench, roughly consistent with the VLFE distribution presented by Matsuzawa et al. (2015). Furthermore, Nishikawa et al. (2019) discovered an approximately 200-km-long tremor gap in the central Japan Trench (37–39° N) (Fig. 1), which corresponds well with the large slip area (10 m or larger)

of the Tohoku-Oki earthquake (Iinuma et al. 2012; the thick red contours in the Japan Trench in Fig. 1).

In 2020, Baba et al. (2020) conducted a comprehensive detection of VLFEs using data recorded by the F-net broadband seismograph network. They used synthetic waveforms of low-angle reverse faulting on the plate interface as templates of the matched filter technique (Shelly et al. 2007) and revealed the spatiotemporal distribution of VLFEs along the entire Japan Trench from 2003 to 2018. The distribution of VLFEs corresponded well with the distribution of tectonic tremors revealed by the S-net (Tanaka et al. 2019; Nishikawa et al. 2019), as expected from the fact that tectonic tremors and VLFEs are seismic waves emanating from the identical slow interplate slip phenomenon (Ide et al. 2007a; Kaneko et al. 2018; Masuda et al. 2020; Sect. 2.2.2). As with the tectonic tremors (Nishikawa et al. 2019), Baba et al. (2020) discovered an approximately 200-km-long VLFE gap in the central Japan Trench, which corresponded well with the large slip area of the Tohoku-Oki earthquake. Furthermore, this VLFE gap is a feature observed both before and after the 2011 Tohoku-Oki earthquake (Baba et al. 2020). This observation indicates that the Tohoku-Oki earthquake ruptured the gap of seismic slow earthquakes.

In 2021, Nishimura (2021) carried out a systematic and comprehensive short-term SSE detection using GNSS data from the GEONET in the southern Japan Trench. Nishimura (2021) discovered a bimodal depth distribution of SSEs (M_w 5.8–6.9) on the shallow (10–30 km depth) and deeper (40–60 km depth) parts of the plate interface (Fig. 1). SSEs avoid a depth of 30–40 km, where past megathrust earthquakes have repeatedly occurred (e.g., Mochizuki et al. 2008; Kubo et al. 2013). The bimodal depth distribution of SSEs is similar to that of shallow and deep slow earthquakes (shallower than 10 km depth and 25–40 km depth, respectively) in the Nankai Trough (Fig. 1).

Research on the relationship between slow and fast earthquakes along the Japan Trench has also made progress in recent years. In 2020, Kubo and Nishikawa (2020) revealed the along-dip complementary distribution of M_w 7 class megathrust earthquake ruptures (30–40 km depth) (e.g., Yamanaga and Kikuchi, 2004) and tectonic tremors (10–20 km depth) (e.g., Nishikawa et al. 2019) in the northern and southern Japan Trench. They suggested that the shallow slow-earthquake-genic regions in the northern and southern Japan Trench impede rupture propagation of megathrust earthquakes. In 2021, synchronous phenomena of tectonic tremors and swarms of small interplate earthquakes were observed in the shallow part of the southern Japan Trench (Obana et al. 2021). This observation implies that SSEs too small for onshore geodetic detection often trigger both tectonic tremors and earthquake swarms on the shallow plate interface of the Japan Trench.

3.2 Observational studies on slow earthquakes in the Japan Trench

In this section, we present the detailed slow earthquake distribution revealed by observational studies in the Japan Trench. We first present the spatiotemporal distribution of slow earthquakes from August 2016 (Sect. 3.2.1) because it is much more clearly resolved than before August 2016 (Sect. 3.2.2); the details of the spatiotemporal distribution of slow earthquakes before August 2016 are still enigmatic. We believe that a clear picture presented in Sect. 3.2.1 facilitates understanding of the subsequent Sects. (3.2.2 and 3.2.3). In the last part of this section, we review studies on repeating earthquakes, earthquake swarms, and foreshocks because the studies are closely related to slow earthquake observations in the Japan Trench (Sects. 3.2.1 and 3.2.2) and provide insights into slow earthquake activity before March 2011.

3.2.1 Spatiotemporal distribution of slow earthquakes from August 2016

The detailed tectonic tremor activity has been revealed by the S-net since August 2016. Figure 5 shows the spatiotemporal distribution of tectonic tremors (Nishikawa et al. 2019), VLFEs (Baba et al. 2020), and short-term SSEs (Nishimura 2021) from August 2016 to December 2021 along the Japan Trench. Nishikawa et al. (2019) detected the tectonic tremors until August 2018 by applying the envelope correlation method (Obara 2002; Ide 2010) to the S-net seismograms. We updated their tremor catalog until December 2021 using the same method as Nishikawa et al. (2019). Baba et al. (2020) detected VLFEs from January 2003 until July 2018 by a matched filter technique using synthetic waveforms of low-angle reverse faulting on the plate interface as templates. The templates were spaced approximately 40 km apart in the latitudinal and longitudinal directions. The SSE distribution was based on Nishimura (2021), who detected SSEs using the GNSS data of the GEONET until December 2019 in the southern Japan Trench. We updated the catalog until September 2021 using the same method as Nishimura (2021).

We observed good correspondence between tectonic tremors and VLFEs in both their epicenters and origin times (Fig. 5b, d, and e). This is not surprising because tectonic tremors and VLFEs originate from the identical slow interplate slip phenomenon (Ide et al. 2007a; Kaneko et al. 2018; Masuda et al. 2020; Sect. 2.2.2; Fig. 3b). Based on this fact, hereafter, we assume that, as with the VLFEs,

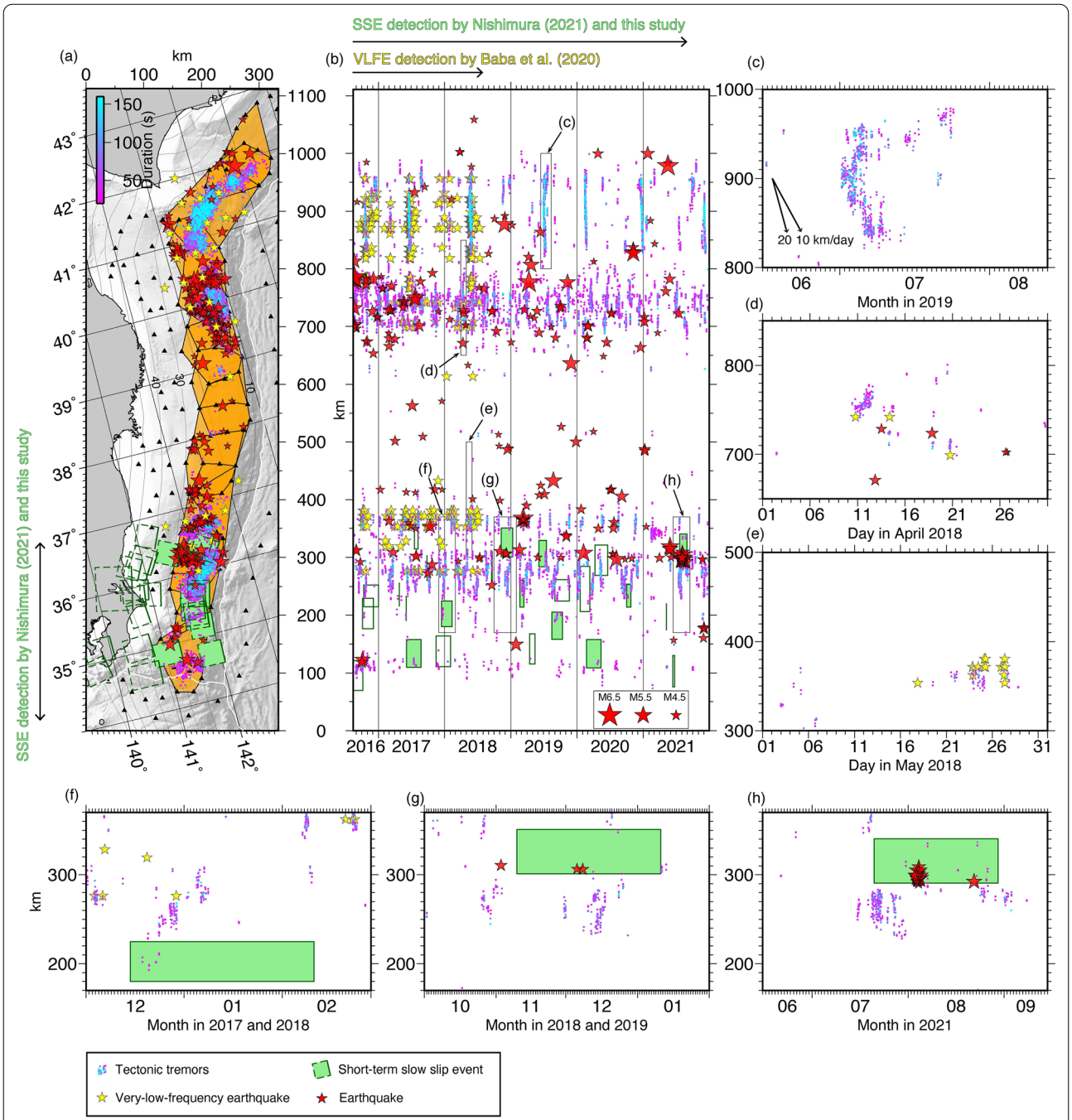

Fig. 5 Tectonic tremor activity in the Japan Trench from August 2016 to December 2021. **a** Epicenters of the tectonic tremors. Colored points indicate the epicenters of the tremors. Yellow and red stars represent VLFEs (Baba et al. 2020) and $M_j \geq 4$ fast earthquakes, respectively. The fast earthquakes are from the Japan Meteorological Agency (JMA) catalog. Open and solid dashed green rectangles denote deep and shallow short-term SSEs, respectively (Nishimura 2021). The upper edges of the SSE fault models are indicated by the green solid lines. Black triangles represent S-net stations. The orange shaded polygons are subregions used for tremor detection by Nishikawa et al. (2019). The upper surface of the subducting Pacific Plate is indicated by the black contours at 10-km-depth intervals. **b** Spatiotemporal distribution of the tectonic tremors. We used Japanese Standard Time (UTC + 9 h). **c**–**h** Enlarged views of (**b**). The spatiotemporal windows of **c**–**h** are shown in (**b**)

the detected tectonic tremors are located along the plate interface, although the source depths of the tectonic tremors are not well constrained (Nishikawa et al. 2019).

In the Japan Trench, tectonic tremors and VLFEs are distributed along the depth contours of 10–20 km of the plate interface (Ohta et al. 2019; Tanaka et al. 2019; Nishikawa et al. 2019; Baba et al. 2020). However, the tremors and VLFEs avoid the central Japan Trench (37–39° N), making the region an approximately 200-km-long gap of seismic slow earthquakes (Fig. 5a). This gap corresponds well with the large slip area of the 2011 Tohoku-Oki earthquake (e.g., Iinuma et al. 2012; the thick red contours in the Japan Trench in Fig. 1). This correspondence is the most prominent feature of the slow earthquake distribution in the Japan Trench.

The tectonic tremor activity along the Japan Trench and the southern end of the Kuril Trench has some common features with tectonic tremor activities in other subduction zones, implying that the slow-earthquake-genic regions in the Japan and Kuril trenches and other subduction zones share basically similar frictional and rheological properties. There are three prominent common features. The first one is tectonic tremor migration. In the southern end of the Kuril Trench, which is located to the north of 41° N, along-strike tremor migration episodes with a speed of ~ 10 km/day are observed approximately once a year (Tanaka et al. 2019; Nishikawa et al. 2019; Fig. 5b and c). Similar along-strike migration episodes with comparable speeds have been observed at the deeper (approximately 10 km/day; Obara 2002) and shallower (approximately 10–60 km/day; Yamashita et al. 2015; Annoura et al. 2017) parts of the Nankai Trough and at the deeper part of the Cascadia subduction zone (approximately 10 km/day; Rogers and Dragert 2003; Houston et al. 2011).

The second common feature is the simultaneous occurrence of tectonic tremors and short-term SSEs (Nishikawa et al. 2019; Fig. 5f and h). This composite fault slip phenomenon, called ETS (Sect. 2.2.1), has also been observed at the deeper part of the Cascadia subduction zone (Rogers and Dragert 2003) and at the deeper and shallower parts (Obara et al. 2004; Araki et al. 2017) of the Nankai Trough. However, in the Japan Trench, many tremor bursts occur without detectable SSEs (Nishimura 2021; Fig. 5b). This is probably because the SSE catalog (Nishimura 2021) is not complete near the trench axis. It is generally difficult to detect small ($M_w \leq 6$) SSEs near the trench axis using only onshore GNSS observations. Furthermore, it is also worth noting that deep ETS has not been reported in the Japan Trench. Although SSEs exhibit a bimodal depth distribution (10–30 km and 40–60 km) (Nishimura 2021; Fig. 5a), tectonic tremors have been observed only on the shallower plate interface.

The third common feature is the correlation between the recurrence intervals of tremor bursts and their seismic energy rates. Yabe et al. (2021) compared the recurrence intervals of tremor bursts with the energy rates of their 2–8 Hz bandpass-filtered seismic waves to find a correlation between them. In the southern end of the Kuril Trench (north of 41° N), tectonic tremor bursts repeated approximately every 0.5–1 year (Fig. 5b), and their median seismic energy rate was high (1700 J/s). In the northern Japan Trench, tremor episodes repeated approximately every 1–2 months (Fig. 5b), and their median seismic energy rate was low (830 J/s). The southern Japan Trench was characterized by medium recurrence intervals of approximately 3 months and medium median seismic energy rates (approximately 1400 J/s). The correlation between recurrence intervals of tremor bursts and their seismic energy rates has also been observed for deep tremors in the Cascadia subduction zone in both the along-strike and along-dip directions (Wech and Creager 2011; Idehara et al. 2014; Yabe and Ide 2014). Yabe et al. (2021) suggested that differences in the frictional strength of faults producing tectonic tremors cause the correlation. A stronger fault may endure stress loading for a longer period and produce more energetic tremors.

The tectonic tremor activity along the Japan Trench also has a feature distinct from that in the other subduction zones: We observed a coincidence of tectonic tremors, short-term SSEs, and a swarm of moderate interplate earthquakes in the Japan Trench. In July and August 2021, a M_w 6.6 short-term SSE and a burst of tectonic tremors occurred in the southern Japan Trench (35.5–36.5° N) (Fig. 5h). In early August, a swarm of moderate interplate earthquakes, with a maximum magnitude of M_w 5.8, occurred in an adjacent region. The fault model of the SSE was located to the north (around 36.4° N) of the earthquake swarm (around 36.2° N), and the tremor burst occurred to the south (around 35.8° N). We also observed a similar coincidence of tectonic tremors, short-term SSEs, and three $M_j \geq 4$ interplate earthquakes in November and December 2018 in the same region (Fig. 5g). Composite fault slip phenomena of tectonic tremors, short-term SSEs, and a swarm of moderate interplate earthquakes have rarely been observed in subduction zones other than the Japan Trench. In the Nankai Trough and Cascadia subduction zone, ETSs on the deeper plate interface are not accompanied by swarms of interplate earthquakes (Rogers and Dragert 2003; Obara et al. 2004). Furthermore, moderate interplate seismicity ($M \geq 4$) is very rare in the Nankai Trough and Cascadia subduction zone (Ide 2013). However, we note that a recent study (Yamamoto et al. 2022) has reported the simultaneous occurrence of a short-term SSE, VLFEs,

and a swarm of interplate microearthquakes ($M \leq 3$) on the shallow plate interface (10 km depth or shallower) of the Nankai Trough. At the Boso Peninsula in the Sagami Trough, eastern Japan, swarms of moderate interplate earthquakes accompany short-term SSEs (Ozawa et al. 2003; Sagiya 2004), but concurrent tectonic tremors have not been observed. These differences in composite fault slip phenomena between subduction zones may reflect differences in interplate frictional properties of slow-earthquake-genic regions between subduction zones. Note, however, that each subduction zone has different observation conditions, such as station density and noise level, and that such differences might lead to apparent differences in composite fault slip phenomena.

3.2.2 Spatiotemporal distribution of slow earthquakes before August 2016

With respect to slow earthquake activity prior to the start of the S-net observations in August 2016, the VLFE activity along the entire Japan Trench (Baba et al. 2020) and SSE activity in the southern Japan Trench (Nishimura 2021) were revealed by the F-net and GEONET, respectively. Systematic and comprehensive detection of SSEs in the central and northern Japan Trench has not yet been conducted. However, in the central Japan Trench, ocean-bottom pressure gauge observations detected short-term SSEs in November 2008 and from the end of January 2011 to just before the largest foreshock (M_w 7.3) of the March 11, 2011, Tohoku-Oki earthquake (Ito et al. 2013). We note that one should be careful of the treatment of the SSE preceding the Tohoku-Oki earthquake, especially when discussing the slow earthquake distribution prior to the Tohoku-Oki earthquake. It is natural that the period just prior to and the region close to the epicenter of the Tohoku-Oki earthquake be analyzed in greater detail than the other periods and regions, given their scientific importance. This causes a spatiotemporal bias in the detectability of SSEs. Moreover, several SSEs similar to the SSE preceding the Tohoku-Oki earthquake (i.e., SSEs accompanied by earthquake swarms and/or tectonic tremors) have recently been reported in the southern Japan Trench (Nishimura 2021; Fig. 5h), implying that such SSEs are more common in the Japan Trench than previously thought.

Figure 6 shows the slow earthquake activity before and after the March 2011 Tohoku-Oki earthquake. VLFEs frequently occurred in the northern and southern Japan Trench both before and after the 2011 Tohoku-Oki earthquake (Fig. 6b and c). In the gap of tectonic tremors and VLFEs that we identified in Fig. 5a (37–39° N), VLFE activity was low even before the Tohoku-Oki earthquake (Fig. 6a and b). The VLFEs before the Tohoku-Oki earthquake appear to have avoided the huge interplate locked zone in the central Japan Trench (Suwa et al. 2006; the red shaded area in Fig. 6a), although ocean-bottom pressure gauge and seismometer observations suggested that a short-term SSE and tectonic tremors preceding the March 2011 Tohoku-Oki earthquake had occurred in the VLFE gap (Ito et al. 2013; Ito et al. 2015; Katakami et al. 2018; a green rectangle within the Tohoku-Oki earthquake rupture in Fig. 6a and b).

As shown in Fig. 6b, short-term SSEs and VLFEs sometimes occur simultaneously in close proximity. These coincidences are potential ETSs (Sect. 2.2.1). Here, if the distance between a VLFE epicenter and an SSE fault model was within 40 km and the VLFE occurred within 2 weeks before or after the short-term SSE period, we considered the event as a potential ETS. As a result, we identified six potential ETSs before the March 2011 Tohoku-Oki earthquake (Fig. 6b). However, Fig. 6b shows that most of the VLFEs were not accompanied by detectable short-term SSEs (Nishimura 2021). This may be due to the incompleteness of the SSE catalog near the trench axis, as mentioned in Sect. 3.2.1 Furthermore, the uncertainty in location of the VLFEs and SSEs may also make the correspondence between the two slow earthquakes worse.

Figure 6 also shows two slow fault slip phenomena similar to SSEs. One is the decade-long acceleration of aseismic slip on the deeper plate interface (approximately 30–60 km depth) of the central Japan Trench, which was discovered by the GEONET (Ozawa et al. 2012; Mavrommatis et al. 2014; Yokota and Koketsu 2015; Sect. 3.1.2; the yellow shaded area in Fig. 6a and b). This transient lasted from around 2002 to just before the 2011 Tohoku-Oki earthquake. Note that this decade-long transient may also have induced slips on the shallower plate interface (approximately 10–30 km depth), as suggested by repeating earthquake data (Mavrommatis et al. 2015). This transient slip resembles long-term SSEs (Yokota and Koketsu 2015). However, the duration of this transient slip (9 years) is longer than that of typical long-term SSEs (several months to several years), and the magnitude of this transient slip (M_w 7.7) is also larger than that of typical long-term SSEs (M_w 6.5–7.5) (Fig. 3a). Furthermore, it is unclear whether this transient slip recurs like the deep long-term SSEs in the Nankai Trough (e.g., Kobayashi 2014; Takagi et al. 2019), as it was observed only once in the decade prior to the 2011 Tohoku-Oki earthquake. Mavrommatis et al. (2014) suggested that this transient slip might be an aseismic slip intruding from the deep plate interface into the inside of the locked region prior to the coseismic rupture. A definite conclusion has not yet been reached as to the identity of this aseismic transient slip.

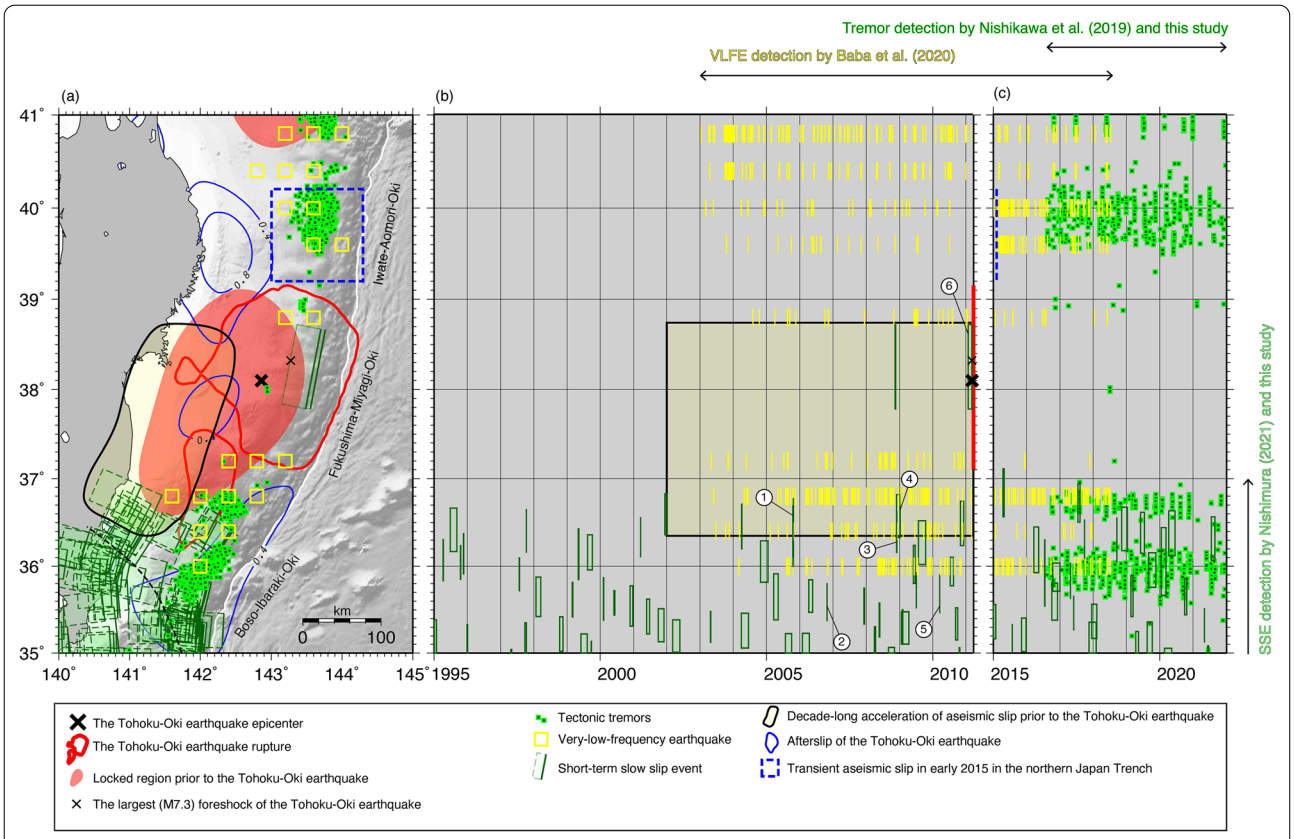

Fig. 6 Slow earthquake activity in the Japan Trench before and after the 2011 Tohoku-Oki earthquake. **a** Epicenters of the slow earthquakes. **b** Spatiotemporal distribution of the slow earthquakes before the March 11, 2011, Tohoku-Oki earthquake. Potential ETSs before the Tohoku-Oki earthquake are numbered 1–6. **c** Spatiotemporal distribution of the slow earthquakes from January 2015 to December 2021. For an explanation of the symbols, refer to the legend in the figure. The epicenter of the Tohoku-Oki earthquake and its largest foreshock are from the JMA catalog. The coseismic slip (10 m or larger) and afterslip (April 23, 2011 to December 10, 2011) of the Tohoku-Oki earthquake are based on Iinuma et al. (2012) and Iinuma et al. (2016), respectively. The afterslip distribution is shown at 0.4 m intervals. The interplate locked region prior to the Tohoku-Oki earthquake is based on the slip deficit distribution estimated by Suwa et al. (2006) (larger than 6 cm/year, i.e., approximately 70% plate coupling). Tectonic tremors and VLFEs are from Nishikawa et al. (2019) and Baba et al. (2020), respectively. In the figure, we showed tectonic tremors with a duration of more than 80 s. Short-term SSEs are from Ito et al. (2013) and Nishimura (2021). The decade-long acceleration of aseismic slip prior to the Tohoku-Oki earthquake (10 cm or larger) is from Yokota and Koketsu (2015). The transient aseismic slip in early 2015 in the northern Japan Trench is based on Honsho et al. (2019)

The other slow fault slip phenomenon similar to SSEs is a transient aseismic slip in the northern part (39.2–40.2° N) of the Japan Trench in early 2015 (Honsho et al. 2019; the blue dashed square in Fig. 6a). Honsho et al. (2019) detected this transient slip (approximately M_w 7.3) based on GNSS-acoustic observations and repeating earthquake activity. Fujiwara et al. (2022) also detected the probably identical transient slip as Honsho et al. (2019) using onshore GNSS observations. Although Honsho et al. (2019) considered this transient slip as a shallow SSE, it may not be a typical SSE. This is because the transient slip followed a large interplate earthquake of M_w 6.7 (Fujiwara et al. 2022). Therefore, one might consider the transient slip as a huge afterslip of the M_w 6.7 interplate earthquake, although it is too large to be a typical afterslip (Alwahedi and Hawthorne 2019). We found that the region where the transient slip was observed significantly overlaps with the region where Kawasaki et al. (1995) observed the 1992 Sanriku-Oki ultraslow earthquake, a transient aseismic slip of M_w 7.3–7.7 that followed a M_w 6.9 interplate earthquake (Sect. 3.1.1 and the blue dashed rectangle in Fig. 1). Due to the similarity and proximity between the 1992 and 2015 transient slip events, we interpret the 2015 event as a slow slip triggered by an earthquake as well as the 1992 event (Sect. 3.1.1). A transient aseismic slip with characteristics intermediate between SSEs and afterslip (Villegas-Lanza et al. 2016) may be a typical slip behavior on the shallow plate interface of the northern part (39–40° N) of the Japan Trench.

3.2.3 Repeating earthquakes, earthquake swarms, and foreshocks before March 2011

Slow earthquake activity along the Japan Trench prior to the 2011 Tohoku-Oki earthquake has been inferred from fast earthquake activity potentially indicative of slow earthquake occurrence (i.e., repeating earthquakes, earthquake swarms, and swarms of foreshocks) (Sect. 2.3). In the Japan Trench, repeating earthquakes have been vigorously studied since the first report by Matsuzawa et al. (2002). The spatiotemporal distribution of repeating earthquakes has been revealed in detail (Igarashi et al. 2003; Igarashi 2010; Uchida and Matsuzawa 2013; Igarashi 2020; red points in Fig. 7). As already described in Sect. 3.1.1, Igarashi et al. (2003) found that few continuous-type small repeating earthquakes (i.e., repeating earthquakes that repeat at almost regular intervals and are not clustered in time) were distributed within the huge locked zone in the central Japan Trench (Ito et al. 2000; Nishimura et al. 2000). Consistent with Igarashi et al. (2003), repeating earthquakes detected by

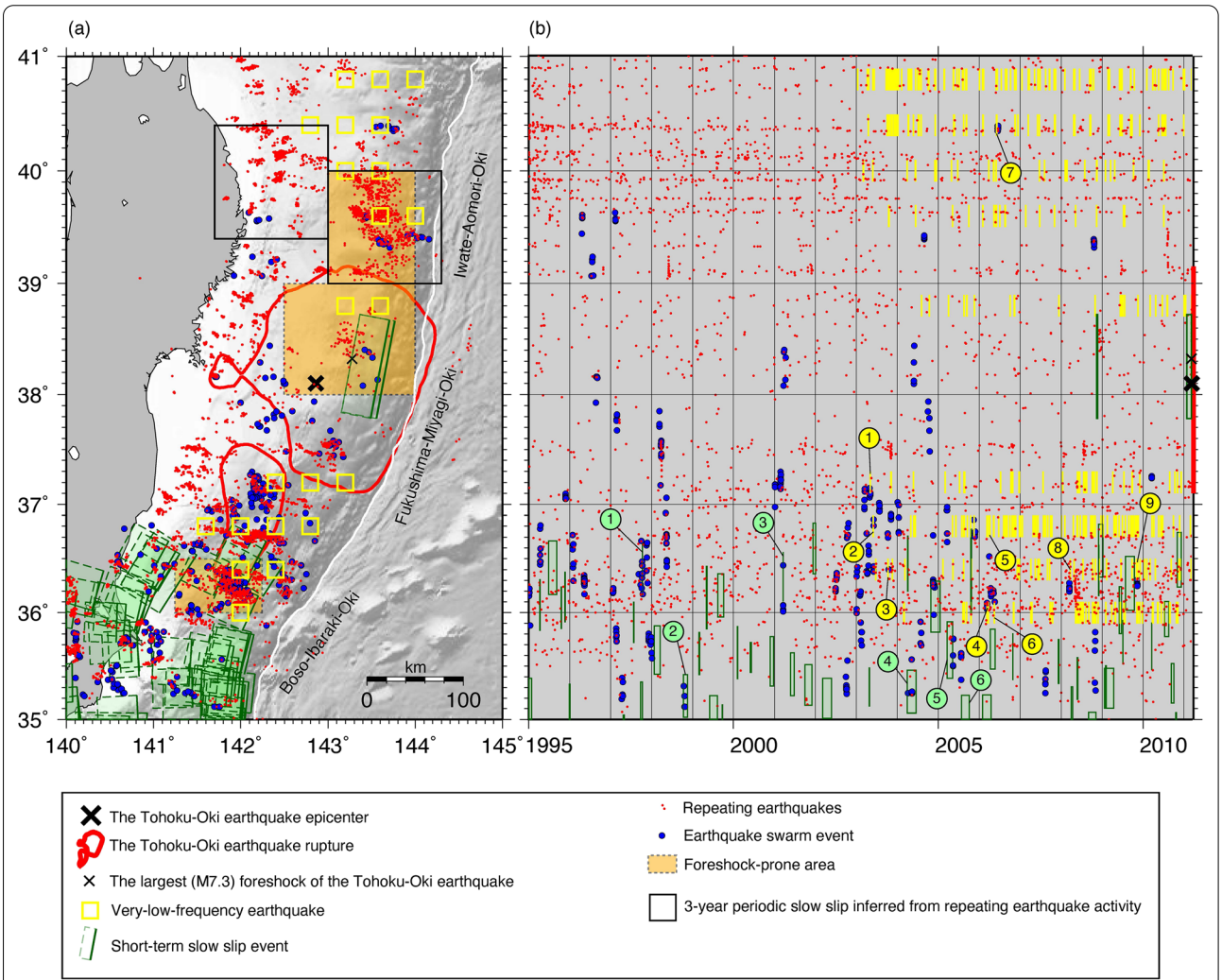

Fig. 7 Activity of repeating earthquakes and earthquake swarms along the Japan Trench before the 2011 Tohoku-Oki earthquake. **a** Epicenters of the repeating earthquakes and earthquake swarm events. **b** Spatiotemporal distribution of the repeating earthquakes and earthquake swarm events before the March 2011 Tohoku-Oki earthquake. Coincident events of SSEs and earthquake swarms are indicated by numbers 1–6 encircled in green. Coincident events of VLFEs and earthquake swarms are indicated by numbers 1–9 encircled in yellow. For an explanation of the other symbols, refer to the legend in the figure. The epicenter of the Tohoku-Oki earthquake and its largest foreshock are from the JMA catalog. The coseismic slip of the Tohoku-Oki earthquake (10 m or larger) is based on Iinuma et al. (2012). The VLFEs are from Baba et al. (2020). The short-term SSEs are from Ito et al. (2013) and Nishimura (2021). The repeating earthquakes are from Uchida and Matsuzawa (2013). The earthquake swarms ($M_j \geq 3$) are from Nishikawa and Ide (2018) and Nishikawa et al. (2019). The foreshock-prone areas are based on Maeda and Hirose (2016) and Hirose et al. (2021). The 3 years periodic slow slip in the northern Japan Trench is from Uchida et al. (2016)

Uchida and Matsuzawa (2013) are sparse within the large slip area of the Tohoku-Oki earthquake in the central Japan Trench (37–39° N) in comparison with the adjacent regions in the northern and southern Japan Trench (39–40° N and 36–37° N) (Fig. 7).

Repeating earthquakes have been used to detect transient aseismic slip on the plate interface in the Japan Trench (Matsuzawa et al. 2004; Uchida et al. 2004, 2016; Kato et al. 2012; Uchida and Matsuzawa 2013; Khoshmanesh et al. 2020). A M_j 5 class earthquake swarm including repeating earthquakes occurred on the shallow plate interface in the central Japan Trench a month before the March 2011 Tohoku earthquake, with their epicenters migrating toward the rupture initiation point of the Tohoku-Oki earthquake (Kato et al. 2012). This observation is a representative example of inferring the occurrence of a propagating SSE from repeating earthquake activity (Sect. 2.3).

Uchida et al. (2016) analyzed repeating earthquake activity from 1984 to 2011 along the entire Japan Trench and found that the interplate slip rates estimated from the repeating earthquake change with periods of 1–6 years. The periodic slip rate changes inferred from repeating earthquakes were widespread in the Japan Trench. They were also suggested by temporal changes in spatial gradients of the surface displacement rate field (Iinuma 2018). Furthermore, Uchida et al. (2016) showed that the occurrence rate of M_j 5 or greater earthquakes was positively correlated with the interplate slip rate. Based on these observations, Uchida et al. (2016) suggested that periodic SSEs widespread in the Japan Trench had stressed the surrounding regions and triggered M_j 5 or greater earthquakes.

Uchida et al. (2016) identified the northern part (39–40.4° N) of the Japan Trench (the black squares in Fig. 7a) as an area of pronounced 3-year periodicity. In and near this region, a repeating earthquake analysis by Uchida et al. (2004) also suggested SSEs preceding the 1989 M_w 7.4, 1992 M_w 6.9, and 1994 M_w 7.7 Sanriku-Oki earthquakes (Sect. 3.1.1). Furthermore, the far offshore region of the pronounced 3-year periodicity significantly overlaps with an area where SSEs triggered by earthquakes were geodetically observed in 1992 (Kawasaki et al. 1995; Kawasaki et al. 2001; Sect. 3.1.1; the blue dashed square in Fig. 1) and 2015 (Honsho et al. 2019; Fujiwara et al. 2022; Sect. 3.2.2; the blue dashed square in Fig. 6a). Uchida et al. (2016) probably captured the recurrence of these SSEs. In fact, the 1992 event (i.e., the 1992 Sanriku-Oki ultraslow earthquake) (Kawasaki et al. 1995, 2001) corresponds with a peak of the periodic interplate slip rate in Uchida et al. (2016).

In the Japan Trench, there have been a number of attempts to infer the occurrence of SSEs from earthquake swarm activity (Marsan et al. 2013; Nishikawa and Ide 2017, 2018; Nishikawa et al. 2019) and activity of swarms of foreshocks (i.e., earthquake swarms followed by megathrust earthquakes) (Matsumura 2010; Kato et al. 2012; Maeda and Hirose 2016; Nishikawa and Ide 2018; Kubo and Nishikawa 2020; Hirose et al. 2021).

Nishikawa and Ide (2018) considered increases in the seismicity rate that do not obey the Omori–Utsu's aftershock law (Utsu 1957; Utsu et al. 1995; Sect. 2.3) as earthquake swarms and detected such seismicity rate increases in the central and southern Japan Trench using a statistical seismicity model called the epidemic-type aftershock-sequence (ETAS) model (e.g., Ogata 1988; Zhuang et al. 2002). The ETAS model usually expresses the seismicity rate as the summation of a constant background seismicity rate and aftershock rates derived from Omori–Utsu's aftershock law. Therefore, increases in the seismicity rate that do not obey the Omori–Utsu's aftershock law appear as anomalous increases in the seismicity rate in the ETAS model analysis (e.g., Llenos et al. 2009; Okutani and Ide 2011). As shown in Fig. 7, $M_j \geq 3$ earthquake swarms frequently occur in the southern Japan Trench. Furthermore, Nishikawa and Ide (2018) found that earthquake swarms including repeating earthquakes had repeatedly occurred in a region around 36.2° N, 142° E (Fig. 7a). The earthquake swarm activity was the most active during the weeks prior to the 1982 and 2008 M_j 7 Ibaraki-Oki earthquakes (Matsumura 2010; Nishikawa and Ide 2018), which ruptured the plate interface downdip of the recurrent earthquake swarms. Nishikawa and Ide (2018) inferred from these observations that SSEs recur in the region around 36.2° N, 142° E and that the SSEs preceding the M_j 7 Ibaraki-Oki earthquakes were possibly aseismic slip acceleration in the nucleation phase of the Ibaraki-Oki earthquakes (e.g., Dieteich, 1992; Ohnaka 1992; McLaskey 2019). Recently, seismic slow earthquakes (i.e., tectonic tremors and VLFEs) were observed in the region around 36.2° N, 142° E (Nishikawa et al. 2019; Baba et al. 2020; Fig. 6a). The coincidence of a short-term SSE, burst of tectonic tremors, and earthquake swarms was also observed in July and August of 2021 in the same region (Fig. 5h). These recent observations are consistent with the inference made by Nishikawa and Ide (2018).

Maeda and Hirose (2016) and Hirose et al. (2021) systematically surveyed foreshock activity (M_j 5 or greater) of $M_j \geq 6$ earthquakes in the Japan Trench from 1961 to 2010. They identified areas of pronounced foreshock activity far offshore in the Japan Trench (the orange shaded areas in Fig. 7a). In these areas, 38% of the $M_j \geq 6$ mainshock earthquakes were preceded by a swarm of foreshocks (three or more $M_j \geq 5$ earthquakes within 10 days before the mainshock) (Maeda and Hirose 2016). These foreshock-prone areas are close to areas where

tectonic tremors and VLFEs occur (Figs. 6a and 7a). Furthermore, Hirose et al. (2021) showed that the occurrence rate of foreshock activity increases as it approaches the time of mainshock occurrence and that this foreshock rate acceleration cannot be fully reproduced by the ETAS model (Ogata 1988; Zhuang et al. 2002), which describes the earthquake-to-earthquake triggering. These results suggest that the foreshock activity in the Japan Trench cannot be explained by earthquake-to-earthquake triggering and that transient aseismic phenomena such as slow earthquakes may be involved in the triggering of the foreshocks. Moreover, Hirose et al. (2021) found that foreshock activity in the northern Japan Trench had been synchronized with the 3-year periodic SSEs reported by Uchida et al. (2016) (the far offshore black square in Fig. 7a) and suggested that the periodic SSEs had excited the foreshock activity.

Although repeating earthquakes and earthquake swarms have been used to infer the occurrence of SSEs in the Japan Trench (e.g., Kato et al. 2012; Marsan et al. 2013; Uchida et al. 2016; Nishikawa and Ide 2018), they have hardly ever been compared with independently observed SSEs or VLFEs in the Japan Trench. Here, we compared the catalogs of small repeating earthquakes (Uchida and Matsuzawa 2013; Nishikawa et al. 2019), $M_j \geq 3$ earthquake swarms (Nishikawa and Ide 2018; Nishikawa et al. 2019), SSEs (Nishimura 2021), and VLFEs (Baba et al. 2020). In Fig. 8a and b, we counted repeating earthquakes and earthquake swarm events around SSE fault models (inside the rectangular faults or within 20 km of the fault models) within 80 days before or after the central dates of the SSE occurrence periods. Here, we excluded SSEs associated with $M_w \geq 5.8$ fast earthquakes (Nishimura 2021) because not SSEs but afterslip following the $M_w \geq 5.8$ earthquakes may have triggered repeating earthquakes and earthquake swarms.

Figure 8a and b shows that the counts of repeating earthquakes and earthquake swarm events have a maximum within 10 days before or after the central dates of the SSE occurrence periods. This is consistent with the idea that SSEs trigger repeating and earthquake swarms in their vicinities (e.g., Kato et al. 2012; Marsan et al. 2013; Uchida et al. 2016; Nishikawa and Ide 2018). However, with respect to earthquake swarms, the sample size (18 earthquake swarm events) was too small to make a statistical argument. As for repeating earthquakes, the tendency that repeating earthquakes are more likely to occur within 10 days before or after the SSE central dates than in the other periods is statistically significant ($p = 1\%$). Here, we conducted a statistical test with a null hypothesis that repeating earthquakes are equally likely to occur on the dates within 80 days before or after the SSE central dates and used a significance level of 5%. However, in Fig. 8a, the repeating earthquakes also occurred on days not close to the central dates of the SSEs. This is probably because repeating earthquakes are triggered by not only SSEs but also interplate steady slip (e.g., Nadeau and Johnson 1998; Nadeau and McEvilly 1999; Matsuzawa et al. 2002; Igarashi et al. 2003). Furthermore, as mentioned in Sect. 3.2.2, the incompleteness of the SSE catalog near the trench axis may have affected the results in Fig. 8a and b.

Figure 8c shows the spatial distribution of coincident events of earthquake swarms and SSEs or earthquake swarms and VLFEs. From January 1995 to March 2011, we observed six coincident events of earthquake swarms and SSEs and nine coincident events of earthquake swarms and VLFEs (Fig. 7b). Here, if an earthquake swarm event occurs within 2 weeks before or after an SSE period inside the SSE rectangular fault or within 20 km of the fault, we regard it as a coincident event. Similarly, if an earthquake swarm event occurs within 2 weeks before or after a VLFE within 40 km of the VLFE epicenter, we regard it as a coincident event. Small repeating earthquakes included in earthquake swarm activity are indicated by colored stars in Fig. 8c. We found that the coincident events had repeatedly occurred at the same locations (Fig. 8c). Specifically, they recurred in regions around 36.3° N, 142.5° E, 36.2° N, 142.0° E, and 35.1° N, 141.4° E. The region around 36.3° N, 142.5° E corresponds with the area where Obana et al. (2021) observed coinciding events of tectonic tremors and swarms of interplate microearthquakes in March and June of 2017 (Sect. 3.1.2). Furthermore, in the region around 36.2° N, 142.0° E, the coincidence of a short-term SSE, burst of tectonic tremors, and an interplate earthquake swarm was also observed in July and August of 2021 (Fig. 5h). These observations imply that coincident events of slow and fast earthquakes are common on the shallow plate interface of the southern Japan Trench.

3.3 Experimental studies on slow earthquakes in the Japan Trench

Experimental studies on slow earthquakes in the Japan Trench have been focused on the slip behavior of the shallow plate interface (Ikari et al. 2015; Ito and Ikari 2015; Ito et al. 2017; Ikari and Kopf 2017; Sawai et al. 2017). These studies were motivated by the observational findings that an SSE preceding the Tohoku-Oki earthquake occurred on the shallow plate interface of the central Japan Trench and that the shallow plate interface subsequently underwent a huge coseismic slip breaching the trench axis (Kato et al. 2012; Ito et al. 2013). Before the 2011 Tohoku-Oki earthquake, the shallow subduction plate interface was thought to exclusively host aseismic creep (e.g., Nishizawa et al. 1992; Ikari et al. 2015).

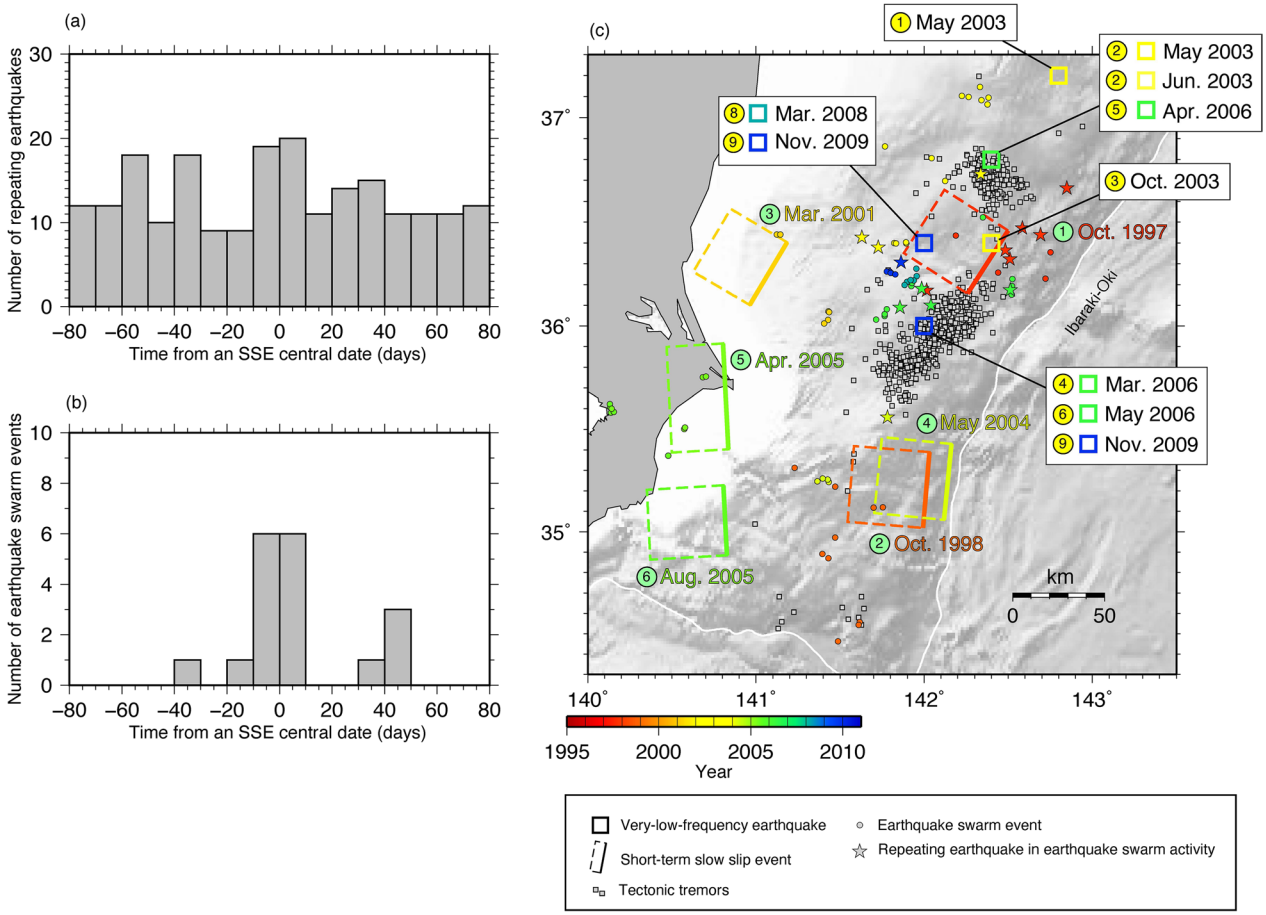

Fig. 8 Coinciding events of repeating earthquakes, earthquake swarms, and slow earthquakes in the southern Japan Trench. **a** and **b** Histograms of the occurrence times of repeating earthquakes and earthquake swarm events, respectively, relative to an SSE central date. These repeating earthquakes and earthquake swarm events occurred inside the SSE fault models or within 20 km of the fault models. **c** Epicenters of the coincident events. The coincident events of earthquake swarms and SSEs are indicated by numbers 1–6 in green, as in Fig. 7b. The coinciding events of earthquake swarms and VLFEs are indicated by numbers 1–9 in yellow, as in Fig. 7b. The VLFEs are from Baba et al. (2020). Note that the VLFEs sometimes have identical epicenters because they were detected using a matched filter technique (Baba et al. 2020). The short-term SSEs are from Nishimura (2021). Tectonic tremors are from Nishikawa et al. (2019) and this study. Repeating earthquakes are based on Uchida and Matsuzawa (2013). The earthquake swarms are from Nishikawa and Ide (2018) and Nishikawa et al. (2019). The VLFEs, SSEs, earthquake swarm events, and repeating earthquakes are colored according to their occurrence time

This is consistent with the standard model of the megathrust slip behavior at that time (Scholz 1998), in which the shallowest part of the plate interface is characterized by rate-strengthening behavior and stable sliding. However, this view was challenged by the aforementioned observations implying the unstable nature of the shallow plate interface. With this background, the above experimental studies reconsidered the frictional behavior of the shallow plate interface using core samples from the shallow plate boundary of the Japan Trench.

Ikari et al. (2015) conducted an experiment in which a core sample retrieved from the shallow plate boundary fault zone (~7 km landward of the trench axis and 822 m below sea floor) by the Japan Trench Fast Drilling Project (JFAST) (Chester et al. 2013) was sheared at a rate comparable to the plate convergence rate (8.5 cm/year). They found that the clay-rich sample exhibited rate-weakening behavior, which is suitable for coseismic rupture propagation, and observed spontaneous slow strength perturbations similar to SSEs. Ikari et al. (2015) proposed that these experimental results explain both the preseismic SSE and coseismic rupture of the Tohoku-Oki earthquake. Furthermore, Ikari and Kopf (2017) showed that weak clay-rich fault samples from shallow parts of several subduction zones also exhibit rate-weakening behavior and produce slow strength perturbations when sheared at

a rate comparable to plate velocities. They suggested that the observed unstable nature of the shallow fault zone materials may facilitate the propagation of coseismic rupture and slip at shallow depths in subduction zones.

Ito et al. (2017) also used a core sample retrieved by JFAST and showed that an increase in the slip rate can induce a change from slip-strengthening friction to slip-weakening friction. They found that velocity steps with initial slip rates consistent with afterslip following the largest (M_w 7.3) foreshock of the Tohoku-Oki earthquake exhibit significant slip weakening. Based on this experiment, they suggested that the accelerated interplate aseismic slip due to the afterslip following the largest foreshock (Ando and Imanishi 2011; Kato et al. 2012; Ohta et al. 2012; Sect. 3.1.2) might have been a favorable initial condition for the huge coseismic slip of the Tohoku-Oki earthquake.

3.4 Numerical simulations on slow earthquakes in the Japan Trench

There are several simulation studies that consider slow earthquakes (especially SSEs) in the Japan Trench (Mitsui et al. 2012; Ohtani et al. 2014; Shibazaki et al. 2019; Barbot 2020; Nakata et al. 2021). These are earthquake cycle simulations based on rate-and-state-dependent friction (Dieterich 1979; Sect. 2.4). Some studies reproduced SSEs in the Japan Trench by assuming large characteristic slip distances (Ohtani et al. 2014; Nakata et al. 2021; Sect. 2.4), and others reproduced the SSEs by assuming friction that exhibits rate-weakening behavior at low slip rates but switches to rate-strengthening behavior at high slip rates (Shibazaki et al. 2019; Sect. 2.4).

Ohtani et al. (2014) assumed that regions outside asperities show rate-weakening behavior but have a large characteristic slip distance. Asperities here mean large slip areas of past megathrust earthquakes (Yamanaka and Kikuchi 2004), as described in Sect. 3.1.1. Ohtani et al. (2014) found that recurrent SSEs occur on the shallow plate interface in the southern Japan Trench and pointed out that these SSEs might correspond to a decrease in the interplate coupling in the southern part (~ 37° N) of the Japan Trench prior to the 2011 Tohoku-Oki earthquake detected by GNSS observations (Geospatial Information Authority of Japan GSI 2011). Shibazaki et al. (2019) assumed that the shallow plate interface near the trench axis has a frictional property that exhibits rate-weakening behavior at low slip rates but switches to rate-strengthening behavior at high slip rates. Their model reproduced the preseismic SSE, the largest foreshock, and coseismic rupture of the Tohoku-Oki earthquake, although the location of the simulated SSE (the shallow part of the northern Japan Trench) was different from that of the observed SSE (the shallow part of the central Japan Trench) (Ito et al. 2013).

No previous simulation studies have reproduced or considered the complex slow earthquake distribution along the Japan Trench (Figs. 5 and 6). However, Nakata et al. (2021) attempted to reproduce along-strike changes in the slip behavior of the Japan Trench. They assumed rate-weakening behavior with a large characteristic slip distance in the southern and northern Japan Trench and rate-weakening behavior with a small characteristic slip distance in the central Japan Trench, considering the along-strike distribution of interplate sedimentary units revealed by multichannel seismic reflection surveys (Tsuru et al. 2002; Sect. 5.1.1). They reproduced the coseismic rupture of the Tohoku-Oki earthquake in the central Japan Trench (e.g., Ide et al. 2011; Iinuma et al. 2012; Lay 2018) and the large afterslip in the shallow part of the southern Japan Trench (Uchida and Matsuzawa 2013; Sun and Wang 2015; Iinuma et al. 2016; Tomita et al. 2017; Honsho et al. 2019; Tomita et al. 2020; Watanabe et al. 2021; the blue contours in Fig. 6a). The simulation results of Nakata et al. (2021) also show that transient slow fault slips repeatedly occur in the southern Japan Trench during interseismic periods. These transient aseismic slips might correspond to the slow earthquakes observed in the southern Japan Trench (Nishikawa et al. 2019; Baba et al. 2020; Nishimura 2021; Figs. 5 and 6), although the characteristic time scale of the transient slips (tens of years) and that of the observed SSEs (tens of days) are different.

4 Comparison of the slow earthquake distribution along the Japan Trench with the distribution of other fault slip phenomena

4.1 Coseismic slip, afterslip, and interseismic interplate coupling of the M_w 9.0 Tohoku-Oki earthquake

As already described in Sect. 3.2.1, the approximately 200-km-long along-strike gap of tectonic tremors in the central Japan Trench corresponds to the region ruptured by the Tohoku-Oki earthquake (Figs. 5a and 6). In other words, the tremor-genic regions in the southern and northern Japan Trench did not slip significantly during the Tohoku-Oki earthquake (Figs. 5a and 6). The huge coseismic slip in the central Japan Trench and the rupture termination in the southern and northern Japan Trench are features common to most coseismic slip models of the Tohoku-Oki earthquake (e.g., Ide et al. 2011; Simons et al. 2011; Iinuma et al. 2012). For more details on the coseismic rupture characteristics of the Tohoku-Oki earthquake, refer to a review paper by Lay (2018).

The northern and southern Japan Trench experienced afterslip following the Tohoku-Oki earthquake. The afterslip on the shallow plate interface has been suggested by

GNSS-acoustic observations and repeating earthquake analyses in both the regions (Uchida and Matsuzawa 2013; Sun and Wang 2015; Iinuma et al. 2016; Tomita et al. 2017; Honsho et al. 2019; Tomita et al. 2020; Watanabe et al. 2021; blue contours in Fig. 6a). The VLFE occurrence rates in the shallow parts of these two regions also sharply increased after the Tohoku-Oki earthquake (Matsuzawa et al. 2015; Baba et al. 2020). A similar correspondence between VLFEs and afterslip following the 2003 M_w 8.0 Tokachi-Oki earthquake has been reported in the southern end of the Kurile Trench (Miyazaki et al. 2004; Asano et al. 2008; Uchida et al. 2009b; Itoh et al. 2019; Baba et al. 2020). Simons et al. (2011) point out that the area near the trench axis of the southern Japan Trench (around 36–37° N, 142.5° E) is a gap of megathrust earthquakes and a region of possible high seismic hazard. However, the large afterslip of the Tohoku-Oki earthquake (Uchida and Matsuzawa 2013; Sun and Wang 2015; Iinuma et al. 2016; Tomita et al. 2017, 2020; Honsho et al. 2019; Watanabe et al. 2021) and the numerous slow earthquakes (i.e., tectonic tremors, VLFEs, and short-term SSEs) (Matsuzawa et al. 2015; Nishikawa et al. 2019; Baba et al. 2020; Nishimura 2021) imply that the accumulated elastic strain in this area has so far been released aseismically.

The spatial distribution of VLFEs before the 2011 Tohoku-Oki earthquake (Matsuzawa et al. 2015; Baba et al. 2020) corresponds well with the spatial distribution of tectonic tremors after the Tohoku-Oki earthquake (Fig. 6). Given the related physical origin of tectonic tremors and VLFEs (Kaneko et al. 2018; Masuda et al. 2020; Sect. 2.2.2), this observation suggests that there was no significant change in the distribution of seismic slow earthquakes (tectonic tremors and VLFEs) before and after the Tohoku-Oki earthquake. Even before the Tohoku-Oki earthquake, a 200-km-long gap of seismic slow earthquakes existed in the central Japan Trench. As already mentioned in Sect. 3.2.2, this gap corresponds well with the huge interplate locked zone revealed by the GNSS observations before the Tohoku-Oki earthquake (Ito et al. 2000; Nishimura et al. 2000; Nishimura et al. 2004; Suwa et al. 2006; Hashimoto et al. 2009; Loveless and Meade 2010; the red shaded area in Fig. 6a). However, we note that these studies could not resolve the slip deficit near the trench axis due to the limited offshore resolution of onshore GNSS stations. The slip deficit near the trench axis is substantially affected by model assumptions. Some assumed complete interplate decoupling at the trench axis (e.g., Suwa et al. 2006), and others assumed complete coupling (Wallace et al. 2009). Lindsey et al. (2021) recently proposed a new method for estimating interplate coupling that assumes nonnegative shear stress accumulation rates on the plate interface during an interseismic period, to improve the offshore resolution. The application of this new method to the Japan Trench (Lindsey et al. 2021) suggested that the region near the trench axis in the central Japan Trench had been almost completely coupled before the 2011 Tohoku-Oki earthquake, while the shallow parts of the northern and southern Japan Trench had been partially coupled. This coupling distribution corresponds well with the spatial distribution of VLFEs before the 2011 Tohoku-Oki earthquake (Matsuzawa et al. 2015; Baba et al. 2020; Fig. 6a).

It is still not clear whether the spatial complementarity between M_w 9 class megathrust coseismic rupture and seismic slow earthquakes (Fig. 6a) is true only for the 2011 Tohoku-Oki earthquake or also for past and future M_w 9 class earthquakes in the Japan Trench. However, Ikehara et al. (2016) examined thick turbidite units in sediment cores collected at the trench axis and suggested that the shallow part of the central Japan Trench had repeatedly experienced huge earthquakes similar to the 2011 Tohoku-Oki earthquake (i.e., the 1454 Kyotoku and 869 Jogan earthquakes). Furthermore, the thick turbidite units related to the 2011 Tohoku-Oki, 1454 Kyotoku, and 869 Jogan earthquakes (Ikehara et al. 2016) were observed only in the central Japan Trench (Ikehara et al. 2018), corresponding well with the observed distribution of slip to the trench during the 2011 Tohoku-Oki earthquake (Kodaira et al. 2020, 2021). In other words, in the northern and southern Japan Trench, they found no evidence implying a slip to the trench during the 1454 Kyotoku and 869 Jogan earthquakes. Therefore, slip-to-the-trench events (i.e., *Mw* 9 class earthquakes breaching the trench axis) might be characteristic of the central Japan Trench (Kodaira et al. 2020), and the spatial complementarity between M_w 9 class megathrust coseismic rupture and seismic slow earthquakes might be true for past M_w 9 class earthquakes in the Japan Trench.

4.2 Large and small interplate earthquakes

Figure 9 shows asperities (i.e., areas where the amount of slip is half the maximum slip or larger) of M_w 7–8 class interplate earthquakes in the Japan Trench from 1936 (Nagai et al. 2001; Murotani et al. 2003; Yamanaka and Kikuchi 2004; Earthquake Research Center 2005; Mochizuki et al. 2008; Research Center for Seismology, Volcanology, and Disaster Mitigation 2008; Ohta et al. 2012, Kubo et al. 2013; Kubo and Nishikawa 2020; Sect. 3.1.1).

The asperities of M_w 7–8 class interplate earthquakes (red contours in Fig. 9) are complementary to the slow earthquake distribution in the entire Japan Trench (green symbols in Fig. 9). The asperities are mainly distributed at 20–40 km depth, whereas slow earthquakes avoid this depth range. The Tohoku-Oki earthquake is the only instrumentally recorded megathrust earthquake that

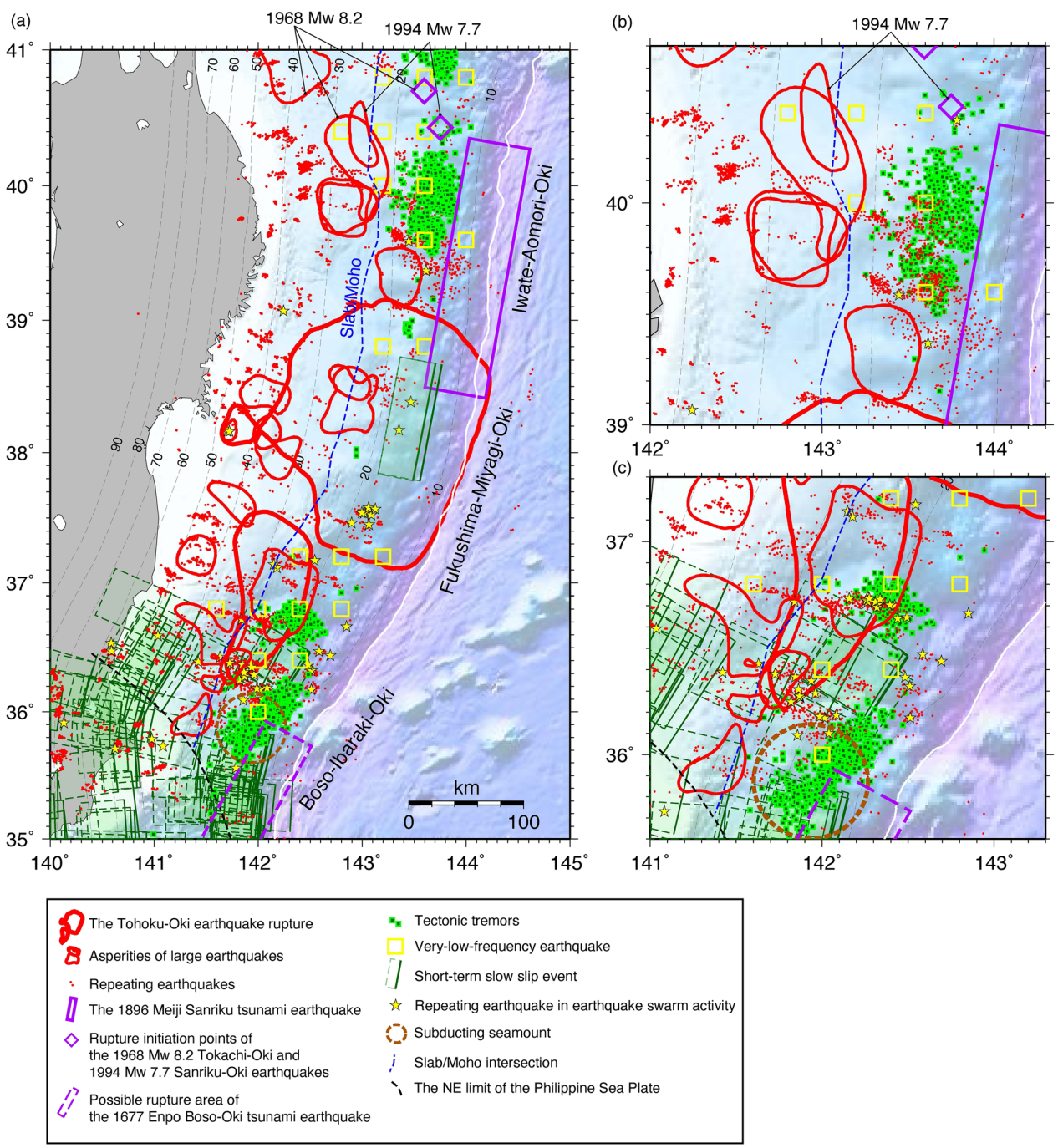

Fig. 9 Comparison between megathrust asperities and the slow earthquake distribution in the Japan Trench. **a** Megathrust asperities and epicenters of the slow earthquakes. **b** and **c** Enlarged views of the northern and southern Japan Trench, respectively. For an explanation of the symbols, refer to the legend in the figure. The megathrust asperities are from Nagai et al. (2001), Murotani et al. (2003), Yamanaka and Kikuchi (2004), Earthquake Research Center (2005), Mochizuki et al. (2008), Research Center for Seismology, Volcanology, and Disaster Mitigation (2008), Ohta et al. (2012), Kubo et al. (2013), and Kubo and Nishikawa (2020). The slip distribution of the March 11, 2011, Tohoku-Oki earthquake and the 1896 Meiji Sanriku tsunami earthquake is from Iinuma et al. (2012) and Tanioka and Seno (2001), respectively. The rupture initiation points of the 1968 M_w 8.2 Tokachi-Oki and 1994 M_w 7.7 Sanriku-Oki earthquakes are from the JMA catalog. The possible rupture area of the 1677 Enpo Boso-Oki tsunami earthquake is based on the Japan Society of Civil Engineers (2002). Small repeating earthquakes are from Uchida and Matsuzawa (2013). Repeating earthquakes included in earthquake swarms are based on Nishikawa and Ide (2018) and Nishikawa et al. (2019). Tectonic tremors are from Nishikawa et al. (2019) and this study. The VLFEs are from Baba et al. (2020). Short-term SSEs are from Ito et al. (2013), Nishimura (2021), and this study. The location of the subducting seamount in the southern Japan Trench is based on Mochizuki et al. (2008). The northeastern limit of the Philippine Sea Plate is from Uchida et al. (2009a). The intersection of slab and upper-plate Moho is based on Bassett et al. (2016)

significantly ruptured the shallow slow-earthquake-genic region (10–20 km depth) in the central Japan Trench (Fig. 9a). Nishimura (2021) pointed out that short-term SSEs in the southern Japan Trench predominantly occur at depths of 10–30 km and greater than 40 km, avoiding the source depths of large interplate earthquakes (30–40 km) (Fig. 9a and c). The complementarity between large coseismic slip areas and shallow slow earthquakes has also been observed at the southern end of the Kuril Trench (north of 41° N) (Asano et al. 2008; Baba et al. 2020). No instrumentally recorded megathrust earthquakes are known to have significantly ruptured the shallow slow-earthquake-genic region (10–20 km depth) at the southern end of the Kuril Trench (Fig. 5a), although the M_w 9 class megathrust earthquake in the seventeenth century, which was identified by tsunami deposits (Nanayama et al. 2003), might have ruptured the shallow slow-earthquake-genic region (Satake et al. 2008; Ioki and Tanioka 2016).

In contrast to large interplate earthquakes, we observed no clear complementarity between small interplate earthquakes and slow earthquakes in the dip direction. The red dots in Fig. 9 show the distribution of small repeating earthquakes on the plate interface (mostly from M_j 2.5–4.5) (Uchida and Matsuzawa 2013). Repeating earthquakes are located at 10–60 km depth in the northern and central Japan Trench. In the southern Japan Trench, they occur at depths ranging from 10–80 km. Note that the upper plate of the deeper part of the southern Japan Trench is the subducting Philippine Sea Plate (Uchida et al. 2009a, b) and not a typical mantle wedge. The subducting Philippine Sea Plate is thought to lower the temperature of the upper surface of the Pacific Plate (Hasegawa et al. 2007) and allow small interplate earthquakes to occur at greater depths in the southern Japan Trench (Nakajima et al. 2009). As shown in Fig. 9, the source depths of the repeating earthquakes significantly overlap those of the slow earthquakes (i.e., 10–30 km and 40 km depth or deeper). These observations indicate that in contrast to large interplate earthquakes of M_w 7–8, small interplate earthquakes and slow earthquakes (i.e., tectonic tremors, VLFEs, and short-term SSEs) can occur under similar pressure–temperature conditions. Furthermore, these observations are slightly incompatible with the widely accepted view that slow earthquakes are intermediate-type fault slips that are transitional between fast earthquakes and stable sliding, with the transition proceeding predominantly in the dip direction (Obara and Kato 2016).

In addition, we note that some of the repeating earthquakes in Fig. 9 (red dots) occurred during periods of earthquake swarm activity (yellow stars). As described in Sect. 2.3, they were potentially triggered by slow earthquakes (Nishikawa and Ide 2018; Nishikawa et al. 2019). Consistent with this idea, they are mainly concentrated in the shallow part of the Japan Trench and located near the source regions of shallow slow earthquakes (i.e., tectonic tremors, VLFEs, and short-term SSEs) (Fig. 9b and c), while the whole of the repeating earthquakes is more widely distributed along the plate interface.

4.3 Tsunami earthquakes

Interplate earthquakes that generate huge tsunamis despite weak ground motions are called tsunami earthquakes. Tsunami earthquakes are considered to be fault slip events with a longer duration than regular earthquakes of comparable seismic moment (Kanamori 1972). They occur on the plate interface near the trench axis (e.g., Kanamori 1972; Ide et al. 1993; Kanamori and Kikuchi 1993). Soft subducted sediments on the shallow plate interface are thought to cause their rupture processes to be slower than those of regular earthquakes (Kanamori and Kikuchi 1993; Tanioka and Sataka 1996).

In 1896, the M_w 8.0 Meiji Sanriku tsunami earthquake occurred in the northern Japan Trench (Kanamori 1972; Tanioka and Sataka 1996; Tanioka and Seno 2001; the open purple rectangle in Fig. 9a and b). The earthquake is considered to have ruptured the very shallow plate interface of the northern Japan Trench. The source region is close to and slightly shallower than the shallow tremor-genic region (approximately 10–20 km depth) in the northern Japan Trench (Fig. 9b). According to a fault slip model inverted from tsunami waveform data of the 2011 Tohoku-Oki earthquake (Satake et al. 2013), this shallow plate interface of the northern Japan Trench slipped again during the 2011 Tohoku-Oki earthquake, and the slip amount reached up to 36 m. However, bathymetry observations (Fujiwara et al. 2017) have not found evidence of such a large slip breaching the trench axis in the northern Japan Trench.

Besides the 1896 Meiji Sanriku tsunami earthquake, many large interplate earthquakes have repeatedly occurred in the northern Japan Trench (Yamanaka and Kikuchi 2004; red contours in Fig. 9b). Among them, the 1994 M_w 7.7 Sanriku-Oki earthquake is known to have started its coseismic rupture like a tsunami earthquake (Nakayama and Takeo 1997). The epicenter of this earthquake was located at 40.43° N and 143.75° E, close to the shallow tremor-genic region (an open purple diamond in Fig. 9a and b). After the rupture initiation, the coseismic rupture propagated downdip toward the west (landward) at a slow speed of approximately 1.8 km/s. To the west of 143°E, the rupture propagated at a speed of 3.0 km/s. A similar slow rupture (1.1–1.5 km/s) was also observed during the 1992 M_w 7.6 Nicaragua tsunami earthquake (Ide et al. 1993; Kanamori and Kikuchi 1993).

Tsunami earthquakes may also have occurred close to the shallow slow-earthquake-genic region of the southern Japan Trench (Fig. 9c). The 1677 Enpo Boso-Oki earthquake is considered a tsunami earthquake because of its huge tsunami and weak ground shaking (the dashed purple rectangle in Fig. 9a and c). From historical documents and tsunami deposits, Yanagisawa et al. (2016) estimated a slip model for this earthquake. They suggested that the earthquake may have ruptured the area near the trench axis of the southern Japan Trench (mainly south of 36° N) and caused a fault slip of 11–16 m.

In the central Japan Trench, a typical tsunami earthquake has not been observed. However, Ide et al. (2011) pointed out that the shallow rupture of the Tohoku-Oki earthquake in the central Japan Trench had only weakly radiated high-frequency seismic waves despite the prodigious slip amount (tens of meters) and resembled tsunami earthquakes.

In summary, the tsunami earthquakes in the Japan Trench ruptured the plate interface close to the shallow slow-earthquake-genic regions (Fig. 9). They are characterized by a duration longer than and a rupture propagation speed slower than regular earthquakes (e.g., Kanamori 1972; Nakayama and Takeo 1997; Ide et al. 2011), which is probably caused by soft subducted sediments on the shallow plate interface (Kanamori and Kikuchi 1993; Tanioka and Satake, 1996). These rupture characteristics of tsunami earthquakes are qualitatively similar to those of slow earthquakes. However, the rupture speed of tsunami earthquakes, which is roughly 50% slower than fast regular earthquakes (Ide et al. 1993; Kanamori and Kikuchi 1993; Nakayama and Takeo 1997), is approximately four orders of magnitude faster than the typical rupture propagation speed (10 km/day) of short-term SSEs (e.g., Dragert et al. 2001). This indicates that tsunami earthquakes and slow earthquakes are quantitatively very different phenomena, although they are both slow compared to fast, regular earthquakes. The difference is also evident in their moment–duration scaling relations (Fig. 3a).

4.4 Seismicity parameters

The Japan Trench has a high interplate seismicity rate compared to the Nankai Trough and Cascadia subduction zone (Ide 2013), and the characteristics of the interplate seismicity have been studied vigorously. In this section, we compare the slow earthquake distribution with the spatial distributions of parameters characterizing seismicity. Here, we selected the Gutenberg–Richter relationship's b value (Nanjo et al. 2012; Tormann et al. 2015), tidal response of seismicity (Tanaka 2012), and p value of the Omori–Utsu's aftershock law (Ogata 2011; Ueda 2021). These parameters showed a good correspondence with the slow earthquake distribution.

4.4.1 *Gutenberg–Richter relationship's b value and tidal response of seismicity*

Spatiotemporal variations of the Gutenberg–Richter relationship's b value (Nanjo et al. 2012; Tormann et al. 2015) and tidal response of seismicity (Tanaka 2012) in the Japan Trench have been investigated in detail (Fig. 10a and b). The b value is the power exponent of the magnitude–frequency distribution of earthquakes (Guternberg and Richter 1944). It reflects the relative number of small earthquakes compared to large ones. A low b value indicates relatively frequent large earthquakes. According to Nanjo et al. (2012) and Tormann et al. (2015), the b value inside the source region of the March 2011 Tohoku-Oki earthquake gradually decreased from around 2005 until the occurrence of the earthquake. The decrease in the b value in the central Japan Trench may reflect an increase in the differential stress in the locked region prior to the Tohoku-Oki earthquake because rock experiments (e.g., Scholz 1968; Goebel et al. 2013) and natural earthquake observations (e.g., Schorlemmer et al. 2005; Spada et al. 2013; Nishikawa and Ide 2014; Scholz 2015; Petruccelli et al. 2019) suggest that the b value is negatively correlated with differential stress in the crust.

Note that the b value also depends on the focal mechanisms of sampled earthquakes, with thrust faults being characterized by lower b values than normal and strike faults (e.g., Schorlemmer et al. 2005; Bürgmann et al. 2016). The decade-scale decrease in the b value might have been affected by a temporal change in the fraction of the faulting types of the earthquakes sampled by Nanjo et al. (2012) and Tormann et al. (2015) because their analyses included small earthquakes whose faulting types were unclear. One should be careful when interpreting spatiotemporal changes in the b value because the fraction of the faulting types can vary in space and time in the Japan Trench (Nakamura et al. 2016). However, the b value changes due to the faulting types are only about 0.2 even in very extreme cases (e.g., 100% thrust to 100% normal faulting) (Bürgmann et al. 2016) and realistically would be about 0.1 or less, considering the observed temporal changes in the faulting types prior to the Tohoku-Oki earthquake (Bürgmann et al. 2016). Therefore, it is unlikely that the decade-scale decrease in the b value (~ 0.4) was solely due to the temporal change in the fraction of the faulting types.

In Fig. 10a, we compared the slow earthquake distribution with the spatial distribution of the b value prior to the Tohoku-Oki earthquake estimated by Tormann et al. (2015) (January 1, 2004, to March 11, 2011). Tectonic tremors and VLFEs are predominantly distributed

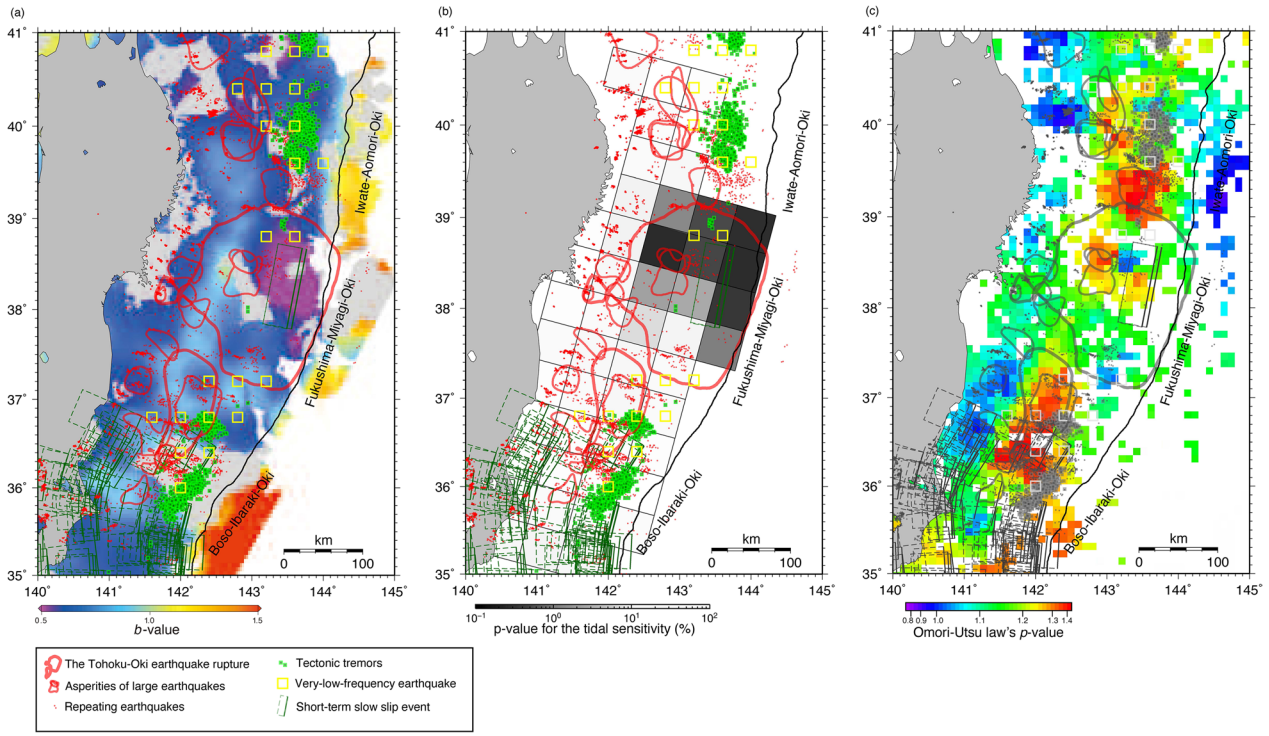

Fig. 10 Comparison between spatial distributions of seismicity parameters and the slow earthquake distribution in the Japan Trench. **a** Gutenberg–Richter relationship's *b* value (Tormann et al. 2015). The *b* values were estimated from January 1, 2004, to March 11, 2011. In gray areas, Tormann et al. (2015) did not estimate *b* values because the magnitude–frequency distributions of the areas were not well described by the Gutenberg–Richter relationship. **b** Tidal response of seismicity (Tanaka 2012). *p* values of Schuster's test during the 3000 days prior to the Tohoku-Oki earthquake are shown. A low *p* value indicates a high tidal response. The *p* values were calculated for seismicity in spatial windows of 200 km × 200 km, whose centers correspond with the centers of the squares of 50 km × 50 km in the figure (the black squares). **c** *p* value of the Omori–Utsu's aftershock law (Ogata 2011). The *p* values were estimated using M_j 5 or greater earthquakes from 1926 to 2008. Note that the slow and fast earthquakes are colored gray in (**c**). For an explanation of the symbols, refer to the legend in the figure. The slow earthquakes, megathrust earthquakes, and small repeating earthquakes are from Fig. 9

outside the region of a particularly low *b* value ($b \leq 0.5$) in the central Japan Trench (the purple area in Fig. 10a), implying that the differential stress in the tremor-genic regions of the northern and southern Japan Trench was relatively low before the Tohoku-Oki earthquake. These observations are consistent with the frequent stress release due to slow earthquakes in the shallow parts of the northern and southern Japan Trench (Fig. 6). However, the SSE that occurred during the month prior to the Tohoku-Oki earthquake ruptured the very region where the *b* value was particularly low ($b \leq 0.5$) (Kato et al. 2012; Ito et al. 2013; a green rectangle within the Tohoku-Oki earthquake rupture in Fig. 10a). This observation implies that the preseismic SSE of the Tohoku-Oki earthquake ruptured the region where the differential stress at the plate boundary was high.

Tanaka (2012) compared the occurrence times of M_w 5 or greater earthquakes in the Japan Trench with tidally induced increases in shear stress. The amplitude of the shear stress perturbation was less than 1 kPa. Tanaka (2012) observed a significant correlation between the tidal stress and earthquake occurrence times from December 2002 to March 2011 in the central Japan Trench ($p = 0.34\%$). The region of high tidal response corresponds well with the region of a particularly low *b* value ($b \leq 0.5$) (Fig. 10a and b). Tanaka (2012) interpreted the high tidal response in the central Japan Trench to indicate that the source region of the Tohoku-Oki earthquake had been critically stressed prior to the Tohoku-Oki earthquake and was sensitive to the small stress perturbations induced by the tides. Figure 10b presents the comparison of the slow earthquake distribution and the spatial distribution of the tidal response prior to the Tohoku-Oki earthquake (December 2002–March 2011). Similar to the *b* value (Fig. 10a), tectonic tremors and VLFEs are mainly distributed outside the region of particularly high tidal response in the central Japan Trench. The SSE during the month prior to the Tohoku-Oki earthquake (Kato et al. 2012; Ito et al. 2013) ruptured the very region

where the tidal response was particularly high (a green rectangle within the Tohoku-Oki earthquake rupture in Fig. 10b).

In summary, the above comparisons of the b values, tidal response, and slow earthquake distribution imply that the SSE during the month prior to the March 2011 Tohoku-Oki earthquake ruptured the region where the differential stress or shear stress on the plate interface was increased and that seismic slow earthquakes (i.e., tectonic tremors and VLFEs) predominantly occurred outside that region both before and after the Tohoku-Oki earthquake (Nishikawa et al. 2019; Baba et al. 2020).

4.4.2 p value of the Omori–Utsu's aftershock law

The p value of the Omori–Utsu's aftershock law (Utsu 1957; Utsu et al. 1995) is the power exponent of the power-law decay of the aftershock occurrence rate; the larger the p value, the faster the aftershock rate decays. Ogata (2011) and Ueda (2021) used the hierarchical space–time ETAS (HIST-ETAS) model, a spatiotemporal statistical model describing earthquake-to-earthquake triggering, to investigate the spatial distribution of the p value of the Omori–Utsu's aftershock law in the Japan Trench. Figure 10c shows the comparison of the p value distribution with the slow earthquake distribution. The p value distribution was estimated using M_j 5 or greater earthquakes from 1926 to 2008 (Ogata 2011). Figure 10c shows that the p value is high (reddish areas) near the tremor-genic regions in the northern and southern Japan Trench ($p \geq 1.3$). That is, aftershock rates decay faster near the tremor-genic regions.

It is not straightforward to understand why the p value is high near the tremor-genic regions. Utsu et al. (1995) pointed out that aftershock rates of earthquakes within earthquake swarm activity tend to decay faster (i.e., a higher p value). Therefore, the high p value in the tremor-genic regions may indicate frequent earthquake swarms in these regions. Consistent with this idea, earthquake swarms ($M_j \geq 5$) have been repeatedly observed in these regions (Kawasaki et al. 1995, 2001; Matsumura 2010; Nishikawa and Ide 2018; Fig. 5h). Furthermore, earthquake swarms in subduction zones are considered to be potential indicators of short-term SSEs (e.g., Marsan et al. 2013; Nishikawa et al. 2019; Sect. 2.3), which are often accompanied by tectonic tremors. Based on the above reasoning, our idea may consistently explain the p value and slow earthquake distributions along the Japan Trench.

Moreover, as mentioned in Sect. 3.2.3, it is known that earthquake swarms cannot be well described within the usual framework of the ETAS model (e.g., Llenos et al. 2009; Okutani and Ide 2011). Therefore, areas that frequently experience earthquake swarms may appear as some kind of anomaly in the ETAS model analysis; the high p values ($p \geq 1.3$) in Fig. 10c might reflect such anomalies.

5 Crustal structure and geological environment of the slow-earthquake-genic regions in the Japan Trench

In this section, we present comparisons of the slow earthquake distribution in the Japan Trench with the crustal structure (Sect. 5.1). We also describe the geological environment of the slow-earthquake-genic regions, focusing on water sources, pressure–temperature conditions, and metamorphism (Sect. 5.2). Through these comparisons, we aim to gain insight into the factors governing the slow earthquake distribution in the Japan Trench.

5.1 Crustal structure of the slow-earthquake-genic regions

5.1.1 Interplate sedimentary units

Many previous studies have investigated the along-strike changes in the crustal structure of the Japan Trench in detail. Tsuru et al. (2002) investigated the distribution of interplate sedimentary units subducted in the Japan Trench by conducting multichannel seismic reflection surveys (Fig. 11). In the northern Japan Trench, a deformed wedge-shaped sedimentary unit is located updip (from the trench axis to approximately 10 km depth) of the tremor-genic regions (Fig. 11a and b). In contrast, in the southern Japan Trench, a channel-like sedimentary unit with a thickness of approximately 2 km extends to depths deeper than 15 km (Fig. 11a and d). Both the sedimentary units are characterized by low P-wave velocity (2–4 km/s) (see also Azuma et al. 2018). In the central Japan Trench, the shape of the sedimentary unit switches from wedge shape to channel-like shape (Fig. 11a and c), and the interplate sedimentary units of the Japan Trench change their shape on a scale of hundreds of kilometers along the strike direction of the plate interface.

Seismic slow earthquakes (i.e., tectonic tremors and VLFEs) are distributed in the northern and southern Japan Trench (Fig. 11a), with an approximately 200-km-long along-strike gap of seismic slow earthquakes in the central Japan Trench. This along-strike change appears to correspond to the along-strike change in the shape of the interplate sedimentary units (Fig. 11a). The low P-wave velocity sedimentary units are thought to contain large amounts of water (Tsuru et al. 2002). Therefore, the along-strike change in the shape of the fluid-rich sedimentary units may cause an along-strike change in the fluid distribution, which, in turn, might affect the distribution of seismic slow earthquakes (Nakajima and Hasegawa 2016; Delph et al. 2018; Yabe et al. 2021; Sect. 2.4). However, the correspondence between the

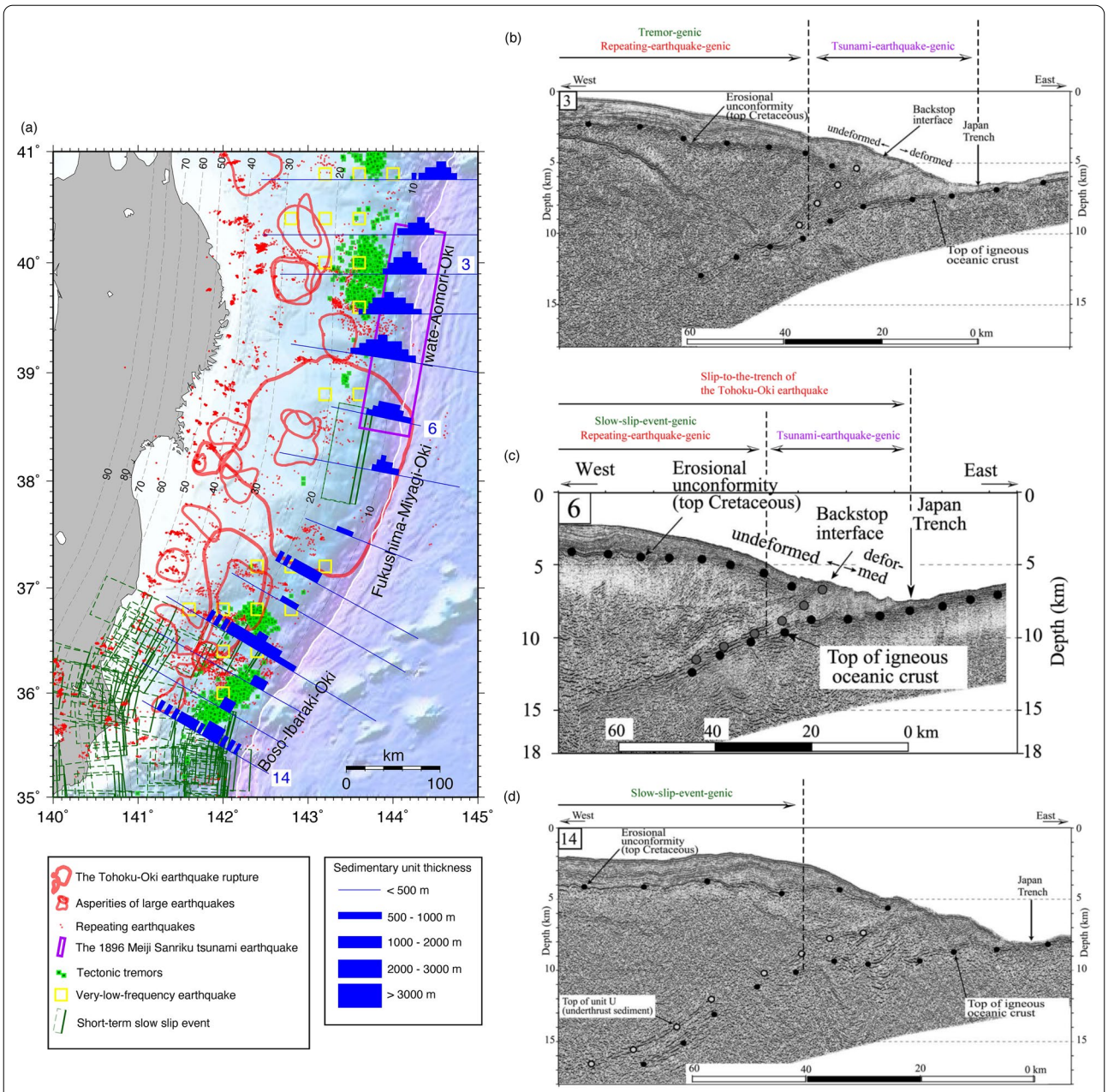

Fig. 11 Comparison between the distribution of interplate sedimentary units and the slow earthquake distribution in the Japan Trench. **a** Map view of the interplate sedimentary units and slow earthquakes. The distribution of the interplate sedimentary units is from Tsuru et al. (2002). For an explanation of the symbols, refer to the legend in the figure. The slow earthquakes, megathrust earthquakes, and small repeating earthquakes are from Fig. 9. **b**–**d** Seismic reflection images of survey line 3, 6, and 14, respectively. The slip behavior of the plate interface is indicated in the images. The seismic reflection images are adapted from Tsuru et al. (2002). Unit U in **d** indicates the channel-like sedimentary unit

interplate sedimentary units and seismic slow earthquakes at a smaller spatial scale (tens of kilometers) is not clear. The tremors prefer some small spots on the shallow plate interface (e.g., 38.9° N and 36.6°–36.8° N), but the correspondence between these spots and the shape of the sedimentary units is unclear.

Figure 11b–d shows the locations of slow earthquakes on seismic reflection images obtained by Tsuru et al. (2002). These images provide insight into the crustal structures generating slow earthquakes. On survey line 3 in the northern Japan Trench, tectonic tremors (Nishikawa et al. 2019) and small repeating earthquakes (Uchida and Matsuzawa

2013) have been observed on the plate interface deeper than the deformed wedge-shaped sedimentary unit (Fig. 11b). Previous ocean-bottom seismic observations (Hino et al. 1996, 2000; Obana et al. 2018) also reported the absence of small interplate seismicity where the wedge-shaped sedimentary unit is present. Soft sediments constituting the wedge-shaped unit may suppress the small interplate seismicity (Hino et al. 1996). In contrast to tectonic tremors and small interplate earthquakes, the 1896 M_w 8.0 Meiji Sanriku tsunami earthquake is thought to have ruptured the plate interface beneath the wedge-shaped sedimentary unit (Kanamori 1972; Tanioka and Satake, 1996; Tanioka and Seno 2001; Sect. 4.3; the purple rectangle in Fig. 11a). The soft sediments on the shallow plate interface probably slowed down the rupture process compared to regular earthquakes (Tanioka and Satake, 1996).

On survey line 6 in the central Japan Trench (Fig. 11c), repeating earthquakes have been observed on the plate interface deeper than the deformed wedge-shaped sedimentary unit, similar to survey line 3. The SSE that occurred during the month prior to the Tohoku-Oki earthquake is also thought to have mainly ruptured this plate interface (Kato et al. 2012; Ito et al. 2013; a green rectangle within the Tohoku-Oki earthquake rupture in Fig. 11a). The plate interface beneath the wedge-shaped sedimentary unit on survey line 6 is thought to have slipped during the 2011 Tohoku-Oki earthquake in addition to the 1896 earthquake (e.g., Tanioka and Seno 2001; Ide et al. 2011; Iinuma et al. 2012; Kodaira et al. 2012; Kodaira et al. 2021).

Figure 11d shows the location of the slow earthquakes on the seismic reflection image of survey line 14 in the southern Japan Trench. In this region, the approximately 2-km-thick channel-like sedimentary unit characterized by low P-wave velocity (3–4 km/s) extends to depths greater than 15 km. Shallow SSEs (Nishimura 2021) probably occur within this possibly fluid-rich sedimentary unit (Fig. 11a).

5.1.2 Subducting seamounts and petit-spot volcanoes

Subducting topographic features such as seamounts and petit-spot volcanoes may affect the slip behavior of the Japan Trench megathrust. Petit-spot volcanoes are volcanoes that are thought to be formed by asthenospheric melts ascending along lithospheric fractures in response to plate flexure during subduction (Hirano et al. 2006), distinct from the other types of volcanoes, such as those at divergent plate boundaries (mid-ocean ridges), convergent plate boundaries (e.g., island arcs), and hotspots. For more details on petit-spot volcanism, refer to a review paper by Hirano (2011).

In the southern Japan Trench, the Joban seamount chain is subducting (Fig. 12a). A seismic survey and gravity anomalies revealed a subducted seamount near 36° N, 142° E on the shallow plate interface (Mochizuki et al. 2008; Bassett et al. 2016; the brown dashed circle in Fig. 12a). Although there is debate as to whether seamounts accumulate elastic strain and host megathrust earthquakes (Scholz and Small 1997) or subduct aseismically (Wang and Bilek 2011; Sun et al. 2020), the seamount in the southern Japan Trench is considered to be subducting aseismically (no megathrust earthquakes but many small earthquakes and slow earthquakes) (Mochizuki et al. 2008; Wang and Bilek 2014; Kubo and Nishikawa 2020). Fluid-rich sediments entrained with the seamount (Mochizuki et al. 2008) and the development of a complex fracture network in the upper plate around it (Wang and Bilek 2011, 2014) are thought to suppress large earthquakes and promote aseismic creep and numerous small earthquakes. Consistent with this idea, tectonic tremors and swarms of small interplate earthquakes have been observed in the vicinity of the subducting seamount (Nishikawa and Ide 2018; Nishikawa et al. 2019; Sun et al. 2020; Yamaya et al. 2022; Figs. 9c and 12a). Rupture areas of megathrust earthquakes are located downdip of the subducting seamount (Mochizuki et al. 2008; Kubo and Nishikwa, 2020; red contours in Figs. 9c and 12a). This might be because the enhanced tectonic compression on the downdip side of the seamount causes large fault-normal stress and promotes sediment consolidation to achieve a favorable condition for fast earthquake rupture (Sun et al. 2020).

In the northern Japan Trench, petit-spot volcanoes are subducting (Hirano et al. 2006; Fig. 12a). According to Fujie et al. (2020), the petit-spot volcanic area near the trench axis of the northern Japan Trench is characterized by thinner sediment ($\leq$ 160 m) than the other areas along the trench axis (240–400 m) (the blue section of the trench axis in Fig. 12a). This may be because the sediments in the petit-spot volcanic area were disturbed by the petit-spot volcanism and thermally metamorphosed (Fujie et al. 2020).

(See figure on next page.)

Fig. 12 Comparison between the crustal structure and the slow earthquake distribution in the Japan Trench. **a** Residual gravity anomalies (Bassett et al. 2016). The residual gravity anomalies are residuals from the along-strike average of satellite-derived free-air gravity anomalies. **b** Residual P-wave velocity (*Vp*) tomography along the upper surface of the subducting Pacific Plate. The residual *Vp* is the residual from the along-strike average of the original Vp model obtained by the tomographic inversion (Hua et al. 2020). **c** Plate boundary PP reflection intensity (Mochizuki et al. 2005; Mochizuki 2017). The colored line segments indicate the spatial variations of reflection intensity from the plate interface. For an explanation of the other symbols, refer to the legend in the figure. The slow earthquakes, megathrust earthquakes, and small repeating earthquakes are from Fig. 9

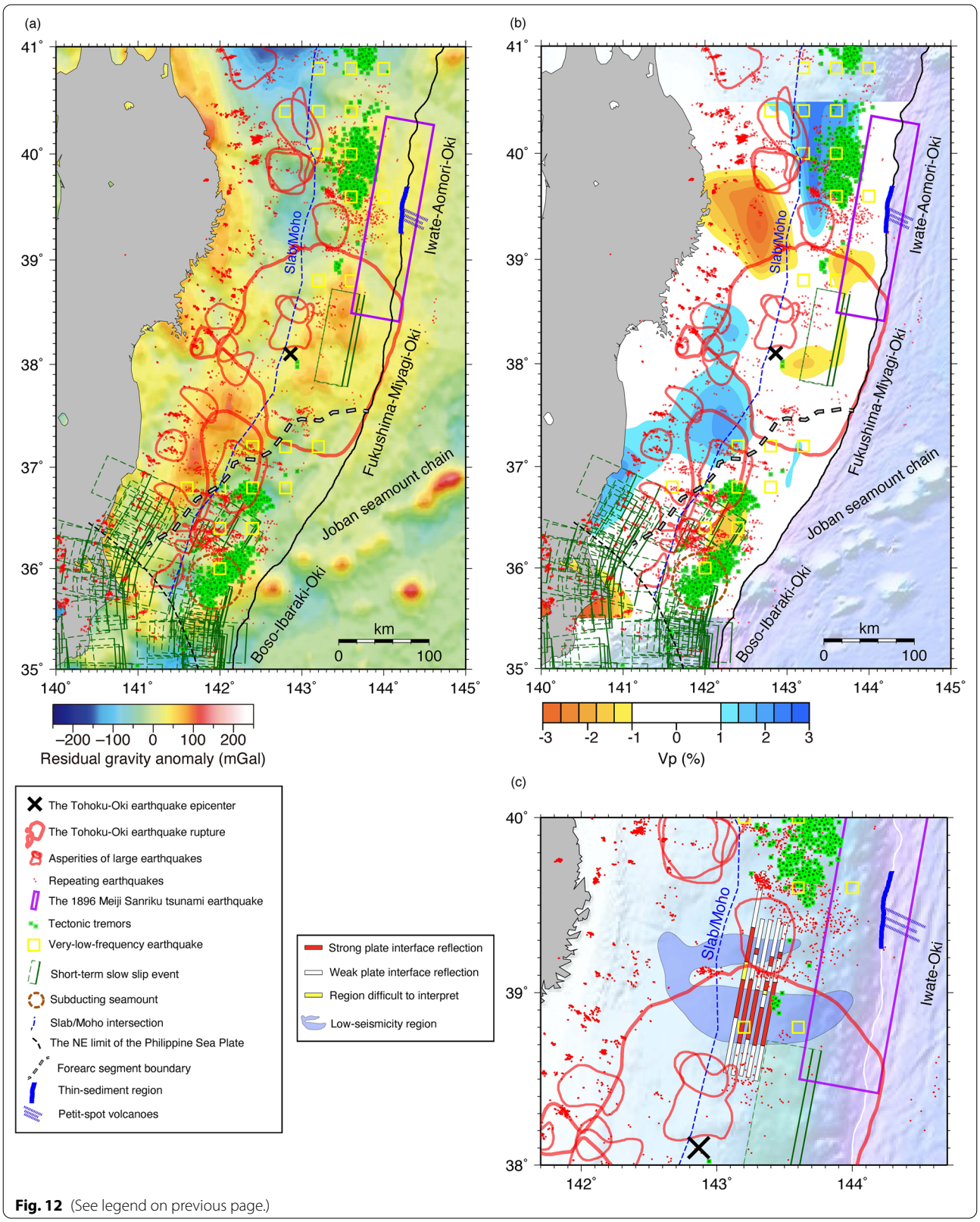

Fig. 12 (See legend on previous page.)

Fujie et al. (2020) also pointed out that the area where the petit-spot volcanoes are subducting corresponds to the northern limit of the coseismic rupture of the 2011 Tohoku-Oki earthquake (Iinuma et al. 2012; Fig. 12a). Furthermore, we found that tectonic tremors and small repeating earthquakes are densely distributed in this area, whereas they are sparse to the south of 39° N (Fig. 12a). These observations indicate a striking change in the slip behavior of the shallow plate interface near the petit-spot volcanic area in the northern Japan Trench. The frictional properties of the plate interface may have been altered by the disturbance and thermal metamorphism of the subducting sediments due to the petit-spot volcanism (Fujie et al. 2020). This, in turn, might have caused the rupture termination of the Tohoku-Oki earthquake (Fujie et al. 2020) and the clear contrasts in the tectonic tremor and repeating earthquake distributions. Due to the disturbance by the petit-spot volcanism, smectite in a pelagic clay layer of the subducting sediments may have transformed into illite, which has a significantly larger frictional coefficient than smectite (Saffer and Marone 2003).

In addition, horst and graben structures are particularly well developed near the petit-spot volcanic area in the northern Japan Trench (Tanioka et al. 1997). Such subducting relief may also influence the frictional properties and slip behavior of the plate interface because it makes the interplate contact rough (Ruff 1989; Tanioka et al. 1997; Heuret et al. 2012). The rough interplate contact may impede the propagation of coseismic rupture.

5.1.3 Residual gravity anomalies

Bassett et al. (2016) investigated residual gravity anomalies along the whole Japan Trench (Fig. 12a). The residual gravity anomalies are residuals from the along-strike average of satellite-derived free-air gravity anomalies. They found that the residual gravity has a particularly large contrast (approximately 60 mGal) between the central (a high residual gravity anomaly) and southern (a low residual gravity anomaly) Japan Trench. Bassett et al. (2016) called the boundary between the high and low residual gravity anomalies the forearc segment boundary (the thick gray dashed line in Fig. 12a). They suggested that this boundary might be the offshore continuation of the Median Tectonic Line, which is the most prominent tectonic boundary in Japan. The crust of the upper plate in the central Japan Trench might be composed of igneous rocks, whereas that of the upper plate in the southern Japan Trench might be composed of accretionary complexes.

When comparing the forearc segment boundary with the tectonic tremor distribution (Nishikawa et al. 2019), we found a striking difference in the tectonic tremor distribution (small dark green squares in Fig. 12a) across the boundary. Numerous tectonic tremors are distributed in the southern Japan Trench, whereas the central Japan Trench lacks tremors and is characterized by megathrust earthquake ruptures, including the 2011 Tohoku-Oki rupture (e.g., Yamanaka and Kikuchi 2004; Iinuma et al. 2012). The difference in the rocks constituting the upper-plate crust (i.e., igneous rocks and accretionary complexes) might contribute to the contrasting tectonic tremor distribution because upper-plate lithology can modulate the frictional behavior of the plate interface (Bassett et al. 2016). However, the residual gravity anomalies alone cannot explain the slow earthquake distribution along the entire Japan Trench. There is no large contrast in the residual gravity between the shallow parts of the northern and central Japan Trench (Bassett et al. 2016), although we observed a striking contrast in the tectonic tremor distribution (Fig. 12a).

5.1.4 Seismic velocity structure

The seismic velocity structure along the plate interface has been investigated in detail in the Japan Trench (e.g., Zhao et al. 2011; Liu and Zhao 2018; Hua et al. 2020). Hua et al. (2020) used S-net ocean-bottom stations and onshore Hi-net stations to obtain the P-wave velocity structure along the plate interface (Fig. 12b). The Hi-net is a high-sensitivity seismograph network operated by NIED (NIED 2019c). They found that the epicenter of the 2011 Tohoku-Oki earthquake (the black cross in Fig. 12b) is located between a deeper high-velocity anomaly (blue) and a shallower low-velocity anomaly (orange) in the central Japan Trench. The deeper high-velocity anomaly corresponds to the large coseismic slip areas of past large interplate earthquakes ($M_w \geq 7$) (e.g., Yamanaka and Kikuchi 2004), and this deeper plate interface strongly radiated high-frequency seismic waves during the Tohoku-Oki earthquake (e.g., Ide et al. 2011; Koper et al. 2011). The shallower low-velocity anomaly corresponds to the large coseismic slip (tens of meters) of the Tohoku-Oki earthquake, and this shallower plate interface only weakly radiated high-frequency seismic waves during the Tohoku-Oki earthquake (e.g., Ide et al. 2011; Koper et al. 2011). Hua et al. (2020) suggested that the shallow low-velocity anomaly may reflect low-rigidity materials such as subducted sediments on the plate interface.

In contrast to the above correspondence between the seismic velocity structure and the Tohoku-Oki earthquake rupture, the correspondence between the seismic velocity structure and the slow-earthquake-genic regions is unclear (Fig. 12b). Hua et al. (2020) pointed out that the SSE during the month prior to the March 2011 Tohoku-Oki earthquake (Kato et al. 2012; Ito et al. 2013; a green rectangle within the Tohoku-Oki earthquake rupture in Fig. 12b) occurred in the vicinity of

the low-velocity anomaly on the shallow plate interface of the central Japan Trench. Tectonic tremors are also distributed near low-velocity anomalies in the central and southern Japan Trench. However, in the northern Japan Trench, tremors are distributed near a high-velocity anomaly. Therefore, no simple relationship can be found between the seismic velocity structure and the slow earthquake distribution.

5.1.5 Plate boundary reflection intensity

Seismic refraction–reflection surveys have been used to investigate the relationship between the plate boundary PP reflection intensity and the distribution of microearthquakes in the shallow part of the north-central Japan Trench (38–40° N) (Fujie et al. 2002; Mochizuki et al. 2005; Mochizuki 2017). These studies pointed out that microearthquakes avoid the plate interface with strong reflection. Figure 12c shows the spatial variation of the plate boundary reflection intensity revealed by these studies. In Fig. 12c, small repeating earthquakes (red points) (Uchida and Matsuzawa 2013), which are repeating ruptures of the identical small areas on the plate interface, are distributed in the vicinity of regions of weak reflection (the white line segments). The regions of strong reflection (the red line segments in Fig. 12c) correspond with the regions of less active microseismicity (the indigo region) (Mochizuki et al. 2005; Mochizuki 2017). Small repeating earthquakes (red points) also avoid the regions of strong reflection.

In contrast to fast earthquakes, tectonic tremors (small dark green squares) and VLFEs (open yellow squares) occur near the regions of strong reflection (around 38.9° N, 143.4° E) (Fig. 12c). The results of the seismic surveys (Fujie et al. 2002; Mochizuki et al. 2005) suggest that a thin layer (approximately 200 m) with a low P-wave velocity of 3–4 km/s exists at the plate boundary in the area of strong reflection. Tectonic tremors and VLFEs probably occur within this thin low-velocity layer. Fujie et al. (2002) suggested that this low-velocity layer may represent a layer of aqueous fluids and/or rocks with hydrated minerals such as serpentine. Such fluids and rocks may generate tectonic tremors and VLFEs and suppress the occurrence of small repeating earthquakes. In contrast, the short-term SSE that occurred during the month prior to the Tohoku-Oki earthquake (Kato et al. 2012; Ito et al. 2013; a green rectangle in Fig. 12c) is considered to have mainly ruptured the plate interface close to a region where the plate boundary reflection is weak and small repeating earthquakes occur. This observation implies that short-term SSEs can occur outside the possibly fluid-rich layer.

5.2 Geological environment of the slow-earthquake-genic regions

In this section, we describe the geological environment of the slow-earthquake-genic regions in the Japan Trench, focusing on their water sources, temperature–pressure conditions, and metamorphism. As described in Sect. 2.4, slow-earthquake-genic regions are characterized by abundant fluids and near-lithostatic pore-fluid pressure (e.g., Kodaira et al. 2004; Shelly et al. 2006; Ujiie et al. 2018; Bürgmann 2018; Behr and Bürgmann 2021; Kirkpatrick et al. 2021). Understanding water sources in the Japan Trench may help identify the factors governing the slow earthquake distribution in the Japan Trench.

Figure 13a and b shows the flux of water released upward from subducted sediments and the oceanic crust in the Japan Trench (Hyndman and Peacock 2003) and the thermal structure of the Japan Trench (Peacock and Wang 1999; Hyndman and Peacock 2003), respectively. Tectonic tremors, VLFEs, and shallow short-term SSEs occur in the shallow part of the Japan Trench (approximately 10–20 km depth). At these depths, the temperature at the plate boundary is estimated to be between 80 °C and 130 °C (Peacock and Wang 1999; Hyndman and Peacock 2003). Under this pressure–temperature condition, subducted sediments provide substantial water. The water sources include sediment compaction, the diagenetic transformation from opal to quartz, and the phase transition from smectite to illite (Hyndman and Peacock 2003; Kimura et al. 2012; Saffer and Tobin 2011; Saffer and Wallace 2015; Katayama 2016; Fig. 13a). The water flux due to the sediment compaction is dominant near the top of the shallow slow-earthquake-genic regions (10 km depth and 80 °C). As the temperature increases, the water flux due to the dehydration reactions becomes significant. At the bottom of the shallow slow-earthquake-genic regions (20 km depth and 130 °C), the phase transition from smectite to illite is the primary water source. Along with the low permeability of marine sediments, the water supplied by these sources may cause near-lithostatic pore-fluid pressure at the plate boundary (Saffer and Tobin 2011; Saffer and Wallace 2015) and enable shallow slow earthquakes to occur.

At the deeper plate interface of the Japan Trench (approximately 40–60 km depth), deep short-term SSEs occur in the southern Japan Trench (Nishimura 2021; Fig. 9a). As mentioned in Sect. 3.2.2, systematic and comprehensive detection of short-term SSEs has not yet been conducted in the central and northern Japan Trench; thus, it is unclear whether deep short-term SSEs occur along the entire Japan Trench. However, the decade-long acceleration of aseismic slip prior to the Tohoku-Oki earthquake, which resembles long-term SSEs, occurred on the plate interface at a depth of approximately

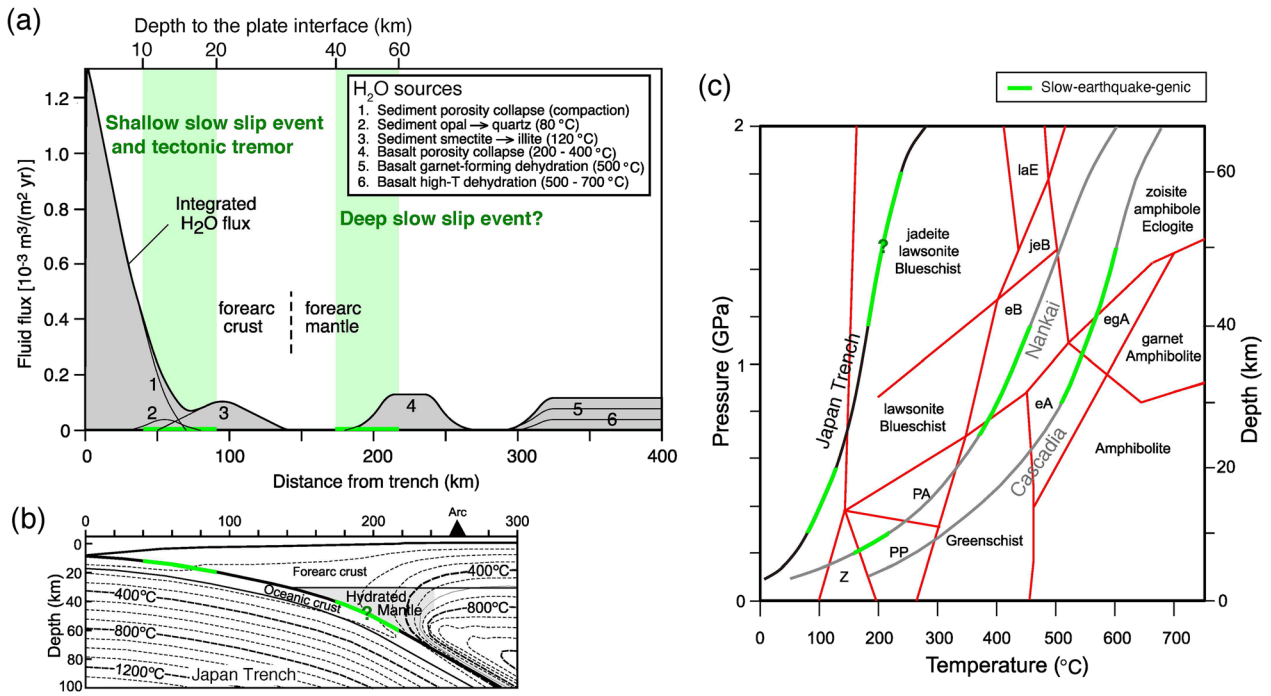

Fig. 13 Thermal and metamorphic environment of the Japan Trench. **a** Amount of water released upward from subducted sediments and the oceanic crust as estimated by Hyndman and Peacock (2003). For the details of the fluid flux estimation, see Hyndman and Peacock (2003). The green areas indicate the locations of the slow-earthquake-genic regions. **b** Thermal structure of the Japan Trench as estimated by Peacock and Wang (1999). This panel is adapted from Hyndman and Peacock (2003). The green sections of the plate interface indicate the locations of the slow-earthquake-genic regions. The question mark indicates the possible deep slow-earthquake-genic region. **c** Pressure–temperature paths for the top of the subducting oceanic crust in the Japan Trench, Nankai Trough, and Cascadia subduction zone (Peacock and Wang 1999; Peacock 2009). The pressure–temperature ranges of the slow-earthquake-genic regions are shown by the green sections of the pressure–temperature paths. The question mark indicates the possible deep slow-earthquake-genic region in the Japan Trench. Metamorphic conditions of the subducting oceanic crust (Peacock 2009) are also shown. eA, epidote–amphibolite; eB, epidote–blueschist; egA, epidote–garnet–amphibolite; jeB, jadeite–epidote–blueschist; laE, lawsonite–amphibole eclogite, PA; prehnite–actinolite; PP, prehnite–pumpellyite; and Z, zeolite facies

30–60 km in the central Japan Trench, possibly accompanied by slips on some areas of the shallower plate interface (10–30 km depth) (Ozawa et al. 2012; Mavrommatis et al. 2014, 2015; Yokota and Koketsu 2015; Sect. 3.2.2). Furthermore, the 3-year periodic slow slip on the deeper plate interface of the northern Japan Trench, which has been inferred from repeating earthquake analyses (Uchida et al. 2016; Khoshmanesh et al. 2020; Sect. 3.2.3; Fig. 7a), is also thought to occur at a similar depth range (approximately 30–60 km depth). Considering these observations, it is possible that certain types of slow earthquakes occur on the deeper plate interface in the central and northern Japan Trench as well as in the southern Japan Trench.

The temperature on the deeper plate interface (40–60 km depth) of the Japan Trench is estimated to be approximately 180–240 °C (Peacock and Wang 1999; Hyndman and Peacock 2003). Pore collapse within basalt constituting the subducting oceanic crust (200–400 °C) can be a water source under this pressure–temperature condition (Hyndman and Peacock 2003; Saffer and Tobin 2011; Katayama 2016; Fig. 13a). The supplied water may be related to the occurrence of deep short-term SSEs (Nishimura 2021) and transient slip phenomena similar to long-term SSEs (e.g., Mavrommatis et al. 2014; Yokota and Koketsu 2015; Uchida et al. 2016; Khoshmanesh et al. 2020; Sects. 3.2.2 and 3.2.3). At the deep plate interface of the Japan Trench, the subducting oceanic crust experiences the blueschist → eclogite facies metamorphism and releases substantial amounts of water (Peacock and Wang 1999). However, this transition occurs on the plate interface at a depth of approximately 110 km (approximately 500 °C) (Peacock and Wang 1999), which is much deeper than the possible deep slow-earthquake-genic region (40–60 km depth).

Figure 13c shows the pressure–temperature ranges of the shallow and deep slow-earthquake-genic regions in the Japan Trench and metamorphic conditions of the subducting oceanic crust. For comparison, the pressure–temperature paths at the plate boundaries of the

Nankai Trough and Cascadia subduction zone are also shown (Peacock and Wang 1999; Peacock 2009). The slow-earthquake-genic pressure–temperature ranges greatly vary among the three subduction zones. The shallow part of the Japan Trench (10–20 km depth) has the lowest temperature in Fig. 13c, ranging from 80–130 °C. In this pressure–temperature range, the subducting oceanic crust has not yet experienced a metamorphic facies transition. The possible deep slow-earthquake-earthquake-genic region of the Japan Trench (40–60 km depth and 180–240 °C) corresponds to the jadeite-lawsonite blueschist facies. The highest temperature in Fig. 13c is found in the deeper part of the Cascadia subduction zone (30–50 km depth and 500–600 °C), where the young and warm Juan de Fuca Plate (less than 10 Ma) (Müller et al. 2008) is subducting. In this pressure–temperature range, the subducting oceanic crust experiences the epidote–amphibolite → epidote–garnet–amphibolite → eclogite facies metamorphism. It is surprising that despite the substantial differences in the pressure–temperature and metamorphic conditions, the same types of slow earthquakes (i.e., tectonic tremors, VLFEs, and short-term SSEs) have been observed at the shallow plate boundaries of the Japan Trench and Nankai Trough and at the deep plate boundaries of the Nankai Trough and Cascadia subduction zone (Dragert et al. 2001; Obara 2002; Rogers and Dragert 2003; Obara et al. 2004; Obara and Ito 2005; Ito et al. 2007; Ghosh et al. 2015; Araki et al. 2017; Ohta et al. 2019; Tanaka et al. 2019; Nishikawa et al. 2019; Baba et al. 2020; Nishimura 2021). This suggests that the global slow earthquake distribution is not governed by a single specific temperature, pressure, mineral dehydration, metamorphic facies, or lithology (Peacock 2009; Saffer and Wallace 2015; Kirkpatrick et al. 2021).

6 Discussion

In this section, by synthesizing the results and implications of slow earthquake studies in the Japan Trench (Sects. 3, 4, and 5), we comprehensively discuss the roles of the slow earthquakes in the occurrence process of the March 11, 2011, M_w 9.0 Tohoku-Oki earthquake (Sect. 6.1), factors governing the slow earthquake distribution in the Japan Trench (Sect. 6.2), and the use of the slow earthquakes for improving the forecasts of interplate seismicity along the Japan Trench (Sect. 6.3).

6.1 Overview of the occurrence process of the 2011 Tohoku-Oki earthquake focusing on the roles of slow earthquakes

6.1.1 Prior to the Tohoku-Oki earthquake

In the interseismic period before the 2011 Tohoku-Oki earthquake, slow earthquake activity on the shallow plate interface of the Japan Trench (10–20 km depth) probably varied substantially in the along-strike direction. As suggested by the VLFE activity from January 2003 (Baba et al. 2020; Sect. 3.2.2; Fig. 6), the slow earthquake activity may have been particularly active in the northern and southern Japan Trench. Note that, however, along-strike variations in moment release due to the shallow slow earthquakes are unclear because the spatiotemporal distribution of SSEs (i.e., slow earthquakes with the largest seismic moments) along the entire Japan Trench is unknown (Nishimura 2021). The interplate coupling ratio before the Tohoku-Oki earthquake was high in the central Japan Trench and relatively low in the northern and southern Japan Trench (Ito et al. 2000; Nishimura et al. 2000, 2004; Suwa et al. 2006; Hashimoto et al. 2009; Loveless and Meade 2010; Uchida and Matsuzawa 2011; Lindsey et al. 2021; Fig. 6a), and this coupling distribution corresponds well to the variation of the shallow slow earthquake activity. However, these observations do not mean that slow earthquakes did not occur in the central Japan Trench before the Tohoku-Oki earthquake. VLFEs repeatedly occurred in a small spot around 38.9° N, 143.4° E (Matsuzawa et al. 2015; Baba et al. 2020; Sect. 5.1.5; Figs. 6a and 12c), which corresponds to the northern edge of the huge locked zone in the central Japan Trench (Suwa et al. 2006; Fig. 6a) and the region of strong plate boundary reflection (Fujie et al. 2002; Mochizuki et al. 2005; Mochizuki 2017; Sect. 5.1.5; Fig. 12c).

Large interplate earthquakes ($M_w \geq 7$) before the Tohoku-Oki earthquake avoided the shallow slow-earthquake-genic regions (10–20 km depth) (Sect. 4.2; Fig. 9). Most of them ruptured the plate interface deeper than the shallow slow-earthquake-genic regions (e.g., Yamanaka and Kikuchi 2004; Mochizuki et al. 2008; Research Center for Seismology, Volcanology, and Disaster Mitigation 2008), although the 1896 Meiji Sanriku tsunami earthquake ruptured the shallow plate interface close to and slightly shallower than the slow-earthquake-genic region in the northern Japan Trench (Tanioka and Satake, 1996; Tanioka and Seno 2001; Sect. 4.3; Figs. 9 and 14). Furthermore, in the southern Japan Trench, large interplate earthquakes (Mochizuki et al. 2008; Research Center for Seismology, Volcanology, and Disaster Mitigation 2008) avoided the source depth of deep short-term SSEs (40 km depth or deeper) as well as that of shallow short-term SSEs (10–30 km depth) (Nishimura 2021; Figs. 9 and 14).

The clear complementarity between the slow-earthquake-genic regions and the rupture areas of the large interplate earthquakes indicates that the coseismic ruptures did not propagate deep into the slow-earthquake-genic regions. Based on this observation, we suggest that the slow-earthquake-genic regions impeded the coseismic rupture propagation. According to linear elastic

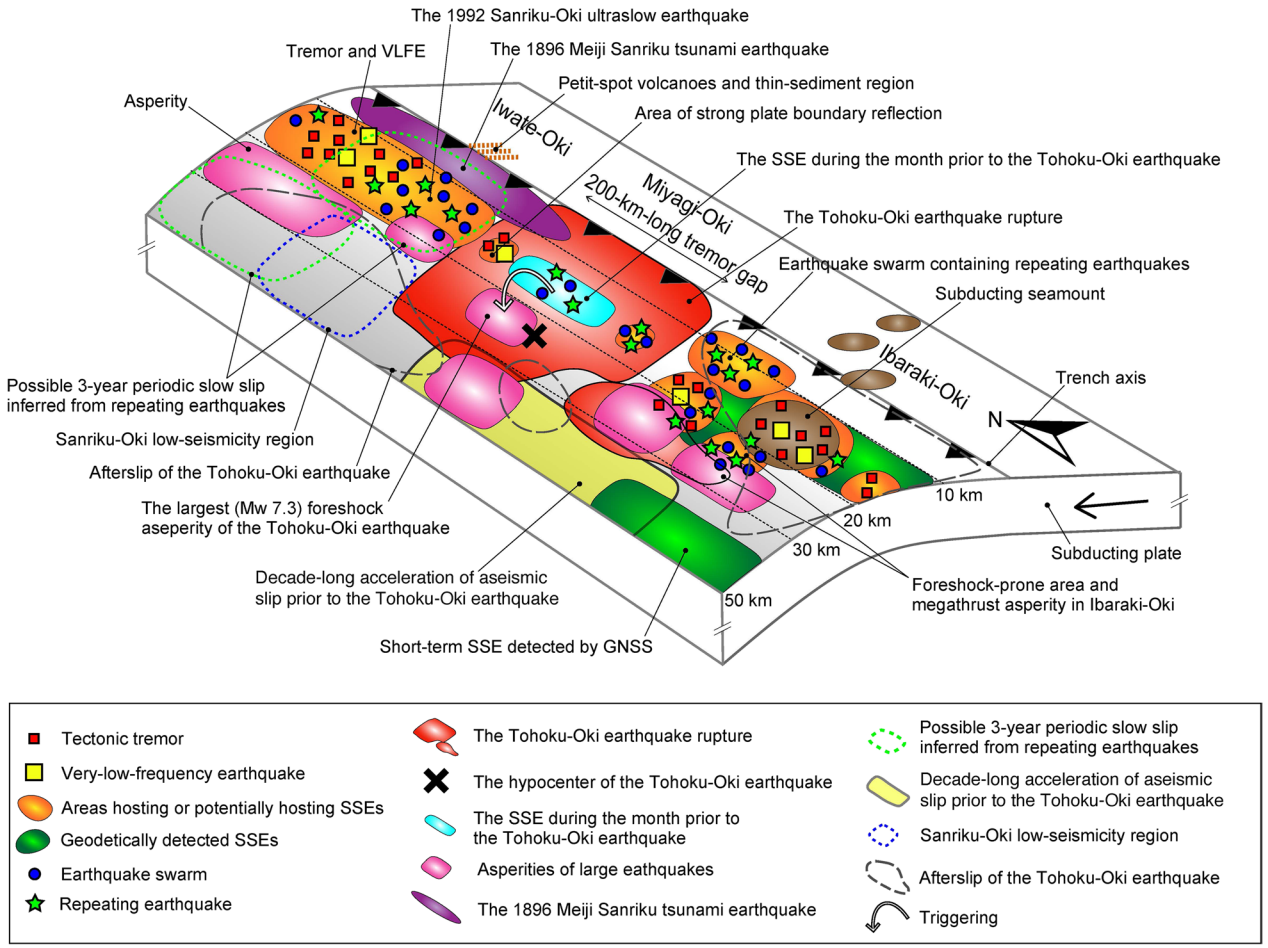

Fig. 14 Schematic of the interplate slip behavior of the Japan Trench. For an explanation of the symbols, refer to the legend in the figure

fracture mechanics, coseismic rupture terminates when the strain energy released by unit rupture advance falls below the fracture energy consumed (e.g., Ke et al. 2018). Based on this idea, a simple interpretation is that during the coseismic rupture propagation in the slow-earthquake-genic regions, the fracture energy consumed by unit rupture propagation might have exceeded the strain energy released. The large fracture energy in the slow-earthquake-genic regions might have been caused by the mechanisms suppressing fault slip rates considered in the physical models of slow earthquakes (Sect. 2.4). Alternatively, it is also possible that the coseismic rupture propagation terminated due to the small strain energy released by unit rupture propagation in the slow-earthquake-genic regions, which may have resulted from a small stress drop. However, we are aware that linear elastic fracture mechanics may be too simplistic to describe the rupture propagation in slow-earthquake-genic regions because fault zone deformation in these regions is thought to involve not only brittle fractures but also viscous flow (e.g., Ando et al. 2012; Behr et al. 2018; Ujiie et al. 2018), which is not within the framework of elastic fracture mechanics.

Slow earthquakes were involved not only in the rupture termination process but also in the rupture initiation process of the large interplate earthquakes before the 2011 Tohoku-Oki earthquake. SSEs triggering swarms of foreshocks are thought to have occurred during the weeks prior to the 1982 and 2008 M_j 7 Ibaraki-Oki earthquakes in the southern part of the Japan Trench (Matsumura 2010; Nishikawa and Ide 2018; Kubo and Nishikawa 2020; Hirose et al. 2021; Sect. 3.2.3; Fig. 14). Moreover, the 3-year periodic slow slip in the northern Japan Trench (Uchida et al. 2016) might have triggered foreshock activity of $M_j \geq 6$ interplate earthquakes (Hirose et al. 2021; Sect. 3.2.3).

In the decade prior to the March 2011 M_w 9.0 Tohoku-Oki earthquake, various changes occurred on the plate

interface of the Japan Trench. From around 2002 until the 2011 Tohoku-Oki earthquake, an acceleration of aseismic slip similar to a long-term SSE occurred on the deeper plate interface (approximately 30–60 km depth) in the central Japan Trench (Ozawa et al. 2012; Mavrommatis et al. 2014, 2015; Yokota and Koketsu 2015; Sect. 3.2.2; Fig. 6a and b). Furthermore, some areas of the shallow plate interface (10–30 km depth) may also have slipped during this transient (Mavrommatis et al. 2015). This transient aseismic slip may have stressed the huge locked zone in the central Japan Trench (Mavrommatis et al. 2015; Yokota and Koketsu 2015). Concurrently, at the shallow part (approximately 10–20 km depth) of the huge locked zone, the Gutenberg–Richter relationship's *b* value (Nanjo et al. 2012; Tormann et al. 2015; Fig. 10a) and the tidal response of seismicity (Tanaka 2012; Fig. 10b) decreased and increased, respectively, on a decadal scale. These decade-scale changes in the seismicity parameters might be due to increased shear stress on the shallow part of the huge locked zone in the central Japan Trench (Nanjo et al. 2012; Tanaka 2012; Tormann et al. 2015; Sect. 4.4.1).

In the month prior to the March 11, 2011, Tohoku-Oki earthquake, an SSE accompanied by a M_j 5 class earthquake swarm and tectonic tremors occurred at the shallow part of the huge locked zone in the central Japan Trench (Kato et al. 2012; Ito et al. 2013, 2015; Katakami et al. 2018; Fig. 14). The SSE ruptured the region of the decreased *b* value (Nanjo et al. 2012; Tormann et al. 2015; Fig. 10a) and increased tidal response (Tanaka 2012; Fig. 10b). The SSE is thought to have induced an increase in the shear stress in the surrounding region and triggered the largest foreshock (M_w 7.3) 2 days before the Tohoku-Oki earthquake (Ito et al. 2013; Fig. 14). The largest foreshock ruptured the plate interface deeper than the SSE source region (Ohta et al. 2012; Ito et al. 2013; Fig. 14), and its coseismic rupture overlapped significantly with that of a M_w 7.1 interplate earthquake in 1981 (Yamanaka and Kikuchi 2004; the two red contours within the Tohoku-Oki earthquake rupture in Fig. 9a). Following the largest foreshock, its afterslip propagated southwestward and eventually triggered the dynamic rupture of the Tohoku-Oki earthquake on the plate interface deeper than the shallow slow-earthquake-genic region (approximately 25 km depth) (Ando and Imanishi 2011; Kato et al. 2012; Ohta et al. 2012; the large black cross in Fig. 14).

6.1.2 During and after the Tohoku-Oki earthquake

It is difficult to discuss the spatiotemporal evolution of the coseismic rupture of the M_w 9.0 Tohoku-Oki earthquake because it differs significantly from one study to another (e.g., Ide et al. 2011; Shao et al. 2011; Yagi and Fukahata 2011; Yagi 2012). A review paper by Yagi (2012) summarized the differences between several studies in the spatiotemporal rupture evolution of the Tohoku-Oki earthquake. Here, we introduce the rupture process estimated by Ide et al. (2011) as an example. According to Ide et al. (2011), the dynamic rupture of the Tohoku-Oki earthquake first propagated downdip toward the west (landward), and the deeper plate interface (40–60 km depth) of the central Japan Trench slipped approximately 40 s after the rupture initiation. This deeper rupture strongly radiated high-frequency waves and corresponds with small areas recognized as strong-motion generation areas by Kurahashi and Irikura (2013). Next, the shallow slow-earthquake-genic region (10–20 km depth) and the vicinity of the trench axis in the central Japan Trench underwent a huge coseismic slip of tens of meters at 60 s. Despite the prodigious slip amount, this huge slip only weakly radiated high-frequency waves and resembles tsunami earthquakes (Sect. 4.3). Then, the rupture again propagated downdip toward the west, and the deeper plate interface (40–60 km depth) slipped again at 90 s. The final coseismic slip distribution of the Tohoku-Oki earthquake was mainly limited to the central Japan Trench and the deeper part of the southern Japan Trench (Figs. 9 and 14). As with the other large interplate earthquakes (e.g., Yamanaka and Kikuchi 2004; Mochizuki et al. 2008; Research Center for Seismology, Volcanology, and Disaster Mitigation 2008; Fig. 9), the Tohoku-Oki earthquake did not substantially rupture the shallow slow-earthquake-genic regions in the northern and southern Japan Trench (Figs. 9 and 14). This is a common feature of most slip inversion results (Lay 2018, and references cited therein).

The fact that the coseismic rupture of the 2011 Tohoku-Oki earthquake terminated at the shallow slow-earthquake-genic regions in the southern and northern Japan Trench is consistent with our idea that the shallow slow-earthquake-genic regions impede fast rupture propagation, as discussed in Sect. 6.1.1. Furthermore, the subducting seafloor features such as the seamounts (Mochizuki et al. 2008; Wang and Bilek 2014; Sun et al. 2020), petit-spot volcanoes (Hirano et al. 2006), sediments thermally metamorphosed by petit-spot volcanism (Fujie et al. 2020), and well-developed horst and graben structures (Tanioka et al. 1997) in the northern and southern Japan Trench may have influenced the frictional behavior of the plate interface and contributed to the termination of the Tohoku-Oki earthquake rupture (Sect. 5.1.2; Figs. 12a and 14). Moreover, a region of low seismicity ($M_j \geq 5.0$) and interplate decoupling, called the Sanriku-Oki low-seismicity region, is located on the plate interface (25–50 km depth) downdip of the slow-earthquake-genic region in the northern Japan Trench

(Ye et al. 2012; the area indicated by the blue dashed line in Fig. 14), corresponding to a prominent low P-wave velocity anomaly in the deeper part of the northern Japan Trench (Hua et al. 2020; Fig. 12b). Little strain accumulation in and stable frictional behavior of the region may also have bounded the Tohoku-Oki rupture (Ye et al. 2012).

In contrast to the northern and southern Japan Trench, the shallow slow-earthquake-genic region in the central Japan Trench was ruptured by the Tohoku-Oki earthquake and underwent a coseismic slip of tens of meters (Figs. 9 and 14). This is contrary to our expectation that slow-earthquake-genic regions impede the coseismic rupture and act as a barrier against it (Sect. 6.1.1). It is unclear why only the shallow slow-earthquake-genic region in the central Japan Trench was ruptured. However, the particularly large slip deficit in the central Japan Trench (Ito et al. 2000; Nishimura et al. 2000; Nishimura et al. 2004; Suwa et al. 2006; Hashimoto et al. 2009; Loveless and Meade 2010; Uchida and Matsuzawa 2011; Lindsey et al. 2021; Fig. 6a) and the huge rupture dimension of the Tohoku-Oki earthquake may have induced substantial stress concentration and elevated the strain energy released by unit rupture advance, eventually enabling the coseismic rupture to break through the frictional barrier (Das and Aki 1977; Kaneko et al. 2010). In addition, substantial dynamic fault weakening due to mechanisms such as thermal pressurization (i.e., thermal expansion of pore fluids due to frictional heating) (e.g., Sibson 1973; Andrews 2002) may have promoted the huge slip in the shallow slow-earthquake-genic region of the central Japan Trench (Shibazaki et al. 2011; Mitsui et al. 2012; Noda and Lapusta 2013; Ujiie et al. 2013; Hirono et al. 2016).

Immediately after the Tohoku-Oki earthquake, the largest interplate aftershocks (M_w 7.8 and M_w 7.4) occurred in the southern and northern Japan Trench, respectively. As with the Tohoku-Oki earthquake, the largest interplate aftershocks did not rupture the shallow slow-earthquake-genic regions in the southern and northern Japan Trench (Kubo and Nishikawa 2020). The occurrence rates of VLFEs in both regions sharply increased after the Tohoku-Oki earthquake (Matsuzawa et al. 2015; Baba et al. 2020). In addition to the VLFEs, numerous tectonic tremors have been observed in the shallow part of the northern and southern Japan Trench (Ohta et al. 2019; Tanaka et al. 2019; Nishikawa et al. 2019; Sect. 3.2.1; Figs. 5 and 14). The large afterslip following the Tohoku-Oki earthquake was also observed in both the regions (Uchida and Matsuzawa 2013; Sun and Wang 2015; Iinuma et al. 2016; Tomita et al. 2017, 2020; Honsho et al. 2019; Watanabe et al. 2021; Figs. 6a and 14). However, it is still unclear how much of the afterslip in the northern and southern Japan Trench was accounted for by the shallow slow earthquakes because the precise cumulative slip of shallow SSEs, which are slow earthquakes with the largest seismic moments, is unknown.

In summary, slow earthquakes in the Japan Trench are related to the rupture initiation and termination processes of megathrust earthquakes in the Japan Trench, including the 2011 Tohoku-Oki earthquake. Due to the interaction of slow and fast earthquakes, the plate boundary of the Japan Trench has been undergoing surprisingly complex deformation processes, as schematically summarized in Fig. 14.

6.2 Factors governing the slow earthquake distribution in the Japan Trench

The slow earthquake distribution along the Japan Trench has two notable characteristics. The first is the complementarity between the source region of the M_w 9.0 Tohoku-Oki earthquake and the distribution of seismic slow earthquakes in the along-strike direction on a scale of hundreds of kilometers (Nishikawa et al. 2019; Baba et al. 2020; Figs. 9 and 14). This is a common feature of the slow earthquake distribution before and after the Tohoku-Oki earthquake (Baba et al. 2020; Sect. 3.2.2; Fig. 6). Seismic slow earthquakes (i.e., tectonic tremors and VLFEs) are much more frequent in the northern and southern Japan Trench than in the central Japan Trench, where the huge coseismic rupture of the Tohoku-Oki earthquake is located. The second notable feature is that the Japan Trench has a very complex distribution of interplate fast and slow earthquakes, with their source areas varying in both the along-strike and along-dip directions on a scale of tens of kilometers (Nishikawa et al. 2019; Nishimura 2021; Obana et al. 2021; Figs. 9 and 14). In summary, the Japan Trench megathrust shows changes in its slip behavior at two spatial scales: hundreds of kilometers and tens of kilometers.

Identifying the factors that produce these features is important for understanding the physical mechanisms governing deformation processes at subduction plate boundaries. Section 5 details the candidate factors. With respect to the along-strike changes in the slow earthquake distribution at the scale of hundreds of kilometers, we have discussed interplate sedimentary units (Tsuru et al. 2002), subducting seamounts (Mochizuki et al. 2008; Wang and Bilek 2014; Sun et al. 2020), subducting petit-spot volcanoes (Hirano et al 2006), trench sediment thickness (Fujie et al. 2020), subducting horst and graben structures (Tanioka et al. 1997), changes in the lithology of the upper-plate crust (Bassett et al. 2016), and seismic velocity structure (Hua et al. 2020) (Figs. 11 and 12). Although we observed some partial correspondences between the slow earthquake distribution and crustal

structure (e.g., fluid-rich interplate sedimentary units and subducting seamounts entraining fluid-rich sediments), none of these factors fully explain the slow earthquake distribution along the entire Japan Trench.

In the Nankai Trough and Cascadia subduction zone, along-strike changes in the tectonic tremor distribution are thought to reflect the distribution of highly overpressured fluids at the plate boundary (Nakajima and Hasegawa 2016; Delph et al. 2018). The distribution of such fluids is thought to be influenced by the flux of fluids from the subducting crust and sediments and the upper-plate permeability. The structural heterogeneity described in Sect. 5 might influence fluid fluxes along the Japan Trench and the permeability structure of the Japan Trench, leading to along-strike changes in the distribution of highly overpressured fluids. We speculate that highly overpressured fluids are more widely distributed on the shallow plate interface in the northern and southern Japan Trench than in the central Japan Trench.

However, it should be noted that the along-strike changes in the shallow slow earthquake distribution on the scale of hundreds of kilometers (Figs. 9 and 14) do not necessarily reflect along-strike changes in the frictional properties of the shallow plate interface. It is possible that a huge frictionally locked region exists on the plate interface deeper than 20 km in the central Japan Trench (Lindsey et al. 2021), and that the stress shadow cast by this deep frictionally locked region causes apparent along-strike changes in the shallow slow earthquake distribution (10–20 km depth). That is, the shallow part of the central Japan Trench may have a low stress accumulation rate due to the stress shadow, which may be responsible for the relatively infrequent slow earthquake activity in the central Japan Trench (Fig. 6). If this is the case, the area where frictional properties change significantly in the along-strike direction is not the shallow slow-earthquake-genic zone but the deeper plate interface. Considering these points, we propose that it is necessary to observe slow earthquake activity at the shallow part of the Japan Trench over a long period to investigate whether there indeed are differences in interplate frictional properties between the shallow parts of the northern, central, and southern Japan Trench. Specifically, it is necessary to ascertain whether there are differences in the types of slow earthquakes that occur and the size of the regions where each type of slow earthquake occurs.

With respect to the changes in the slow earthquake distribution on the scale of tens of kilometers (Fig. 9), the causes of the changes are largely unknown. However, the distribution of tectonic tremors, VLFEs, and small interplate earthquakes around 39° N was found to clearly correlate with the changes in the plate boundary PP reflection (Fujie et al. 2002; Mochizuki et al. 2005; Mochizuki 2017) (Sect. 5.1.5; Fig. 12c). The areas of strong reflection are associated with tectonic tremors and VLFEs, whereas the areas of weak reflection are associated with small repeating earthquakes. The strong reflection is thought to indicate the presence of a thin layer (approximately 200 m) composed of aqueous fluids or rocks with hydrous minerals at the plate boundary (Fujie et al. 2002; Mochizuki et al. 2005; Mochizuki 2017). This interplate thin layer probably produces the seismic slow earthquakes. It is important to confirm whether such a correlation between strong plate boundary reflection and slow earthquake distribution is common in other areas of the Japan Trench.

Tectonic tremors in the Japan Trench (Ohta et al. 2019; Tanaka et al. 2019; Nishikawa et al. 2019) are distributed along 10–20 km depth contours (Fig. 5a). Shallow SSEs also occur at similar depths (10–30 km) (Nishimura 2021; Fig. 5a). These observations imply that the distribution of slow earthquakes in the Japan Trench strongly depends on pressure–temperature conditions of the plate interface, which predominantly vary in the dip direction. The shallow plate boundary where the tectonic tremors occur (10–20 km depth and 80–130 °C) corresponds to the site where opal and smectite dehydrate (Hyndman and Peacock 2003; Kimura et al. 2012). Along with sediment compaction, these dehydration reactions may provide the water necessary for shallow slow earthquakes to occur (Sect. 5.2; Fig. 13a).

However, upon comparing the slow earthquake distribution in the Japan Trench with the slow earthquake distribution in other subduction zones (i.e., the shallow and deeper parts of the Nankai Trough and the deeper part of the Cascadia subduction zone), we found that the pressure–temperature conditions and hence metamorphic conditions of the slow-earthquake-genic regions are very different for each subduction zone and have little in common (Peacock 2009; Kirkpatrick et al. 2021; Fig. 13c). Despite the substantial differences, the characteristics of the deep and shallow slow earthquakes (e.g., types of slow earthquakes, occurrence of ETS, migration speed, and scaled energy) are similar (e.g., Dragert et al 2001; Obara 2002; Rogers and Dragert 2003; Bartlow et al. 2011; Araki et al. 2017; Annoura et al. 2017; Nishikawa et al. 2019; Sakaue et al. 2019; Yabe et al. 2021; Takemura et al. 2022), although tremor seismic energy rates and VLFE seismic moment rates in the deeper parts of the Nankai Trough and Cascadia subduction zone are known to be smaller than those in the shallow parts of the Nankai Trough and Japan Trench (Ide and Yabe 2014; Ide 2016; Yabe et al. 2019, 2021). It is paradoxical that the slow earthquake distribution within each subduction zone appears to

strongly depend on pressure–temperature conditions, yet the pressure–temperature conditions of the global slow earthquake distribution have little in common (Fig. 13c).

Slow earthquakes might occur under a very wide range of pressure–temperature and metamorphic conditions, provided that abundant, highly overpressured fluids exist at the plate boundary. Based on geological observations of quartz-filled veins in subduction mélange exhumed from a frictional–viscous transition depth, Ujiie et al. (2018) suggested that tectonic tremors on the deeper plate interface of the Nankai Trough might be brittle shear fractures within ductile shear zones under near-lithostatic pore-fluid pressure. Ductile shear deformation and near-lithostatic pore-fluid pressure can be achieved under a wide range of pressure–temperature conditions and are not limited to specific pressures or temperatures, although microscale mechanisms of ductility (e.g., granular flow, pressure-solution creep, dislocation creep, and diffusion creep) may vary with the pressure–temperature conditions (e.g., Bürgmann 2018). Therefore, the hypothesis proposed by Ujiie et al. (2018) might be applicable not only to deep tectonic tremors in the Nankai Trough but also to shallow and deep tectonic tremors in other subduction zones. In addition, we note that Namiki et al. (2014) used a viscoelastic gel and conducted an analogue experiment of slow earthquakes in which both ductile deformation and episodic frictional sliding occur. Such deformation may correspond to brittle shear fractures within ductile shear zones that are geologically observed.

Furthermore, the diversity of the slow-earthquake-genic pressure–temperature conditions among subduction zones (Fig. 13c) might reflect differences between subduction zones in the depths at which highly overpressured fluids accumulate. Locations where fluids accumulate in each subduction zone depend not only on the pressure–temperature conditions, which decide the sites of fluid release by subducting sediments and the oceanic crust, but also on the permeability structure of each subduction zone, given that the released fluids migrate (Iwamori 1998; Katayama et al. 2012; Katayama 2016). Therefore, it may be necessary to consider both the pressure–temperature conditions and the permeability structure of each subduction zone to understand the global slow earthquake distribution (Fig. 13c).

As described above, the factors governing the slow earthquake distribution in the Japan Trench are still largely unclear. Further detailed investigation of the correspondence of the slow earthquake distribution with crustal structure and geological environment in the Japan Trench is expected to provide important insights into the slow-earthquake-genesis in the Japan Trench and the physical mechanisms of slow earthquakes.

6.3 Use of slow earthquakes for improving forecasts of interplate seismicity along the Japan Trench

The detailed slow and fast earthquake distributions have been revealed in the Japan Trench (Fig. 9), and the relationship between slow earthquakes and megathrust earthquakes is becoming clear. Considering these recent advances, we propose that it is important to utilize the results of slow earthquake studies in the near future to improve forecasts of interplate seismicity along the Japan Trench.

Along the Japan Trench, slow earthquakes and interplate fast earthquakes occur in close proximity (Tanaka et al. 2019; Nishikawa et al. 2019; Takahashi et al. 2021; Yamaya et al. 2022; Figs. 5 and 9), and the slow earthquakes seem to be involved in the occurrence process of the fast earthquakes. The simultaneous occurrence of slow earthquakes and earthquake swarms has been observed (Sects. 3.2.1 and 3.2.3; Figs. 5h and 8). Several previous studies suggest that SSEs in the Japan Trench trigger both large and small interplate earthquakes (e.g., Ito et al. 2013; Uchida et al. 2016; Nishikawa and Ide 2018; Obana et al. 2021). Furthermore, the 2011 M_w 9.0 Tohoku-Oki earthquake was preceded by slow earthquakes (Kato et al. 2012; Ito et al. 2013, 2015; Katakami et al. 2018).

Considering the seismicity-triggering effects of slow earthquakes may improve short-term seismic risk assessment in the Japan Trench. It has been pointed out that slow earthquakes may have triggered foreshocks of large interplate earthquakes along the Japan Trench (Matsumura 2010; Kato et al. 2012; Ito et al. 2013; Nishikawa and Ide 2018; Hirose et al. 2021). Therefore, monitoring seismicity near the slow-earthquake-genic regions and detecting interplate earthquake swarms accompanying slow earthquakes in real time may enable us to find foreshock activity of impending large earthquakes in advance. Furthermore, the rupture initiation points of M_w 8 class megathrust earthquakes in the northern Japan Trench (the 1968 M_w 8.2 Tokachi-Oki and 1994 M_w 7.7 Sanriku-Oki earthquakes) (Yamanaka and Kikuchi 2004; the open purple diamonds in Fig. 9a) and the southern end of the Kuril Trench (the 1952 M_w 8.1 and 2003 M_w 8.0 Tokachi-Oki earthquakes) (Yamanaka and Kikuchi 2003) are very close to the shallow slow-earthquake-genic regions (10–20 km depth) (Tanaka et al. 2019). Therefore, seismic and geodetic observations near the slow-earthquake-genic regions may be effective to capture the preparatory and rupture initiation processes of megathrust earthquakes in the Japan and Kuril trenches. It might be possible to detect changes in characteristics of slow earthquake activity prior to the megathrust earthquakes, as suggested by Nishikawa and Ide (2018) in the southern Japan Trench (Sect. 3.2.3). Moreover, considering the

seismicity-triggering effects of slow earthquakes in physical and statistical seismicity models (e.g., Ogata 1988; Dieterich 1994) may improve short-term forecasts of interplate seismicity along the Japan Trench.

However, it is difficult to know in advance whether a slow earthquake will only cause a swarm of small earthquakes or will lead to a megathrust earthquake. The probability of a slow earthquake triggering a megathrust earthquake is also unknown. It is necessary to accumulate more observations to clarify the amount of seismicity triggered by a slow earthquake, the probability of megathrust earthquake occurrence increased by a slow earthquake, and the presence/absence of unique characteristics of slow earthquakes that precede megathrust earthquakes. If a slow earthquake preceding a megathrust earthquake is a preslip, which is a transient aseismic slip expected to precede a megathrust earthquake based on mechanics of fault friction (e.g., Dieterich 1992) and rock friction experiments (e.g., Ohnaka 1992; McLaskey 2019), then characteristics unique to a preslip, such as aseismic slip acceleration immediately before a megathrust earthquake (e.g., Dieterich 1992), may be observed. For example, Nishikawa and Ide (2018) claimed to have identified preslip-like features (i.e., sharp increases in the seismicity rate and interplate aseismic slip rate just before a mainshock) in the foreshock activity of the 1982 and 2008 M_j 7 Ibaraki-Oki earthquakes in the southern Japan Trench (Sect. 3.2.3). However, aseismic slip a few days before the March 11, 2011, M_w 9.0 Tohoku-Oki earthquake did not show preslip-like features (Ohta et al. 2012; Hino et al. 2014). Based on the ocean-bottom pressure gauge observations, Hino et al. (2014) concluded the Tohoku-Oki earthquake was not preceded by a M_w 6.2 or larger preslip in the vicinity of its rupture initiation point. Furthermore, simulation studies (Ide and Aochi 2005, 2013; Noda et al. 2013) and natural earthquake observations (Okuda and Ide 2018; Ide 2019a) suggested that the observable preslip of a large earthquake can be skipped due to the cascading process from a small rupture to a large one.

Currently, it may be challenging to utilize slow earthquakes to forecast megathrust earthquakes because the frequency of megathrust earthquake occurrence is very low and sufficient observations are lacking. However, we can conduct trials of forecasts for small-to-moderate earthquakes ($M_w \leq 6$). The Japan Trench is an ideal subduction zone for such trials, because the occurrence rate of small-to-moderate interplate earthquakes is much higher than in other subduction zones with advanced slow earthquake research (e.g., the Nankai Trough and Cascadia subduction zone) (Ide 2013).

In addition, the complementarity between the slow-earthquake-genic regions and the rupture areas of megathrust earthquakes (Nishikawa et al. 2019; Baba et al. 2020; Kubo and Nishikawa 2020; Nishimura 2021; Sect. 4.2) may be useful for inferring the possible source regions of future megathrust earthquakes. The 2011 Tohoku-Oki earthquake is the only instrumentally recorded megathrust earthquake that has been confirmed to have significantly ruptured the shallow slow-earthquake-genic regions in the Japan Trench (Fig. 9). From a purely statistical point of view, even if a megathrust earthquake of M_w 7 or greater occurs in the Japan Trench in the future, it is not highly likely that the earthquake will significantly rupture the shallow slow-earthquake-genic regions. The slow-earthquake-genic regions may impede the fast rupture propagation of megathrust earthquakes (Sect. 6.1.1). However, the slow-earthquake-genic regions do not always arrest the rupture of megathrust earthquakes, as evidenced by the slip to the trench of the Tohoku-Oki earthquake in the central Japan Trench. Under what conditions do the slow-earthquake-genic regions slip coseismically? Will future megathrust earthquakes rupture the slow-earthquake-genic regions in the northern and southern Japan Trench? Are there significant differences in the interplate frictional properties between the shallow part of the central Japan Trench and the shallow parts of the northern and southern Japan Trench? Answering these questions is essential for utilizing the complementarity between the slow-earthquake-genic regions and the rupture areas of megathrust earthquakes to infer the possible source regions of future megathrust earthquakes.

7 Conclusions

In this paper, we reviewed studies on slow earthquakes along the Japan Trench from the first report of a large transient aseismic slip to the present (Sect. 3). We compared the slow earthquake distribution along the Japan Trench with the distribution of other interplate slip phenomena (Sect. 4). We also described the crustal structure and geological environment of the slow-earthquake-genic regions in the Japan Trench (Sect. 5). By synthesizing the insights provided by the slow earthquake studies in the Japan Trench, we discussed the roles of the slow earthquakes in the occurrence process of the March 11, 2011, M_w 9.0 Tohoku-Oki earthquake, factors governing the slow earthquake distribution in the Japan Trench, and the use of slow earthquakes for improving forecasts of interplate seismicity along the Japan Trench (Sect. 6).

The studies reviewed in this paper revealed a surprisingly complex distribution of slow and fast earthquakes along the Japan Trench. These slow and fast earthquakes interact, and the plate boundary of the Japan Trench has been undergoing extremely complex deformation processes. The slow earthquakes are related to the rupture

initiation and termination processes of megathrust earthquakes in the Japan Trench, including the 2011 Tohoku-Oki earthquake. The causes of the complexity in the megathrust slip behavior of the Japan Trench are still largely unclear, although we observed some correspondences between the slow earthquake distribution and crustal structure (e.g., fluid-rich interplate sedimentary units, subducting seamounts entraining fluid-rich sediments, and strong plate boundary reflection suggesting the existence of a thin fluid-rich layer) and between the slow earthquake distribution and the geological environment (e.g., the site where opal and smectite dehydrate). Highly overpressured fluids along the plate interface are probably a key to understanding the complex slow earthquake distribution. Further attempts to understand the slow earthquake distribution based on the crustal structure and geological environment of the Japan Trench are expected to provide important insights into the slow-earthquake-genesis in the Japan Trench and the physical mechanisms of slow earthquakes. Moreover, we expect that further investigations of the complex interaction between slow and fast earthquakes and detailed monitoring of slow earthquake activity in the Japan Trench will lead to a better understanding of the occurrence process of megathrust earthquakes and an improved forecast of interplate seismicity in the Japan Trench.

Abbreviations

ETS: Episodic tremor and slip; GNSS: Global navigation satellite system; GSI: Geospatial Information Authority of Japan; JMA: Japan Meteorological Agency; LFE: Low-frequency earthquake; NIED: National Research Institute for Earth Science and Disaster Resilience; SSE: Slow slip event; VLFE: Very-low-frequency earthquake.

Acknowledgements

We thank Dr. Suguru Yabe for providing their tectonic tremor catalog (Yabe et al. 2019). We thank Dr. Takeshi Iinuma for providing their distribution of the afterslip following the 2011 Tohoku-Oki earthquake (Iinuma et al. 2016). We thank Dr. Naoki Uchida and Dr. David Shelly for their helpful and constructive comments.

Author contributions

TN proposed the topic, drew all the figures, and wrote the manuscript. SI carried out the detection of tectonic tremors. TN carried out the detection of short-term SSEs. All authors read, commented on, and approved the final manuscript.

Funding

This work was supported by JSPS KAKENHI Grant Number 21K20382 and 22H05307. This work was also supported by JSPS KAKENHI Grant Number JP16H06472 in Scientific Research on Innovative Areas "Science of Slow Earthquakes."

Availability of data and materials

The tectonic tremor catalog of the Japan Trench is based on Nishikawa et al. (2019) and is included in its supplementary material. The VLFE catalog of the Japan Trench is from Baba et al. (2020) and is included in its supplementary material. The short-term SSE catalog of the southern Japan Trench is based on Nishimura (2021) and is included in its supplementary material. The repeating earthquake catalog of the Japan Trench is based on Uchida and Matsuzawa (2013) and is included in its supplementary material. The earthquake swarm catalog of the Japan Trench is from Nishikawa and Ide (2018) and Nishikawa et al. (2019) and is included in their supplementary materials. The above catalogs of the tectonic tremors, VLFEs, repeating earthquakes, and earthquake swarms are also available at https://www.aob.gp.tohoku.ac.jp/~uchida/page_3e.html. The distributions of the asperities in the Japan Trench (e.g., Yamanaka and Kikuchi 2004), the interplate coupling in the Japan Trench (Suwa et al. 2006), and the coseismic slip of the 2011 Tohoku-Oki earthquake (Iinuma et al. 2012) are available at https://www.aob.gp.tohoku.ac.jp/~uchida/page_3_aspe.html. The tectonic tremor and short-term SSE catalogs (Nishimura et al. 2013; Idehara et al. 2014; Nishimura 2014; Yamashita et al. 2015, 2021) of the Nankai Trough are from the Slow Earthquake Database (Kano et al. 2018a; http://www-solid.eps.s.u-tokyo.ac.jp/~sloweq/). The repeating earthquake catalog of the Nankai Trough is from Igarashi (2020) and is included in its supplementary material. The asperity distribution in the Nankai Trough (Yagi et al. 1998, 1999) is from the Earthquake Source Model Database (http://equake-rc.info/srcmod/). The depth contours of the upper surface of the Pacific and Philippine Sea plates are available at https://www.mri-jma.go.jp/Dep/sei/fhirose/plate/en.PlateData.html. The Japan Meteorological Agency (JMA) earthquake catalog is available at https://www.data.jma.go.jp/svd/eqev/data/bulletin/hypo.html (in Japanese). The seismograms recorded by the S-net ocean-bottom stations are available at https://www.seafloor.bosai.go.jp/outline/ (in Japanese). The GNSS data recorded by the GEONET stations are available at https://www.gsi.go.jp/ENGLISH/geonet_english.html. The seafloor topography data (Smith and Sandwell 1997) are available at https://topex.ucsd.edu/marine_topo/. The figures are prepared using the Generic Mapping Tools (Wessel et al. 2019), which are available at https://www.generic-mapping-tools.org.

Declarations

Competing interests

The authors declare that they have no competing interests.

Author details

[1]Disaster Prevention Research Institute, Kyoto University, Gokasho, Uji, Kyoto, Japan. [2]Department of Earth and Planetary Science, The University of Tokyo, 7-3-1, Hongo, Bunkyo, Tokyo, Japan.

Received: 12 September 2022 Accepted: 3 December 2022
Published online: 03 January 2023

References

Aguiar AC, Melbourne TI, Scrivner CW (2009) Moment release rate of Cascadia tremor constrained by GPS. J Geophys Res 114(B7):B00A05. https://doi.org/10.1029/2008JB005909

Aki K (1967) Scaling law of seismic spectrum. J Geophys Res 72(4):1217–1231. https://doi.org/10.1029/JZ072i004p01217

Alwahedi MA, Hawthorne JC (2019) Intermediate-magnitude postseismic slip follows intermediate-magnitude (*M* 4 to 5) earthquakes in California. Geophys Res Lett 46(7):3676–3687. https://doi.org/10.1029/2018GL081001

Ando R, Takeda N, Yamashita T (2012) Propagation dynamics of seismic and aseismic slip governed by fault heterogeneity and Newtonian rheology. J Geophys Res 117(B11):B11308. https://doi.org/10.1029/2012JB009532

Ando R, Imanishi K. (2011) Possibility of M_w 9.0 mainshock triggered by diffusional propagation of after-slip from M_w 7.3 foreshock. Earth Planet Space 63(7):767–771. doi:/https://doi.org/10.5047/eps.2011.05.016.

Andrews DJ (2002) A fault constitutive relation accounting for thermal pressurization of pore fluid. J Geophys Res 107(B12):2363. https://doi.org/10.1029/2002JB001942

Annoura S, Hashimoto T, Kamaya N, Katsumata A (2017) Shallow episodic tremor near the Nankai Trough axis off southeast Mie prefecture. Japan Geophys Res Lett 44(8):3564–3571. https://doi.org/10.1002/2017GL073006

Araki E, Saffer DM, Kopf AJ, Wallace LM, Kimura T, Machida Y, Ide S, Davis E, IODP Expedition 365 Shipboard Scientists (2017) Recurring and triggered slow-slip events near the trench at the Nankai Trough subduction megathrust. Science 356(6343):1157–1160. https://doi.org/10.1126/science.aan3120

Asano Y, Obara K, Ito Y (2008) Spatiotemporal distribution of very-low frequency earthquakes in Tokachi-oki near the junction of the Kuril and Japan trenches revealed by using array signal processing. Earth Planet Space 60(8):871–875. https://doi.org/10.1186/BF03352839

Aso N, Ando R, Ide S (2019) Ordinary and slow earthquakes reproduced in a simple continuum system with stochastic temporal stress fluctuations. Geophys Res Lett 46(24):14347–14357. https://doi.org/10.1029/2019GL085010

Azuma R, Hino R, Ohta Y, Ito Y, Mochizuki K, Uehira K, Murai Y, Sato T, Takanami T, Shinohara M, Kanazawa T (2018) Along-arc heterogeneity of the seismic structure around a large coseismic shallow slip area of the 2011 Tohoku-Oki earthquake: 2-D Vp structural estimation through an air gun-ocean bottom seismometer experiment in the Japan Trench Subduction Zone. J Geophys Res 123(6):5249–5264. https://doi.org/10.1029/2017JB015361

Baba T, Tanioka Y, Cummins PR, Uhira K (2002) The slip distribution of the 1946 Nankai earthquake estimated from tsunami inversion using a new plate model. Phys Earth Planet Inter 132:59–73. https://doi.org/10.1016/S0031-9201(02)00044-4

Baba S, Takeo A, Obara K, Matsuzawa T, Maeda T (2020) Comprehensive detection of very low frequency earthquakes off the Hokkaido and Tohoku Pacific coasts, northeastern Japan. J Geophys Res 125(1):e2019JB017988. https://doi.org/10.1029/2019JB017988

Barbot S (2019) Slow-slip, slow earthquakes, period-two cycles, full and partial ruptures, and deterministic chaos in a single asperity fault. Tectonophysics 768:228171. https://doi.org/10.1016/j.tecto.2019.228171

Barbot S (2020) Frictional and structural controls of seismic super-cycles at the Japan trench. Earth Planet Space 72:63. https://doi.org/10.1186/s40623-020-01185-3

Bartlow NM, Miyazaki SI, Bradley AM, Segall P (2011) Space-time correlation of slip and tremor during the 2009 Cascadia slow slip event. Geophys Res Lett 38(18):L18309. https://doi.org/10.1029/2011GL048714

Bassett D, Sandwell DT, Fialko Y, Watts AB (2016) Upper-plate controls on co-seismic slip in the 2011 magnitude 9.0 Tohoku-oki earthquake. Nature 531(7592):92–96. https://doi.org/10.1038/nature16945

Beeler NM, Lockner DL, Hickman SH (2001) A simple stick-slip and creep-slip model for repeating earthquakes and its implication for microearthquakes at Parkfield. Bull Seismol Soc Am 91(6):1797–1804. https://doi.org/10.1785/0120000096

Behr WM, Bürgmann R (2021) What's down there? The structures, materials and environment of deep-seated slow slip and tremor. Philos Trans R Soc A 379(2193):20200218. https://doi.org/10.1098/rsta.2020.0218

Behr WM, Kotowski AJ, Ashley KT (2018) Dehydration-induced rheological heterogeneity and the deep tremor source in warm subduction zones. Geology 46(5):475–478. https://doi.org/10.1130/G40105.1

Beroza GC, Ide S (2011) Slow earthquakes and nonvolcanic tremor. Annu Rev Earth Planet Sci 39:271–296. https://doi.org/10.1146/annurev-earth-040809-152531

Bird P (2003) An updated digital model of plate boundaries. Geochem Geophys Geosyst 4(3):1027. https://doi.org/10.1029/2001GC000252

Bostock MG, Thomas AM, Savard G, Chuang L, Rubin AM (2015) Magnitudes and moment-duration scaling of low-frequency earthquakes beneath southern Vancouver Island. J Geophys Res 120(9):6329–6350. https://doi.org/10.1002/2015JB012195

Bouchon M, Karabulut H, Aktar M, Özalaybey S, Schmittbuhl J, Bouin MP (2011) Extended nucleation of the 1999 M_w 7.6 Izmit earthquake. Science 331(6019):877–880. https://doi.org/10.1126/science.1197341

Bürgmann R (2018) The geophysics, geology and mechanics of slow fault slip. Earth Planet Sci Lett 495:112–134. https://doi.org/10.1016/j.epsl.2018.04.062

Bürgmann R, Uchida N, Hu Y, Matsuzawa T (2016) Tohoku rupture reloaded? Nat Geosci 9(3):183–183. https://doi.org/10.1038/ngeo2649

Chang TW, Ide S (2021) Hypocenter hotspots illuminated using a new cross-correlation-based hypocenter and centroid relocation method. J Geophys Res 126(9):e2021JB021991. https://doi.org/10.1029/2021JB021991

Chen T, Lapusta N (2009) Scaling of small repeating earthquakes explained by interaction of seismic and aseismic slip in a rate and state fault model. J Geophys Res 114(B1):B01311. https://doi.org/10.1029/2008JB005749

Chester FM, Mori JJ, Eguchi N, Toczko S, Expedition 343/343T Scientists (2013) Integrated Ocean Drilling Program, vol 343/343T (Integrated Ocean Drilling Program Management International, Inc.)

Collot JY, Sanclemente E, Nocquet JM, Leprêtre A, Ribodetti A, Jarrin P, Chlieh M, Graindorge D, Charvis P (2017) Subducted oceanic relief locks the shallow megathrust in central Ecuador. J Geophys Res 122(5):3286–3305. https://doi.org/10.1002/2016JB013849

Das S, Aki K (1977) Fault plane with barriers: A versatile earthquake model. J Geophys Res 82(36):5658–5670. https://doi.org/10.1029/JB082i036p05658

Delahaye EJ, Townend J, Reyners ME, Rogers G (2009) Microseismicity but no tremor accompanying slow slip in the Hikurangi subduction zone, New Zealand. Earth Planet Sci Lett 277(1–2):21–28. https://doi.org/10.1016/j.epsl.2008.09.038

Delph JR, Levander A, Niu F (2018) Fluid controls on the heterogeneous seismic characteristics of the Cascadia margin. Geophys Res Lett 45(20):11–021. https://doi.org/10.1029/2018GL079518

Dieterich JH (1979) Modeling of rock friction: 1. Experimental results and constitutive equations. J Geophys Res 84(B5):2161–2168. https://doi.org/10.1029/JB084iB05p02161

Dieterich JH (1992) Earthquake nucleation on faults with rate-and state-dependent strength. Tectonophysics 211(1–4):115–134. https://doi.org/10.1016/0040-1951(92)90055-B

Dieterich J (1994) A constitutive law for rate of earthquake production and its application to earthquake clustering. J Geophys Res 99(B2):2601–2618. https://doi.org/10.1029/93JB02581

Dragert H, Wang K, James TS (2001) A silent slip event on the deeper Cascadia subduction interface. Science 292(5521):1525–1528. https://doi.org/10.1126/science.1060152

Dragert H, Wang K, Rogers G (2004) Geodetic and seismic signatures of episodic tremor and slip in the northern Cascadia subduction zone. Earth Planet Space 56(12):1143–1150. https://doi.org/10.1186/BF03353333

Earthquake Research Center, The University of Tokyo (2005) Miyagi-oki earthquake (Mj7.2) on August 16 (in Japanese), EIC seismological note No.168. http://wwweic.eri.u-tokyo.ac.jp/sanchu/Seismo_Note/2005/EIC168.html. Accessed 19 July 2022

Frank WB, Brodsky EE (2019) Daily measurement of slow slip from low-frequency earthquakes is consistent with ordinary earthquake scaling. Sci Adv 5(10):eaaw9386. https://doi.org/10.1126/sciadv.aaw9386

Frank WB, Rousset B, Lasserre C, Campillo M (2018) Revealing the cluster of slow transients behind a large slow slip event. Sci Adv 4(5):eaat0661. https://doi.org/10.1126/sciadv.aat0661

Fujie G, Kasahara J, Hino R, Sato T, Shinohara M, Suyehiro K (2002) A significant relation between seismic activities and reflection intensities in the Japan Trench region. Geophys Res Lett 29(7):1100. https://doi.org/10.1029/2001GL013764

Fujie G, Kodaira S, Nakamura Y, Morgan JP, Dannowski A, Thorwart M, Grevemeyer I, Miura S (2020) Spatial variations of incoming sediments at the northeastern Japan arc and their implications for megathrust earthquakes. Geology 48(6):614–619. https://doi.org/10.1130/G46757.1

Fujiwara T, Kodaira S, No T, Kaiho Y, Takahashi N, Kaneda Y (2011) The 2011 Tohoku-Oki earthquake: displacement reaching the trench axis. Science 334(6060):1240–1240. https://doi.org/10.1126/science.12115

Fujiwara T, dos Santos FC, Bachmann AK, Strasser M, Wefer G, Sun T, Kanamatsu T, Kodaira S (2017) Seafloor displacement after the 2011 Tohoku-Oki earthquake in the northern Japan trench examined by repeated bathymetric surveys. Geophys Res Lett 44(23):11–833. https://doi.org/10.1002/2017GL075839

Fujiwara S, Tobita M, Ozawa S (2022) Spatiotemporal functional modeling of postseismic deformations after the 2011 Tohoku-Oki earthquake. Earth Planet Space 74:13. https://doi.org/10.1186/s40623-021-01568-0

Fukao Y, Kubota T, Sugioka H, Ito A, Tonegawa T, Shiobara H, Yamashita M, Saito T (2021) Detection of "rapid" aseismic slip at the Izu-Bonin Trench. J Geophys Res 126(9):e2021JB022132. https://doi.org/10.1029/2021JB022132

Fukuda JI (2018) Variability of the space-time evolution of slow slip events off the Boso Peninsula, central Japan, from 1996 to 2014. J Geophys Res 123(1):732–760. https://doi.org/10.1002/2017JB014709

Gardonio B, Marsan D, Socquet A, Bouchon M, Jara J, Sun Q, Cotte N, Campillo M (2018) Revisiting slow slip events occurrence in Boso Peninsula, Japan, combining GPS data and repeating earthquakes analysis. J Geophys Res Solid Earth 123(2):1502–1515. https://doi.org/10.1002/2017JB014469

Geospatial Information Authority of Japan (GSI) (2011) Estimated slip deficit distribution in northeast and southwest Japan (in Japanese). Report of Coordinating Committee for Earthquake Prediction 86:226
Ghosh A, Huesca-Pérez E, Brodsky E, Ito Y (2015) Very low frequency earthquakes in Cascadia migrate with tremor. Geophys Res Lett 42(9):3228–3232. https://doi.org/10.1002/2015GL063286
Goebel THW, Schorlemmer D, Becker TW, Dresen G, Sammis CG (2013) Acoustic emissions document stress changes over many seismic cycles in stick-slip experiments. Geophys Res Lett 40(10):2049–2054. https://doi.org/10.1002/grl.50507
Gomberg J, Wech A, Creager K, Obara K, Agnew D (2016) Reconsidering earthquake scaling. Geophys Res Lett 43(12):6243–6251. https://doi.org/10.1002/2016GL069967
Gutenberg B, Richter CF (1944) Frequency of earthquakes in California. Bull Seismol Soc Am 34(4):185–188. https://doi.org/10.1785/BSSA0340040185
Hasegawa A, Nakajima J, Kita S, Okada T, Matsuzawa T, Kirby SH (2007) Anomalous deepening of a belt of intraslab earthquakes in the Pacific slab crust under Kanto, central Japan: possible anomalous thermal shielding, dehydration reactions, and seismicity caused by shallower cold slab material. Geophys Res Lett 34(9):L09305. https://doi.org/10.1029/2007GL029616
Hashimoto C, Noda A, Sagiya T, Matsu'ura M (2009) Interplate seismogenic zones along the Kuril–Japan trench inferred from GPS data inversion. Nat Geosci 2(2):141–144. https://doi.org/10.1038/ngeo421
Heki K, Miyazaki SI, Tsuji H (1997) Silent fault slip following an interplate thrust earthquake at the Japan Trench. Nature 386(6625):595–598. https://doi.org/10.1038/386595a0
Heuret A, Conrad CP, Funiciello F, Lallemand S, Sandri L (2012) Relation between subduction megathrust earthquakes, trench sediment thickness and upper plate strain. Geophys Res Lett 39(5):L05304. https://doi.org/10.1029/2011GL050712
Hino R, Kanazawa T, Hasegawa A (1996) Interplate seismic activity near the northern Japan Trench deduced from ocean bottom and land-based seismic observations. Phys Earth Planet Inter 93(1–2):37–52. https://doi.org/10.1016/0031-9201(95)03087-5
Hino R, Ito S, Shiobara H, Shimamura H, Sato T, Kanazawa T, Kasahara J, Hasegawa A (2000) Aftershock distribution of the 1994 Sanriku-oki earthquake (M_w 7.7) revealed by ocean bottom seismographic observation. J Geophys Res Solid Earth 105(B9):21697–21710. https://doi.org/10.1029/2000JB900174
Hino R, Inazu D, Ohta Y, Ito Y, Suzuki S, Iinuma T, Osada Y, Kdo M, Fujimoto H, Kaneda Y (2014) Was the 2011 Tohoku-Oki earthquake preceded by aseismic preslip? Examination of seafloor vertical deformation data near the epicenter. Mar Geophys Res 35(3):181–190
Hirano N (2011) Petit-spot volcanism: a new type of volcanic zone discovered near a trench. Geochem J 45(2):157–167. https://doi.org/10.2343/geochemj.1.0111
Hirano N, Takahashi E, Yamamoto J, Abe N, Ingle SP, Kaneoka I, Hirata T, Kimura J, Ishii T, Ogawa Y, Machida S, Suyehiro K (2006) Volcanism in response to plate flexure. Science 313(5792):1426–1428. https://doi.org/10.1126/science.1128235
Hirono T, Tsuda K, Tanikawa W, Ampuero JP, Shibazaki B, Kinoshita M, Mori JJ (2016) Near-trench slip potential of megaquakes evaluated from fault properties and conditions. Sci Rep 6:28184. https://doi.org/10.1038/srep28184
Hirose H, Obara K (2005) Repeating short-and long-term slow slip events with deep tremor activity around the Bungo channel region, southwest Japan. Earth Planet Space 57(10):961–972. https://doi.org/10.1186/BF03351875
Hirose H, Obara K (2010) Recurrence behavior of short-term slow slip and correlated nonvolcanic tremor episodes in western Shikoku, southwest Japan. J Geophys Res. https://doi.org/10.1029/2008JB006050
Hirose H, Hirahara K, Kimata F, Fujii N, Miyazaki SI (1999) A slow thrust slip event following the two 1996 Hyuganada earthquakes beneath the Bungo Channel, southwest Japan. Geophys Res Lett 26(21):3237–3240. https://doi.org/10.1029/1999GL010999
Hirose I, Kawasaki I, Okada Y, Sagiya T, Tamura Y (2000) A silent earthquake of December 9, 1989, in the Tokyo Bay, as revealed by the continuous observation of crustal movements in southern Kanto district, central Japan (in Japanese with English abstract and figure captions). Zisin (j Seismol Soc Jpn) 53(1):11–23. https://doi.org/10.4294/zisin1948.53.1_11
Hirose F, Nakajima J, Hasegawa A (2008) Three-dimensional seismic velocity structure and configuration of the Philippine Sea slab in southwestern Japan estimated by double-difference tomography. J Geophys Res 113:B09315. https://doi.org/10.1029/2007JB005274
Hirose F, Tamaribuchi K, Maeda K (2021) Characteristics of foreshocks revealed by an earthquake forecasting method based on precursory swarm activity. J Geophys Res 126(9):e2021JB021673. https://doi.org/10.1029/2021JB021673
Holtkamp SG, Brudzinski MR (2011) Earthquake swarms in circum-Pacific subduction zones. Earth Planet Sci Lett 305(1–2):215–225. https://doi.org/10.1016/j.epsl.2011.03.004
Honsho C, Kido M, Tomita F, Uchida N (2019) Offshore postseismic deformation of the 2011 Tohoku earthquake revisited: application of an improved GPS-acoustic positioning method considering horizontal gradient of sound speed structure. J Geophys Res 124(6):5990–6009. https://doi.org/10.1029/2018JB017135
Houston H, Delbridge BG, Wech AG, Creager KC (2011) Rapid tremor reversals in Cascadia generated by a weakened plate interface. Nat Geosci 4(6):404–409. https://doi.org/10.1038/ngeo1157
Hua Y, Zhao D, Toyokuni G, Xu Y (2020) Tomography of the source zone of the great 2011 Tohoku earthquake. Nat Commun 11:1163. https://doi.org/10.1038/s41467-020-14745-8
Hughes L, Chamberlain CJ, Townend J, Thomas AM (2021) A repeating earthquake catalog from 2003 to 2020 for the Raukumara Peninsula, northern Hikurangi subduction margin, New Zealand. Geochem Geophys Geosyst 22(5):e2021GC009670. https://doi.org/10.1029/2021GC009670
Hyndman RD, Peacock SM (2003) Serpentinization of the forearc mantle. Earth Planet Sci Lett 212(3–4):417–432. https://doi.org/10.1016/S0012-821X(03)00263-2
Ide S (2008) A Brownian walk model for slow earthquakes. Geophys Res Lett 35(17):L17301. https://doi.org/10.1029/2008GL034821
Ide S (2010) Striations, duration, migration and tidal response in deep tremor. Nature 466(7304):356–359. https://doi.org/10.1038/nature09251
Ide S (2013) The proportionality between relative plate velocity and seismicity in subduction zones. Nat Geosci 6(9):780–784. https://doi.org/10.1038/ngeo1901
Ide S (2014) Modeling fast and slow earthquakes at various scales. Proc Jpn Acad Ser B 90(8):259–277. https://doi.org/10.2183/pjab.90.259
Ide S (2016) Characteristics of slow earthquakes in the very low frequency band: application to the Cascadia subduction zone. J Geophys Res 121(8):5942–5952. https://doi.org/10.1002/2016JB013085
Ide S (2019a) Frequent observations of identical onsets of large and small earthquakes. Nature 573(7772):112–116. https://doi.org/10.1038/s41586-019-1508-5
Ide S (2019b) Detection of low-frequency earthquakes in broadband random time sequences: are they independent events? J Geophys Res 124(8):8611–8625. https://doi.org/10.1029/2019JB017643
Ide S, Aochi H (2005) Earthquakes as multiscale dynamic ruptures with heterogeneous fracture surface energy. J Geophys Res 110:B11303. https://doi.org/10.1029/2004JB003591
Ide S, Aochi H (2013) Historical seismicity and dynamic rupture process of the 2011 Tohoku-Oki earthquake. Tectonophysics 600:1–13. https://doi.org/10.1016/j.tecto.2012.10.018
Ide S, Yabe S (2014) Universality of slow earthquakes in the very low frequency band. Geophys Res Lett 41(8):2786–2793. https://doi.org/10.1002/2014GL059712
Ide S, Yabe S (2019) Two-dimensional probabilistic cell automaton model for broadband slow earthquakes. Pure Appl Geophys 176(3):1021–1036. https://doi.org/10.1007/s00024-018-1976-9
Ide S, Imamura F, Yoshida Y, Abe K (1993) Source characteristics of the Nicaraguan tsunami earthquake of September 2, 1992. Geophys Res Lett 20(9):863–866. https://doi.org/10.1029/93GL00683
Ide S, Beroza GC, Shelly DR, Uchide T (2007a) A scaling law for slow earthquakes. Nature 447(7140):76–79. https://doi.org/10.1038/nature05780
Ide S, Imanishi K, Yoshida Y, Beroza GC, Shelly DR (2008) Bridging the gap between seismically and geodetically detected slow earthquakes. Geophys Res Lett 35(10):L10305. https://doi.org/10.1029/2008GL034014

Ide S, Baltay A, Beroza GC (2011) Shallow dynamic overshoot and energetic deep rupture in the 2011 M_w 9.0 Tohoku-Oki earthquake. Science 332(6036):1426–1429

Ide S, Shelly DR, Beroza GC (2007b) Mechanism of deep low frequency earthquakes: Further evidence that deep non-volcanic tremor is generated by shear slip on the plate interface. Geophys Res Lett, 34(3).

Idehara K, Yabe S, Ide S (2014) Regional and global variations in the temporal clustering of tectonic tremor activity. Earth Planet Space 66:66. https://doi.org/10.1186/1880-5981-66-66

Igarashi T (2010) Spatial changes of inter-plate coupling inferred from sequences of small repeating earthquakes in Japan. Geophys Res Lett 37(20):L20304. https://doi.org/10.1029/2010GL044609

Igarashi T (2020) Catalog of small repeating earthquakes for the Japanese Islands. Earth Planet Space 72:73. https://doi.org/10.1186/s40623-020-01205-2

Igarashi T, Matsuzawa T, Hasegawa A (2003) Repeating earthquakes and interplate aseismic slip in the northeastern Japan subduction zone. J Geophys Res 108(B5):2249. https://doi.org/10.1029/2002JB001920

Iinuma T (2018) Monitoring of the spatio-temporal change in the interplate coupling at northeastern Japan subduction zone based on the spatial gradients of surface velocity field. Geophys J Int 213(1):30–47. https://doi.org/10.1093/gji/ggx527

Iinuma T, Hino R, Kido M, Inazu D, Osada Y, Ito Y, Ohzono M, Tsushima H, Suzuki S, Fujimoto H, Miura S (2012) Coseismic slip distribution of the 2011 off the Pacific Coast of Tohoku Earthquake (M9.0) refined by means of seafloor geodetic data. J Geophys Res 117(B7):B07409. https://doi.org/10.1029/2012JB009186

Iinuma T, Hino R, Uchida N, Nakamura W, Kido M, Osada Y, Miura S (2016) Seafloor observations indicate spatial separation of coseismic and postseismic slips in the 2011 Tohoku earthquake. Nat Commun 7:13506. https://doi.org/10.1038/ncomms13506

Ikari MJ, Kopf AJ (2017) Seismic potential of weak, near-surface faults revealed at plate tectonic slip rates. Sci Adv 3(11):e1701269. https://doi.org/10.1126/sciadv.170126

Ikari MJ, Ito Y, Ujiie K, Kopf AJ (2015) Spectrum of slip behaviour in Tohoku fault zone samples at plate tectonic slip rates. Nat Geosci 8(11):870–874. https://doi.org/10.1038/ngeo2547

Ikehara K, Kanamatsu T, Nagahashi Y, Strasser M, Fink H, Usami K, Irino T, Wefer G (2016) Documenting large earthquakes similar to the 2011 Tohoku-oki earthquake from sediments deposited in the Japan Trench over the past 1500 years. Earth Planet Sci Lett 445:48–56. https://doi.org/10.1016/j.epsl.2016.04.009

Ikehara K, Usami K, Kanamatsu T, Arai K, Yamaguchi A, Fukuchi R (2018) Spatial variability in sediment lithology and sedimentary processes along the Japan Trench: use of deep-sea turbidite records to reconstruct past large earthquakes. Geol Soc London Spec Publ 456:75–89. https://doi.org/10.1144/SP456.9

Im K, Saffer D, Marone C, Avouac JP (2020) Slip-rate-dependent friction as a universal mechanism for slow slip events. Nat Geosci 13(10):705–710. https://doi.org/10.1038/s41561-020-0627-9

Ioki K, Tanioka Y (2016) Re-estimated fault model of the 17th century great earthquake off Hokkaido using tsunami deposit data. Earth Planet Sci Lett 433:133–138. https://doi.org/10.1016/j.epsl.2015.10.009

Ishihara Y (2003) Major existence of very low frequency earthquakes in background seismicity along subduction zone of south-western Japan, Eos Trans. AGU, 84(46).

Itaba S, Ando R (2011) A slow slip event triggered by teleseismic surface waves. Geophys Res Lett 38(21):L21306. https://doi.org/10.1029/2011GL049593

Ito Y, Ikari MJ (2015) Velocity- and slip-dependent weakening in simulated fault gouge: implications for multimode fault slip. Geophys Res Lett 42(21):9247–9254. https://doi.org/10.1002/2015GL065829

Ito Y, Obara K (2006) Very low frequency earthquakes within accretionary prisms are very low stress-drop earthquakes. Geophys Res Lett 33(9):L09302. https://doi.org/10.1029/2006GL025883

Ito T, Yoshioka S, Miyazaki SI (2000) Interplate coupling in northeast Japan deduced from inversion analysis of GPS data. Earth Planet Sci Lett 176(1):117–130. https://doi.org/10.1016/S0012-821X(99)00316-7

Ito Y, Obara K, Shiomi K, Sekine S, Hirose H (2007) Slow earthquakes coincident with episodic tremors and slow slip events. Science 315(5811):503–506. https://doi.org/10.1126/science.1134454

Ito Y, Hino R, Kido M, Fujimoto H, Osada Y, Inazu D, Ohta Y, Iinuma T, Ohzono M, Miura S, Mishima M, Suzuki K, Tsuji T, Ashi J (2013) Episodic slow slip events in the Japan subduction zone before the 2011 Tohoku-Oki earthquake. Tectonophysics 600:14–26. https://doi.org/10.1016/j.tecto.2012.08.022

Ito Y, Hino R, Suzuki S, Kaneda Y (2015) Episodic tremor and slip near the Japan Trench prior to the 2011 Tohoku-Oki earthquake. Geophys Res Lett 42(6):1725–1731. https://doi.org/10.1002/2014GL062986

Ito Y, Ikari MJ, Ujiie K, Kopf A (2017) Coseismic slip propagation on the Tohoku plate boundary fault facilitated by slip-dependent weakening during slow fault slip. Geophys Res Lett 44(17):8749–8756. https://doi.org/10.1002/2017GL074307

Itoh Y, Nishimura T, Ariyoshi K, Matsumoto H (2019) Interplate slip following the 2003 Tokachi-oki earthquake from ocean bottom pressure gauge and land GNSS data. J Geophys Res 124(4):4205–4230. https://doi.org/10.1029/2018JB016328

Iwamori H (1998) Transportation of H_2O and melting in subduction zones. Earth Planet Sci Lett 160(1–2):65–80. https://doi.org/10.1016/S0012-821X(98)00080-6

Japan Society of Civil Engineers (2002) Tsunami Assessment Method for Nuclear Power Plants in Japan. Tsunami Eval Subcomm, The Nucl Civil Eng Comm. http://committees.jsce.or.jp/ceofnp/system/files/JSCE_Tsunami_060519.pdf. Accessed 19 July 2022

Kanamori H (1972) Mechanism of tsunami earthquakes. Phys Earth Planet Inter 6(5):346–359. https://doi.org/10.1016/0031-9201(72)90058-1

Kanamori H, Kikuchi M (1993) The 1992 Nicaragua earthquake: a slow tsunami earthquake associated with subducted sediments. Nature 361(6414):714–716. https://doi.org/10.1038/361714a0

Kaneko Y, Avouac JP, Lapusta N (2010) Towards inferring earthquake patterns from geodetic observations of interseismic coupling. Nat Geosci 3(5):363–369. https://doi.org/10.1038/ngeo843

Kaneko L, Ide S, Nakano M (2018) Slow earthquakes in the microseism frequency band (0.1–1.0 Hz) off Kii Peninsula, Japan. Geophys Res Lett 45(6):2618–2624. https://doi.org/10.1002/2017GL076773

Kano M, Aso N, Matsuzawa T, Ide S, Annoura S, Arai R, Baba S, Bostock M, Chao K, Heki K, Itaba S, Ito Y, Kamaya N, Maeda T, Maury J, Nakamura M, Nishimura T, Obana K, Ohta K, Poiata N, Rousset B, Sugioka H, Takagi R, Takahashi T, Takeo A, Tu Y, Uchida N, Yamashita Y, Obara K (2018a) Development of a slow earthquake database. Seismol Res Lett 89(4):1566–1575. https://doi.org/10.1785/0220180021

Kano M, Fukuda JI, Miyazaki SI, Nakamura M (2018b) Spatiotemporal evolution of recurrent slow slip events along the southern Ryukyu subduction zone, Japan, from 2010 to 2013. J Geophys Res 123(8):7090–7107. https://doi.org/10.1029/2018JB016072

Katakami S, Ito Y, Ohta K, Hino R, Suzuki S, Shinohara M (2018) Spatiotemporal variation of tectonic tremor activity before the Tohoku-Oki earthquake. J Geophys Res 123(11):9676–9688. https://doi.org/10.1029/2018JB016651

Katayama I (2016) Water circulation system at subduction zones (in Japanese with English abstract and figure captions). Kazan (bull Volcanol Soc Jpn) 61(1):69–77. https://doi.org/10.18940/kazan.61.1_69

Katayama I, Terada T, Okazaki K, Tanikawa W (2012) Episodic tremor and slow slip potentially linked to permeability contrasts at the Moho. Nat Geosci 5(10):731–734. https://doi.org/10.1038/ngeo1559

Kato N (2004) Interaction of slip on asperities: Numerical simulation of seismic cycles on a two-dimensional planar fault with nonuniform frictional property. J Geophys Res 109(B12):B12306. https://doi.org/10.1029/2004JB003001

Kato A, Nakagawa S (2020) Detection of deep low-frequency earthquakes in the Nankai subduction zone over 11 years using a matched filter technique. Earth Planet Space 72:128. https://doi.org/10.1186/s40623-020-01257-4

Kato A, Obara K, Igarashi T, Tsuruoka H, Nakagawa S, Hirata N (2012) Propagation of slow slip leading up to the 2011 M_w 9.0 Tohoku-Oki earthquake. Science 335(6069):705–708. https://doi.org/10.1126/science.1215141

Kato A, Igarashi T, Obara K (2014) Detection of a hidden Boso slow slip event immediately after the 2011 M_w 9.0 Tohoku-Oki earthquake, Japan. Geophys Res Lett 41(16):5868–5874. https://doi.org/10.1002/2014GL061053

Katsumata A, Kamaya N (2003) Low-frequency continuous tremor around the Moho discontinuity away from volcanoes in the southwest Japan. Geophys Res Lette 30(1):20–21. https://doi.org/10.1029/2002GL015981

Kawasaki I, Asai Y, Tamura Y, Sagiya T, Mikami N, Okada Y, Sakata M, Kasahara M (1995) The 1992 Sanriku-oki, Japan, ultra-slow earthquake. J Phys Earth 43(2):105–116. https://doi.org/10.4294/jpe1952.43.105

Kawasaki I, Asai Y, Tamura Y (2001) Space–time distribution of interplate moment release including slow earthquakes and the seismo-geodetic coupling in the Sanriku-oki region along the Japan trench. Tectonophysics 330(3–4):267–283. https://doi.org/10.1016/S0040-1951(00)00245-6

Ke CY, McLaskey GC, Kammer DS (2018) Rupture termination in laboratory-generated earthquakes. Geophys Res Lett 45(23):12–784. https://doi.org/10.1029/2018GL080492

Khoshmanesh M, Shirzaei M, Nadeau RM (2015) Time-dependent model of aseismic slip on the central San Andreas Fault from InSAR time series and repeating earthquakes. J Geophys Res 120(9):6658–6679. https://doi.org/10.1002/2015JB012039

Khoshmanesh M, Shirzaei M, Uchida N (2020) Deep slow-slip events promote seismicity in northeastern Japan megathrust. Earth Planet Sci Lett 540:116261. https://doi.org/10.1016/j.epsl.2020.116261

Kim A, Dreger DS, Taira TA, Nadeau RM (2016) Changes in repeating earthquake slip behavior following the 2004 Parkfield main shock from waveform empirical Green's functions finite-source inversion. J Geophys Res 121:1910–1926. https://doi.org/10.1002/2015JB012562

Kimura G, Hina S, Hamada Y, Kameda J, Tsuji T, Kinoshita M, Yamaguchi A (2012) Runaway slip to the trench due to rupture of highly pressurized megathrust beneath the middle trench slope: the tsunamigenesis of the 2011 Tohoku earthquake off the east coast of northern Japan. Earth Planet Sci Lett 339:32–45. https://doi.org/10.1016/j.epsl.2012.04.002

Kirkpatrick JD, Fagereng Å, Shelly DR (2021) Geological constraints on the mechanisms of slow earthquakes. Nat Rev Earth Env 2(4):285–301. https://doi.org/10.1038/s43017-021-00148-w

Kita S, Okada T, Hasegawa A, Nakajima J, Matsuzawa T (2010) Anomalous deepening of a seismic belt in the upper-plane of the double seismic zone in the Pacific slab beneath the Hokkaido corner: possible evidence for thermal shielding caused by subducted forearc crust materials. Earth Planet Science Lett 290:415–426. https://doi.org/10.1016/j.epsl.2009.12.038

Kobayashi A (2014) A long-term slow slip event from 1996 to 1997 in the Kii Channel, Japan. Earth Planet Space 66:9. https://doi.org/10.1186/1880-5981-66-9

Kodaira S, Takahashi N, Nakanishi A, Miura S, Kaneda Y (2000) Subducted seamount imaged in the rupture zone of the 1946 Nankaido earthquake. Science 289(5476):104–106. https://doi.org/10.1126/science.289.5476.104

Kodaira S, Iidaka T, Kato A, Park JO, Iwasaki T, Kaneda Y (2004) High pore fluid pressure may cause silent slip in the Nankai Trough. Science 304(5675):1295–1298. https://doi.org/10.1126/science.10965

Kodaira S, No T, Nakamura Y, Fujiwara T, Kaiho Y, Miura S, Takahashi N, Kaneda Y, Taira A (2012) Coseismic fault rupture at the trench axis during the 2011 Tohoku-oki earthquake. Nat Geosci 5(9):646–650. https://doi.org/10.1038/ngeo1547

Kodaira S, Fujiwara T, Fujie G, Nakamura Y, Kanamatsu T (2020) Large coseismic slip to the trench during the 2011 Tohoku-Oki earthquake. Annu Rev Earth Planet Sci 48:321–343. https://doi.org/10.1146/annurev-earth-071719-055216

Kodaira S, Iinuma T, Imai K (2021) Investigating a tsunamigenic megathrust earthquake in the Japan Trench. Science 371(6534):eabe1169. https://doi.org/10.1126/science.abe1169

Koper KD, Hutko AR, Lay T (2011) Along-dip variation of teleseismic short-period radiation from the 11 March 2011 Tohoku earthquake (M_w 9.0). Geophys Res Lett 38(21):L21309. https://doi.org/10.1029/2011GL049689

Kostoglodov V, Singh SK, Santiago JA, Franco SI, Larson KM, Lowry AR, Bilham R (2003) A large silent earthquake in the Guerrero seismic gap, Mexico. Geophys Res Lett 30(15):1807. https://doi.org/10.1029/2003GL017219

Kubo H, Nishikawa T (2020) Relationship of preseismic, coseismic, and post-seismic fault ruptures of two large interplate aftershocks of the 2011 Tohoku earthquake with slow-earthquake activity. Sci Rep 10:12044. https://doi.org/10.1038/s41598-020-68692-x

Kubo H, Asano K, Iwata T (2013) Source-rupture process of the 2011 Ibaraki-Oki, Japan, earthquake (M_w 7.9) estimated from the joint inversion of strong-motion and GPS data: relationship with seamount and Philippine Sea Plate. Geophys Res Lett 40(12):3003–3007. https://doi.org/10.1002/grl.50558

Kurahashi S, Irikura K (2013) Short-period source model of the 2011 M_w 9.0 off the Pacific coast of Tohoku earthquake. Bull Seismol Soc Am 103(2B):1373–1393. https://doi.org/10.1785/0120120157

Lay T (2018) A review of the rupture characteristics of the 2011 Tohoku-oki M_w 9.1 earthquake. Tectonophysics 733:4–36. https://doi.org/10.1016/j.tecto.2017.09.022

Lindsey EO, Mallick R, Hubbard JA, Bradley KE, Almeida RV, Moore JD, Bürgmann R, Hill EM (2021) Slip rate deficit and earthquake potential on shallow megathrusts. Nat Geosci 14(5):321–326. https://doi.org/10.1038/s41561-021-00736-x

Liu Y, Rice JR (2005) Aseismic slip transients emerge spontaneously in three-dimensional rate and state modeling of subduction earthquake sequences. J Geophys Res 110(B8):B08307. https://doi.org/10.1029/2004JB003424

Liu X, Zhao D (2018) Upper and lower plate controls on the great 2011 Tohoku-oki earthquake. Sci Adv 4(6):eaat4396. https://doi.org/10.1126/sciadv.aat4396

Liu Y, Rice JR, Larson KM (2007) Seismicity variations associated with aseismic transients in Guerrero, Mexico, 1995–2006. Earth Planet Sci Lett 262(3–4):493–504. https://doi.org/10.1016/j.epsl.2007.08.018

Llenos AL, McGuire JJ (2011) Detecting aseismic strain transients from seismicity data. J Geophys Res 116(B6):B06305. https://doi.org/10.1029/2010JB007537

Llenos AL, McGuire JJ, Ogata Y (2009) Modeling seismic swarms triggered by aseismic transients. Earth Planet Sci Lett 281(1–2):59–69. https://doi.org/10.1016/j.epsl.2009.02.011

Loveless JP, Meade BJ (2010) Geodetic imaging of plate motions, slip rates, and partitioning of deformation in Japan. J Geophys Res 115(B2):B02410. https://doi.org/10.1029/2008JB006248

Maeda K, Hirose F (2016) Empirical forecast of occurrence of mainshocks based on foreshock activities (in Japanese with English figure captions). Report of the Coordinating Committee for Earthquake Prediction vol 95, pp 415–419

Marsan D, Reverso T, Helmstetter A, Enescu B (2013) Slow slip and aseismic deformation episodes associated with the subducting Pacific plate offshore Japan, revealed by changes in seismicity. J Geophys Res 118(9):4900–4909. https://doi.org/10.1002/jgrb.50323

Masuda K, Ide S, Ohta K, Matsuzawa T (2020) Bridging the gap between low-frequency and very-low-frequency earthquakes. Earth Planet Space 72:47. https://doi.org/10.1186/s40623-020-01172-8

Matsumura S (2010) Discrimination of a preparatory stage leading to M7 characteristic earthquakes off Ibaraki Prefecture, Japan. J Geophys Res 115(B1):B01301. https://doi.org/10.1029/2009JB006584

Matsuzawa T, Igarashi T, Hasegawa A (2002) Characteristic small-earthquake sequence off Saiku, northeastern Honshu, Japan. Geophys Res Lett 29(11):38. https://doi.org/10.1029/2001GL014632

Matsuzawa T, Uchida N, Igarashi T, Okada T, Hasegawa A (2004) Repeating earthquakes and quasi-static slip on the plate boundary east off northern Honshu, Japan. Earth Planet Space 56(8):803–811. https://doi.org/10.1186/BF03353087

Matsuzawa T, Asano Y, Obara K (2015) Very low frequency earthquakes off the Pacific coast of Tohoku, Japan. Geophys Res Lett 42(11):4318–4325. https://doi.org/10.1002/2015GL063959

Mavrommatis AP, Segall P, Johnson KM (2014) A decadal-scale deformation transient prior to the 2011 M_w 9.0 Tohoku-oki earthquake. Geophys Res Lett 41(13):4486–4494. https://doi.org/10.1002/2014GL060139

Mavrommatis AP, Segall P, Uchida N, Johnson KM (2015) Long-term acceleration of aseismic slip preceding the M_w 9 Tohoku-oki earthquake: constraints from repeating earthquakes. Geophys Res Lett 42(22):9717–9725. https://doi.org/10.1002/2015GL066069

McGuire JJ, Collins JA, Davis E, Becker K, Heesemann M (2018) A lack of dynamic triggering of slow slip and tremor indicates that the shallow Cascadia megathrust offshore Vancouver Island is likely locked. Geophys Res Lett 45(20):11095–11103. https://doi.org/10.1029/2018GL079519

McLaskey GC (2019) Earthquake initiation from laboratory observations and implications for foreshocks. J Geophys Res 124(12):12882–12904. https://doi.org/10.1029/2019JB018363

Michel S, Gualandi A, Avouac JP (2019) Similar scaling laws for earthquakes and Cascadia slow-slip events. Nature 574(7779):522–526. https://doi.org/10.1038/s41586-019-1673-6

Mitsui Y, Kato N, Fukahata Y, Hirahara K (2012) Megaquake cycle at the Tohoku subduction zone with thermal fluid pressurization near the surface. Earth Planet Sci Lett 325:21–26. https://doi.org/10.1016/j.epsl.2012.01.026

Miura S, Iinuma T, Yui S, Uchida N, Sato T, Tachibana K, Hasegawa A (2006) Co- and post-seismic slip associated with the 2005 Miyagi-oki earthquake (M7.2) as inferred from GPS data. Earth Planet Space 58(12):1567–1572. https://doi.org/10.1186/BF03352662

Miura S, Tachibana K, Sato T, Hashimoto K, Mishina M, Hirasawa T (1993) Post-seismic slip events following interplate thrust earthquakes occurring in subduction zone. Abstract B56 presented at the Seismological Society of Japan Fall Meeting 1993

Miura S, Tachibana K, Sato T, Hashimoto K, Mishina M, Kato N, Hirasawa T (1994) Postseismic slip events following interplate thrust earthquake occurring in subduction zone.In: Proceedings of the eighth international symposium on recent crustal movements, pp 84–85.

Miyazaki SI, Segall P, Fukuda J, Kato T (2004) Space time distribution of afterslip following the 2003 Tokachi-oki earthquake: implications for variations in fault zone frictional properties. Geophys Res Lett 31(6):L06623. https://doi.org/10.1029/2003GL019410

Miyazaki SI, Segall P, McGuire JJ, Kato T, Hatanaka Y (2006) Spatial and temporal evolution of stress and slip rate during the 2000 Tokai slow earthquake. J Geophys Res 111(B3):B03409. https://doi.org/10.1029/2004JB003426

Miyazawa M, Mori J (2005) Detection of triggered deep low-frequency events from the 2003 Tokachi-oki earthquake. Geophys Res Lett 32(10):L10307. https://doi.org/10.1029/2005GL022539

Mochizuki K (2017) Relationship between heterogeneity of plate interface- and seismicity at subduction zones: the Japan Trench and Hikurangi subduction zones as examples (in Japanese with English abstract and figure captions). J Geosci (chigaku Zasshi) 126(2):207–221. https://doi.org/10.5026/jgeography.126.207

Mochizuki K, Nakamura M, Kasahara J, Hino R, Nishino M, Kuwano A, Nakamura Y, Yamada T, Shinohara M, Sato T, Moghaddam PP, Kanazawa T (2005) Intense PP reflection beneath the aseismic forearc slope of the Japan Trench subduction zone and its implication of aseismic slip subduction. J Geophys Res 110(B1):B01302. https://doi.org/10.1029/2003JB002892

Mochizuki K, Yamada T, Shinohara M, Yamanaka Y, Kanazawa T (2008) Weak interplate coupling by seamounts and repeating $M \sim 7$ earthquakes. Science 321(5893):1194–1197. https://doi.org/10.1126/science.1160250

Müller RD, Sdrolias M, Gaina C, Roest WR (2008) Age, spreading rates, and spreading asymmetry of the world's ocean crust. Geochem Geophys Geosyst 9(4):Q04006. https://doi.org/10.1029/2007GC001743

Murotani T, Kikuchi M, Yamanaka Y (2003) Rupture processes of large Fukushima-oki earthquakes in 1938. Abstract S052-003 presented at Japan Earth Planetary Science Joint Meeting 2003, Makuhari, Japan, 26–29 May 2003. https://www2.jpgu.org/meeting/2003/index.htm. Accessed 19 July 2022

Nadeau RM, Johnson LR (1998) Seismological studies at Parkfield VI: moment release rates and estimates of source parameters for small repeating earthquakes. Bull Seismol Soc Am 88(3):790–814. https://doi.org/10.1785/BSSA0880030790

Nadeau RM, McEvilly TV (1999) Fault slip rates at depth from recurrence intervals of repeating microearthquakes. Science 285(5428):718–721. https://doi.org/10.1126/science.285.5428.718

Nadeau RM, McEvilly TV (2004) Periodic pulsing of characteristic microearthquakes on the San Andreas fault. Science 303(5655):220–222. https://doi.org/10.1126/science.1090353

Nagai R, Kikuchi M, Yamanaka Y (2001) Comparative study on the source processes of recurrent large earthquakes in Sanriku-oki Region: the 1968 Tokachi-oki earthquake and the 1994 Sanriku-oki earthquake (in Japanese with English abstract and figure captions). Zisin (j Seismol Soc Jpn) 54(2):267–280

Nakajima J, Hasegawa A (2006) Anomalous low-velocity zone and linear alignment of seismicity along it in the subducted Pacific slab beneath Kanto, Japan: reactivation of subducted fracture zone? Geophys Res Lett 33:L16309. https://doi.org/10.1029/2006GL026773

Nakajima J, Hasegawa A (2007) Subduction of the Philippine Sea plate beneath southwestern Japan: slab geometry and its relationship to arc magmatism. J Geophys Res 112:B08306. https://doi.org/10.1029/2006JB004770

Nakajima J, Hasegawa A (2016) Tremor activity inhibited by well-drained conditions above a megathrust. Nat Commun 7:13863. https://doi.org/10.1038/ncomms13863

Nakajima J, Hirose F, Hasegawa A (2009) Seismotectonics beneath the Tokyo metropolitan area, Japan: effect of slab-slab contact and overlap on seismicity. J Geophys Res 114:B08309. https://doi.org/10.1029/2008JB006101

Nakamura W, Uchida N, Matsuzawa T (2016) Spatial distribution of the faulting types of small earthquakes around the 2011 Tohoku-oki earthquake: a comprehensive search using template events. J Geophys Res 121(4):2591–2607. https://doi.org/10.1002/2015JB012584

Nakata R, Suda N, Tsuruoka H (2008) Non-volcanic tremor resulting from the combined effect of Earth tides and slow slip events. Nat Geosci 1(10):676–678. https://doi.org/10.1038/ngeo288

Nakata R, Ando R, Hori T, Ide S (2011) Generation mechanism of slow earthquakes: numerical analysis based on a dynamic model with brittle-ductile mixed fault heterogeneity. J Geophys Res 116(B8):B08308. https://doi.org/10.1029/2010JB008188

Nakata R, Hori T, Miura S, Hino R (2021) Presence of interplate channel layer controls of slip during and after the 2011 Tohoku-Oki earthquake through the frictional characteristics. Sci Rep 11:6480. https://doi.org/10.1038/s41598-021-86020-9

Nakayama W, Takeo M (1997) Slip history of the 1994 Sanriku-Haruka-Oki, Japan, earthquake deduced from strong-motion data. Bull Seismol Soc Am 87(4):918–931. https://doi.org/10.1785/BSSA0870040918

Namiki A, Yamaguchi T, Sumita I, Suzuki T, Ide S (2014) Earthquake model experiments in a viscoelastic fluid: a scaling of decreasing magnitudes of earthquakes with depth. J Geophys Res 119(4):3169–3181. https://doi.org/10.1002/2014JB011135

Nanayama F, Satake K, Furukawa R, Shimokawa K, Atwater BF, Shigeno K, Yamaki S (2003) Unusually large earthquakes inferred from tsunami deposits along the Kuril trench. Nature 424(6949):660–663. https://doi.org/10.1038/nature01864

Nanjo KZ, Hirata N, Obara K, Kasahara K (2012) Decade-scale decrease in *b* value prior to the *M*9-class 2011 Tohoku and 2004 Sumatra quakes. Geophys Res Lett 39(20):L20304. https://doi.org/10.1029/2012GL052997

National Research Institute for Earth Science and Disaster Resilience (NIED) (2019a) NIED S-net, National Research Institute for Earth Science and Disaster Resilience. DOI: https://doi.org/10.17598/nied.0005

National Research Institute for Earth Science and Disaster Resilience (NIED) (2019b) NIED F-net, National Research Institute for Earth Science and Disaster Resilience. DOI: https://doi.org/10.17598/nied.0007

National Research Institute for Earth Science and Disaster Resilience (NIED) (2019c) NIED Hi-net, National Research Institute for Earth Science and Disaster Resilience. DOI: https://doi.org/10.17598/nied.0003

Nishide N, Hashimoto T, Funasaki J, Nakazawa H, Oka M, Ueno H, Yamada N, Sasakawa I, Maeda K, Sugimoto K, Takashima T (2000) Nationwide activity of low-frequency earthquakes in the lower crust in Japan. Abstract Sk-P002 presented at the Jpn Earth Planet Sci Joint Meeting 2000, Tokyo, Japan, 25–28 June 2003. Accessed 20 July 2022

Nishikawa T, Ide S (2014) Earthquake size distribution in subduction zones linked to slab buoyancy. Nat Geosci 7(12):904–908. https://doi.org/10.1038/ngeo2279

Nishikawa T, Ide S (2017) Detection of earthquake swarms at subduction zones globally: insights into tectonic controls on swarm activity. J Geophys Res 122(7):5325–5343. https://doi.org/10.1002/2017JB014188

Nishikawa T, Ide S (2018) Recurring slow slip events and earthquake nucleation in the source region of the *M* 7 Ibaraki-Oki earthquakes revealed by earthquake swarm and foreshock activity. J Geophys Res 123(9):7950–7968. https://doi.org/10.1029/2018JB015642

Nishikawa T, Matsuzawa T, Ohta K, Uchida N, Nishimura T, Ide S (2019) The slow earthquake spectrum in the Japan Trench illuminated by the S-net seafloor observatories. Science 365(6455):808–813. https://doi.org/10.1126/science.aax5618

Nishikawa T, Nishimura T, Okada Y (2021) Earthquake swarm detection along the Hikurangi Trench, New Zealand: insights into the relationship between seismicity and slow slip events. J Geophys Res 126(4):e2020JB020618. https://doi.org/10.1029/2020JB020618
Nishimura T (2014) Short-term slow slip events along the Ryukyu Trench, southwestern Japan, observed by continuous GNSS. Prog Earth Planet Sci 1:22. https://doi.org/10.1186/s40645-014-0022-5
Nishimura T (2021) Slow slip events in the kanto and tokai regions of central Japan detected using global navigation satellite system data during 1994–2020. Geochem Geophys Geosyst 22(2):e2020GC009329. https://doi.org/10.1029/2020GC009329
Nishimura T, Miura S, Tachibana K, Hashimoto K, Sato T, Hori S, Murakami E, Kono T, Nida K, Mishina M, Hirasawa T, Miyazaki SI (2000) Distribution of seismic coupling on the subducting plate boundary in northeastern Japan inferred from GPS observations. Tectonophysics 323(3–4):217–238. https://doi.org/10.1016/S0040-1951(00)00108-6
Nishimura T, Hirasawa T, Miyazaki SI, Sagiya T, Tada T, Miura S, Tanaka K (2004) Temporal change of interplate coupling in northeastern Japan during 1995–2002 estimated from continuous GPS observations. Geophys J Int 157(2):901–916. https://doi.org/10.1111/j.1365-246X.2004.02159.x
Nishimura T, Matsuzawa T, Obara K (2013) Detection of short-term slow slip events along the Nankai Trough, southwest Japan, using GNSS data. J Geophys Res 118(6):3112–3125. https://doi.org/10.1002/jgrb.50222
Nishizawa A, Kanazawa T, Iwasaki T, Shimamura H (1992) Spatial distribution of earthquakes associated with the Pacific plate subduction off northeastern Japan revealed by ocean bottom and land observation. Phys Earth Planet Inter 75:168–175. https://doi.org/10.1016/0031-9201(92)90127-H
Noda H, Lapusta N (2013) Stable creeping fault segments can become destructive as a result of dynamic weakening. Nature 493(7433):518–521. https://doi.org/10.1038/nature11703
Noda H, Nakatani M, Hori T (2013) Large nucleation before large earthquakes is sometimes skipped due to cascade-up—implications from a rate and state simulation of faults with hierarchical asperities. J Geophys Res 118(6):2924–2952. https://doi.org/10.1002/jgrb.50211
Nomura S, Ogata Y, Uchida N, Matsu'ura M (2016) Spatiotemporal variations of interplate slip rates in northeast Japan inverted from recurrence intervals of repeating earthquakes. Geophys J Int 208(1):468–481. https://doi.org/10.1093/gji/ggw395
Obana K, Nakamura Y, Fujie G, Kodaira S, Kaiho Y, Yamamoto Y, Miura S (2018) Seismicity in the source areas of the 1896 and 1933 Sanriku earthquakes and implications for large near-trench earthquake faults. Geophys J Int 212(3):2061–2072. https://doi.org/10.1093/gji/ggx532
Obana K, Fujie G, Yamamoto Y, Kaiho Y, Nakamura Y, Miura S, Kodaira S (2021) Seismicity around the trench axis and outer-rise region of the southern Japan Trench, south of the main rupture area of the 2011 Tohoku-oki earthquake. Geophys J Int 226(1):131–145. https://doi.org/10.1093/gji/ggab093
Obara K (2002) Nonvolcanic deep tremor associated with subduction in southwest Japan. Science 296(5573):1679–1681. https://doi.org/10.1126/science.1070378
Obara K (2010) Phenomenology of deep slow earthquake family in southwest Japan: spatiotemporal characteristics and segmentation. J Geophys Res 115(B8):B00A25. https://doi.org/10.1029/2008JB006048
Obara K (2020) Characteristic activities of slow earthquakes in Japan. Proc Jpn Acad Ser B 96(7):297–315. https://doi.org/10.2183/pjab.96.022
Obara K, Ito Y (2005) Very low frequency earthquakes excited by the 2004 off the Kii peninsula earthquakes: a dynamic deformation process in the large accretionary prism. Earth Planet Space 57(4):321–326. https://doi.org/10.1186/BF03352570
Obara K, Kato A (2016) Connecting slow earthquakes to huge earthquakes. Science 353(6296):253–257. https://doi.org/10.1126/science.aaf1512
Obara K, Hirose H, Yamamizu F, Kasahara K (2004) Episodic slow slip events accompanied by non-volcanic tremors in southwest Japan subduction zone. Geophys Res Lett. https://doi.org/10.1029/2004GL020848
Ogata Y (1988) Statistical models for earthquake occurrences and residual analysis for point processes. J Am Stat Assoc 83(401):9–27
Ogata Y (2011) Significant improvements of the space-time ETAS model for forecasting of accurate baseline seismicity. Earth Planet Space 63(3):217–229. https://doi.org/10.5047/eps.2010.09.001
Ohnaka M (1992) Earthquake source nucleation: a physical model for short-term precursors. Tectonophysics 211(1–4):149–178. https://doi.org/10.1016/0040-1951(92)90057-D
Ohta Y, Freymueller JT, Hreinsdóttir S, Suito H (2006) A large slow slip event and the depth of the seismogenic zone in the south central Alaska subduction zone. Earth Planet Sci Lett 247(1–2):108–116. https://doi.org/10.1016/j.epsl.2006.05.013
Ohta Y, Hino R, Inazu D, Ohzono M, Ito Y, Mishina M, Iinuma T, Nakajima J, Osada Y, Suzuki K, Fujimoto H, Tachibana K, Demachi T, Miura S (2012) Geodetic constraints on afterslip characteristics following the March 9, 2011, Sanriku-oki earthquake, Japan. Geophys Res Lett 39(16):L16304. https://doi.org/10.1029/2012GL052430
Ohta K, Ito Y, Hino R, Ohyanagi S, Matsuzawa T, Shiobara H, Shinohara M (2019) Tremor and inferred slow slip associated with afterslip of the 2011 Tohoku earthquake. Geophys Res Lett 46(9):4591–4598. https://doi.org/10.1029/2019GL082468
Ohtani M, Hirahara K, Hori T, Hyodo M (2014) Observed change in plate coupling close to the rupture initiation area before the occurrence of the 2011 Tohoku earthquake: implications from an earthquake cycle model. Geophys Res Lett 41(6):1899–1906. https://doi.org/10.1002/2013GL058751
Okada T, Matsuzawa T, Hasegawa A (2003) Comparison of source areas of M4.8 ± 0.1 repeating earthquakes off Kamaishi, NE Japan: are asperities persistent features? Earth Planet Sci Lett 213(3–4):361–374. https://doi.org/10.1016/S0012-821X(03)00299-1
Okada Y, Nishimura T, Tabei T, Matsushima T, Hirose H (2022) Development of a detection method for short-term slow slip events using GNSS data and its application to the Nankai subduction zone. Earth Planet Space 74:18. https://doi.org/10.1186/s40623-022-01576-8
Okuda T, Ide S (2018) Hierarchical rupture growth evidenced by the initial seismic waveforms. Nat Commun 9(1):3714. https://doi.org/10.1038/s41467-018-06168-3
Okutani T, Ide S (2011) Statistic analysis of swarm activities around the Boso Peninsula, Japan: slow slip events beneath Tokyo Bay? Earth Planet Space 63(5):419–426. https://doi.org/10.5047/eps.2011.02.010
Ozawa S, Murakami M, Kaidzu M, Tada T, Sagiy T, Hatanaka Y, Yarai H, Nishimura T (2002) Detection and monitoring of ongoing aseismic slip in the Tokai region, central Japan. Science 298(5595):1009–1012. https://doi.org/10.1126/science.1076780
Ozawa S, Miyazaki S, Hatanaka Y, Imakiire T, Kaidzu M, Murakami M (2003) Characteristic silent earthquakes in the eastern part of the Boso peninsula, central Japan. Geophys Res Lett 30(6):1238. https://doi.org/10.1029/2002GL016665
Ozawa S, Nishimura T, Munekane H, Suito H, Kobayashi T, Tobita M, Imakiire T (2012) Preceding, coseismic, and postseismic slips of the 2011 Tohoku earthquake, Japan. J Geophys Res 117(B7):B07404. https://doi.org/10.1029/2011JB009120
Park JO, Moore GF, Tsuru T, Kodaira S, Kaneda Y (2004) A subducted oceanic ridge influencing the Nankai megathrust earthquake rupture. Earth Planet Sci Lett 217(1–2):77–84. https://doi.org/10.1016/S0012-821X(03)00553-3
Peacock SM (2009) Thermal and metamorphic environment of subduction zone episodic tremor and slip. J Geophys Res 114(B8):B00A07. https://doi.org/10.1029/2008JB005978
Peacock SM, Wang K (1999) Seismic consequences of warm versus cool subduction metamorphism: examples from southwest and northeast Japan. Science 286(5441):937–939. https://doi.org/10.1126/science.286.5441.937
Peng Z, Gomberg J (2010) An integrated perspective of the continuum between earthquakes and slow-slip phenomena. Nat Geosci 3(9):599–607. https://doi.org/10.1038/ngeo940
Peterson J (1993) Observations and modelling of background seismic noise. Open-file report 93–322, U. S. Geological Survey, Albuquerque, New Mexico
Petruccelli A, Schorlemmer D, Tormann T, Rinaldi AP, Wiemer S, Gasperini P, Vannucci G (2019) The influence of faulting style on the size-distribution of global earthquakes. Earth Planet Sci Lett 527:115791. https://doi.org/10.1016/j.epsl.2019.115791

Radiguet M, Perfettini H, Cotte N, Gualandi A, Valette B, Kostoglodov V, Lhomme T, Walpersdorf A, Cabral Cano E, Campillo M (2016) Triggering of the 2014 M_w 7.3 Papanoa earthquake by a slow slip event in GuerreroroMexico. Nat Geosci 9(11):829–833. https://doi.org/10.1038/ngeo2817

Research Center for Seismology, Volcanology, and Disaster Mitigation, Nagoya University (2008) Ibaraki-oki earthquake (M6.4, M7.2) on May 8 (in Japanese), NGY seismological note No.7. https://www.seis.nagoya-u.ac.jp/sanchu/Seismo_Note/2008/NGY7.html. Accessed 19 Jul 2022

Reverso T, Marsan D, Helmstetter A (2015) Detection and characterization of transient forcing episodes affecting earthquake activity in the Aleutian Arc system. Earth Planet Sci Lett 412:25–34. https://doi.org/10.1016/j.epsl.2014.12.012

Rogers G, Dragert H (2003) Episodic tremor and slip on the Cascadia subduction zone: the chatter of silent slip. Science 300(5627):1942–1943. https://doi.org/10.1126/science.1084783

Rolandone F, Nocquet JM, Mothes PA, Jarrin P, Vallée M, Cubas N, Hernandez S, Plain M, Vaca S, Font Y (2018) Areas prone to slow slip events impede earthquake rupture propagation and promote afterslip. Sci Adv 4(1):eaao6596. https://doi.org/10.1126/sciadv.aao659

Romanet P, Ide S (2019) Ambient tectonic tremors in manawatu, Cape Turnagain, marlborough, and Puysegur, New Zealand. Earth Planet Space 71:59. https://doi.org/10.1186/s40623-019-1039-1

Ross ZE, Cochran ES, Trugman DT, Smith JD (2020) 3D fault architecture controls the dynamism of earthquake swarms. Science 368(6497):1357–1361. https://doi.org/10.1126/science.abb0779

Rousset B, Campillo M, Lasserre C, Frank WB, Cotte N, Walpersdorf A, Socquet A, Kostoglodov V (2017) A geodetic matched filter search for slow slip with application to the Mexico subduction zone. J Geophys Res 122(12):10498–10514. https://doi.org/10.1002/2017JB014448

Rousset B, Fu Y, Bartlow N, Bürgmann R (2019) Weeks-long and years-long slow slip and tectonic tremor episodes on the south central Alaska Megathrust. J Geophys Res 124(12):13392–13403. https://doi.org/10.1029/2019JB018724

Rubinstein JL, Vidale JE, Gomberg J, Bodin P, Creager KC, Malone SD (2007) Non-volcanic tremor driven by large transient shear stresses. Nature 448(7153):579–582. https://doi.org/10.1038/nature06017

Rubinstein JL, La Rocca M, Vidale JE, Creager KC, Wech AG (2008) Tidal modulation of nonvolcanic tremor. Science 319(5860):186–189. https://doi.org/10.1126/science.1150558

Ruff LJ (1989) Do trench sediments affect great earthquake occurrence in subduction zones? Pure Appl Geophys 129:263–282. https://doi.org/10.1007/978-3-0348-9140-0_9

Ruiz S, Metois M, Fuenzalida A, Ruiz J, Leyton F, Grandin R, Vigny C, Madariaga R, Campos J (2014) Intense foreshocks and a slow slip event preceded the 2014 Iquique M_w 8.1 earthquake. Science 345(6201):1165–1169. https://doi.org/10.1126/science.1256074

Saffer DM, Marone C (2003) Comparison of smectite-and illite-rich gouge frictional properties: application to the updip limit of the seismogenic zone along subduction megathrusts. Earth Planet Sci Lett 215(1–2):219–235. https://doi.org/10.1016/S0012-821X(03)00424-2

Saffer DM, Tobin HJ (2011) Hydrogeology and mechanics of subduction zone forearcs: fluid flow and pore pressure. Annu Rev Earth Planet Sci 39:157–186. https://doi.org/10.1146/annurev-earth-040610-133408

Saffer DM, Wallace LM (2015) The frictional, hydrologic, metamorphic and thermal habitat of shallow slow earthquakes. Nat Geosci 8(8):594–600. https://doi.org/10.1038/ngeo2490

Sagiya T (1997) Anomalous transients in crustal movements of the Boso peninsula, Japan—is it a slow earthquake?-. Eos Trans AGU 78(S214):S31C – S37

Sagiya T (2004) Interplate coupling in the Kanto district, central Japan, and the Boso peninsula silent earthquake in May 1996. Pure Appl Geophys 161:2327–2342. https://doi.org/10.1007/s00024-004-2566-6

Sakaue H, Nishimura T, Fukuda JI, Kato T (2019) Spatiotemporal evolution of long-and short-term slow slip events in the Tokai region, central Japan, estimated from a very dense GNSS network during 2013–2016. J Geophys Res 124(12):13207–13226. https://doi.org/10.1029/2019JB018650

Satake K, Nanayama F, Yamaki S (2008) Fault models of unusual tsunami in the 17th century along the Kuril trench. Earth Planet Space 60(9):925–935. https://doi.org/10.1186/BF03352848

Satake K, Fujii Y, Harada T, Namegaya Y (2013) Time and space distribution of coseismic slip of the 2011 Tohoku earthquake as inferred from tsunami waveform data. Bull Seismol Soc Am 103(2B):1473–1492. https://doi.org/10.1785/0120120122

Sawai M, Niemeijer AR, Hirose T, Spiers CJ (2017) Frictional properties of JFAST core samples and implications for slow earthquakes at the Tohoku subduction zone. Geophys Res Lett 44(17):8822–8831. https://doi.org/10.1002/2017GL073460

Scholz CH (1968) The frequency-magnitude relation of microfracturing in rock and its relation to earthquakes. Bull Seismol Soc Am 58(1):399–415. https://doi.org/10.1785/BSSA0580010399

Scholz CH (1998) Earthquakes and friction laws. Nature 391(6662):37–42. https://doi.org/10.1038/34097

Scholz CH (2015) On the stress dependence of the earthquake *b* value. Geophys Res Lett 42(5):1399–1402. https://doi.org/10.1002/2014GL062863

Scholz CH, Small C (1997) The effect of seamount subduction on seismic coupling. Geology 25(6):487–490. https://doi.org/10.1130/0091-7613(1997)025%3c0487:TEOSSO%3e2.3.CO;2

Schorlemmer D, Wiemer S, Wyss M (2005) Variations in earthquake-size distribution across different stress regimes. Nature 437(7058):539–542. https://doi.org/10.1038/nature04094

Segall P, Rubin AM, Bradley AM, Rice JR (2010) Dilatant strengthening as a mechanism for slow slip events. J Geophys Res 115(B12):B12305. https://doi.org/10.1029/2010JB007449

Shaddox HR, Schwartz SY (2019) Subducted seamount diverts shallow slow slip to the forearc of the northern Hikurangi subduction zone, New Zealand. Geology 47(5):415–418. https://doi.org/10.1130/G45810.1

Shao G, Li X, Ji C, Maeda T (2011) Focal mechanism and slip history of the 2011 M_w 9.1 off the Pacific coast of Tohoku Earthquake, constrained with teleseismic body and surface waves. Earth Planet Space 63(7):559–564. https://doi.org/10.5047/eps.2011.06.028

Shelly DR, Beroza GC, Ide S, Nakamula S (2006) Low-frequency earthquakes in Shikoku, Japan, and their relationship to episodic tremor and slip. Nature 442(7099):188–191. https://doi.org/10.1038/nature04931

Shelly DR, Beroza GC, Ide S (2007) Non-volcanic tremor and low-frequency earthquake swarms. Nature 446(7133):305–307. https://doi.org/10.1038/nature05666

Shibazaki B, Iio Y (2003) On the physical mechanism of silent slip events along the deeper part of the seismogenic zone. Geophys Res Lett 30(9):1489. https://doi.org/10.1029/2003GL017047

Shibazaki B, Shimamoto T (2007) Modelling of short-interval silent slip events in deeper subduction interfaces considering the frictional properties at the unstable—stable transition regime. Geophys J Int 171(1):191–205. https://doi.org/10.1111/j.1365-246X.2007.03434.x

Shibazaki B, Matsuzawa T, Tsutsumi A, Ujiie K, Hasegawa A, Ito Y (2011) 3D modeling of the cycle of a great Tohoku-oki earthquake, considering frictional behavior at low to high slip velocities. Geophys Res Lett 38(21):L21305. https://doi.org/10.1029/2011GL049308

Shibazaki B, Noda H, Ikari MJ (2019) Quasi-dynamic 3D modeling of the generation and afterslip of a Tohoku-oki Earthquake considering thermal pressurization and frictional properties of the shallow plate boundary. Pure Appl Geophys 176(9):3951–3973. https://doi.org/10.1007/s00024-018-02089-w

Sibson RH (1973) Interactions between temperature and pore-fluid pressure during earthquake faulting and a mechanism for partial or total stress relief. Nat Phys Sci 243(126):66–68. https://doi.org/10.1038/physci243066a0

Simons M, Minson SE, Sladen A, Ortega F, Jiang J, Owen SE, Meng L, Ampuero J, Wei S, Chu R, Helmberger DV, Kanamori H, Hetland E, Moore AW, Webb FH (2011) The 2011 magnitude 9.0 Tohoku-Oki earthquake: mosaicking the megathrust from seconds to centuries. Science 332(6036):1421–1425

Skarbek RM, Rempel AW, Schmidt DA (2012) Geologic heterogeneity can produce aseismic slip transients. Geophys Res Lett 39(21):L21306. https://doi.org/10.1029/2012GL053762

Smith WH, Sandwell DT (1997) Global sea floor topography from satellite altimetry and ship depth soundings. Science 277(5334):1956–1962. https://doi.org/10.1126/science.277.5334.1956

Socquet A, Valdes JP, Jara J, Cotton F, Walpersdorf A, Cotte N, Specht S, Ortega-Culaciati F, Carrizo D, Norabuena E (2017) An 8 month slow slip event

triggers progressive nucleation of the 2014 Chile megathrust. Geophys Res Lett 44(9):4046–4053. https://doi.org/10.1002/2017GL073023
Spada M, Tormann T, Wiemer S, Enescu B (2013) Generic dependence of the frequency-size distribution of earthquakes on depth and its relation to the strength profile of the crust. Geophys Res Lett 40(4):709–714. https://doi.org/10.1029/2012GL054198
Sun T, Wang K (2015) Viscoelastic relaxation following subduction earthquakes and its effects on afterslip determination. J Geophys Res 120(2):1329–1344. https://doi.org/10.1002/2014JB011707
Sun T, Saffer D, Ellis S (2020) Mechanical and hydrological effects of seamount subduction on megathrust stress and slip. Nat Geosci 13(3):249–255. https://doi.org/10.1038/s41561-020-0542-0
Suwa Y, Miura S, Hasegawa A, Sato T, Tachibana K (2006) Interplate coupling beneath NE Japan inferred from three-dimensional displacement field. J Geophys Res 111(B4):B04402. https://doi.org/10.1029/2004JB003203
Suzuki T, Yamashita T (2009) Dynamic modeling of slow earthquakes based on thermoporoelastic effects and inelastic generation of pores. J Geophys Res. https://doi.org/10.1029/2008JB006042
Takagi R, Obara K, Maeda T (2016) Slow slip event within a gap between tremor and locked zones in the Nankai subduction zone. Geophys Res Lett 43(3):1066–1074. https://doi.org/10.1002/2015GL066987
Takagi R, Uchida N, Obara K (2019) Along-strike variation and migration of long-term slow slip events in the western Nankai subduction zone, Japan. J Geophys Res 124(4):3853–3880. https://doi.org/10.1029/2018JB016738
Takahashi H, Tateiwa K, Yano K, Kano M (2021) A convolutional neural network-based classification of local earthquakes and tectonic tremors in Sanriku-oki, Japan, using S-net data. Earth Planet Space 73:186. https://doi.org/10.1186/s40623-021-01524-y
Takemura S, Obara K, Shiomi K, Baba S (2022) Spatiotemporal variations of shallow very low frequency earthquake activity southeast off the Kii Peninsula, along the Nankai Trough, Japan. J Geophys Res 127(3):e2021JB023073. https://doi.org/10.1029/2021JB023073
Tanaka S (2012) Tidal triggering of earthquakes prior to the 2011 Tohoku-Oki earthquake (M_w 9.1). Geophys Res Lett 39(7):L00G26. https://doi.org/10.1029/2012GL051179
Tanaka S, Matsuzawa T, Asano Y (2019) Shallow low-frequency tremor in the northern Japan Trench subduction zone. Geophys Res Lett 46(10):5217–5224. https://doi.org/10.1029/2019GL082817
Tanioka Y, Sataka K (1996) Fault parameters of the 1896 Sanriku tsunami earthquake estimated from tsunami numerical modeling. Geophys Res Lett 23(13):1549–1552. https://doi.org/10.1029/96GL01479
Tanioka Y, Seno T (2001) Sediment effect on tsunami generation of the 1896 Sanriku tsunami earthquake. Geophys Res Lett 28(17):3389–3392. https://doi.org/10.1029/2001GL013149
Tanioka Y, Ruff L, Satake K (1997) What controls the lateral variation of large earthquake occurrence along the Japan Trench? Isl Arc 6(3):261–266. https://doi.org/10.1111/j.1440-1738.1997.tb00176.x
Toda S, Stein RS, Sagiya T (2002) Evidence from the AD 2000 Izu islands earthquake swarm that stressing rate governs seismicity. Nature 419(6902):58–61. https://doi.org/10.1038/nature00997
Todd EK, Schwartz SY (2016) Tectonic tremor along the northern Hikurangi Margin, New Zealand, between 2010 and 2015. J Geophys Res 121(12):8706–8719. https://doi.org/10.1002/2016JB013480
Todd EK, Schwartz SY, Mochizuki K, Wallace LM, Sheehan AF, Webb SC, Williams CA, Nakai J, Yarce J, Fry B, Henrys S, Ito Y (2018) Earthquakes and tremor linked to seamount subduction during shallow slow slip at the Hikurangi margin, New Zealand. J Geophys Res 123(8):6769–6783. https://doi.org/10.1029/2018JB016136
Tomita F, Kido M, Ohta Y, Iinuma T, Hino R (2017) Along-trench variation in seafloor displacements after the 2011 Tohoku earthquake. Sci Adv 3(7):e1700113. https://doi.org/10.1126/sciadv.17001
Tomita F, Iinuma T, Ohta Y, Hino R, Kido M, Uchida N (2020) Improvement on spatial resolution of a coseismic slip distribution using postseismic geodetic data through a viscoelastic inversion. Earth Planet Space 72:84. https://doi.org/10.1186/s40623-020-01207-0
Tormann T, Enescu B, Woessner J, Wiemer S (2015) Randomness of megathrust earthquakes implied by rapid stress recovery after the Japan earthquake. Nat Geosci 8(2):152–158. https://doi.org/10.1038/ngeo2343
Tse ST, Rice JR (1986) Crustal earthquake instability in relation to the depth variation of frictional slip properties. J Geophys Res 91(B9):9452–9472. https://doi.org/10.1029/JB091iB09p09452
Tsuru T, Park JO, Miura S, Kodaira S, Kido Y, Hayashi T (2002) Along-arc structural variation of the plate boundary at the Japan Trench margin: Implication of interplate coupling. J Geophys Res 107(B12):2357. https://doi.org/10.1029/2001JB001664
Uchida N (2019) Detection of repeating earthquakes and their application in characterizing slow fault slip. Prog Earth Planet Sci 6:40. https://doi.org/10.1186/s40645-019-0284-z
Uchida N, Bürgmann R (2019) Repeating earthquakes. Annu Rev Earth Planet Sci 47(1):305–332. https://doi.org/10.1146/annurev-earth-053018-060119
Uchida N, Bürgmann R (2021) A Decade of Lessons Learned from the 2011 Tohoku-Oki Earthquake. Rev Geophys 59(2):e2020RG000713. https://doi.org/10.1029/2020RG000713
Uchida N, Matsuzawa T (2011) Coupling coefficient, hierarchical structure, and earthquake cycle for the source area of the 2011 off the Pacific coast of Tohoku earthquake inferred from small repeating earthquake data. Earth Planet Space 63(7):675–679. https://doi.org/10.5047/eps.2011.07.006
Uchida N, Matsuzawa T (2013) Pre- and postseismic slow slip surrounding the 2011 Tohoku-oki earthquake rupture. Earth Planet Sci Lett 374:81–91. https://doi.org/10.1016/j.epsl.2013.05.021
Uchida N, Hasegawa A, Matsuzawa T, Igarashi T (2004) Pre- and post-seismic slow slip on the plate boundary off Sanriku, NE Japan associated with three interplate earthquakes as estimated from small repeating earthquake data. Tectonophysics 385(1–4):1–15. https://doi.org/10.1016/j.tecto.2004.04.015
Uchida N, Matsuzawa T, Ellsworth WL, Imanishi K, Okada T, Hasegawa A (2007) Source parameters of a M4.8 and its accompanying repeating earthquakes off Kamaishi, NE Japan: implications for the hierarchical structure of asperities and earthquake cycle. Geophys Res Lett 34(20):L20313. https://doi.org/10.1029/2007GL031263
Uchida N, Nakajima J, Hasegawa A, Matsuzawa T (2009a) What controls interplate coupling?: evidence for abrupt change in coupling across a border between two overlying plates in the NE Japan subduction zone. Earth Planet Sci Lett 283(1–4):111–121. https://doi.org/10.1016/j.epsl.2009.04.003
Uchida N, Yui S, Miura S, Matsuzawa T, Hasegawa A, Motoya Y, Kasahara M (2009b) Quasi-static slip on the plate boundary associated with the 2003 M8.0 Tokachi-oki and 2004 M7.1 off-Kushiro earthquakes, Japan. Gondwana Res 16(3–4):527–533. https://doi.org/10.1016/j.gr.2009.04.002
Uchida N, Shimamura K, Matsuzawa T, Okada T (2015) Postseismic response of repeating earthquakes around the 2011 Tohoku-oki earthquake: moment increases due to the fast loading rate. J Geophys Res 120(1):259–274
Uchida N, Iinuma T, Nadeau RM, Bürgmann R, Hino R (2016) Periodic slow slip triggers megathrust zone earthquakes in northeastern Japan. Science 351(6272):488–492. https://doi.org/10.1126/science.aad3108
Uchida N, Takagi R, Asano Y, Obara K (2020) Migration of shallow and deep slow earthquakes toward the locked segment of the Nankai megathrust. Earth Planet Sci Lett 531:115986. https://doi.org/10.1016/j.epsl.2019.115986
Ueda T (2021) Seismicity analysis based on statistical modeling: connection with stress change. Dissertation, The University of Tokyo, Tokyo
Ujiie K, Tanaka H, Saito T, Tsutsumi A, Mori JJ, Kameda J, Brodsky EE, Chester FM, Eguchi N, Toczko S, Expedition 343 and 343T Scientists (2013) Low coseismic shear stress on the Tohoku-Oki megathrust determined from laboratory experiments. Science 342(6163):1211–1214. https://doi.org/10.1126/science.1243485
Ujiie K, Saishu H, Fagereng Å, Nishiyama N, Otsubo M, Masuyama H, Kagi H (2018) An explanation of episodic tremor and slow slip constrained by crack-seal veins and viscous shear in subduction mélange. Geophys Res Lett 45(11):5371–5379. https://doi.org/10.1029/2018GL078374
Utsu T (1957) Magnitudes of earthquakes and occurrence of their aftershocks (in Japanese with English figure captions). Zisin (j Seismol Soc Jpn) 10(2):35–45

Utsu T, Ogata Y, Matsu'ura R (1995) The centenary of the Omori formula for a decay law of aftershock activity. J Phys Earth 43(1):1–33. https://doi.org/10.4294/jpe1952.43.1

Vallée M, Nocquet JM, Battaglia J, Font Y, Segovia M, Régnier M, Mothes P, Jarrin P, Cisneros D, Vaca S, Yepes H, Martin X, Béthoux N, Chlieh M (2013) Intense interface seismicity triggered by a shallow slow slip event in the Central Ecuador subduction zone. J Geophys Res 118(6):2965–2981. https://doi.org/10.1002/jgrb.50216

Villegas-Lanza JC, Nocquet JM, Rolandone F, Vallée M, Tavera H, Bondoux F, Tran T, Martin X, Chlieh M (2016) A mixed seismic–aseismic stress release episode in the Andean subduction zone. Nat Geosci 9(2):150–154. https://doi.org/10.1038/ngeo2620

Wallace LM, Beavan J, Miura S, McCaffrey R (2009) Using global positioning system data to assess tectonic hazards. In: Connor C, Connor L, Chapman N (eds) Volcanism, tectonism and siting of nuclear facilities. Cambridge University Press, Cambridge

Wallace LM, Beavan J, Bannister S, Williams C (2012) Simultaneous long-term and short-term slow slip events at the Hikurangi subduction margin, New Zealand: implications for processes that control slow slip event occurrence, duration, and migration. J Geophys Res 117(B11):B11402. https://doi.org/10.1029/2012JB009489

Walter JI, Schwartz SY, Protti M, Gonzalez V (2013) The synchronous occurrence of shallow tremor and very low frequency earthquakes offshore of the Nicoya Peninsula, Costa Rica. Geophys Res Lett 40(8):1517–1522. https://doi.org/10.1002/grl.50213

Wang K, Bilek SL (2011) Do subducting seamounts generate or stop large earthquakes? Geology 39(9):819–822. https://doi.org/10.1130/G31856.1

Wang K, Bilek SL (2014) Invited review paper: fault creep caused by subduction of rough seafloor relief. Tectonophysics 610:1–24. https://doi.org/10.1016/j.tecto.2013.11.024

Watanabe SI, Ishikawa T, Nakamura Y, Yokota Y (2021) Co- and postseismic slip behaviors extracted from decadal seafloor geodesy after the 2011 Tohoku-oki earthquake. Earth Planet Space 73:162. https://doi.org/10.1186/s40623-021-01487-0

Wech AG, Creager KC (2011) A continuum of stress, strength and slip in the Cascadia subduction zone. Nat Geosci 4(9):624–628. https://doi.org/10.1038/ngeo1215

Wech AG, Creager KC, Houston H, Vidale JE (2010) An earthquake-like magnitude-frequency distribution of slow slip in northern Cascadia. Geophys Res Lett 37(22):L22310. https://doi.org/10.1029/2010GL044881

Wessel P, Luis JF, Uieda L, Scharroo R, Wobbe F, Smith WHF, Tian D (2019) The generic mapping tools version 6. Geochem Geophys Geosyst 20:5556–5564. https://doi.org/10.1029/2019GC008515

Wu B, Oglesby DD, Ghosh A, Li B (2019) A dynamic rupture source model for very low-frequency earthquake signal without detectable nonvolcanic tremors. Geophys Res Lett 46(21):11934–11943. https://doi.org/10.1029/2019GL084135

Yabe S, Ide S (2014) Spatial distribution of seismic energy rate of tectonic tremors in subduction zones. J Geophys Res 119(11):8171–8185. https://doi.org/10.1002/2014JB011383

Yabe S, Tonegawa T, Nakano M (2019) Scaled energy estimation for shallow slow earthquakes. J Geophys Res 124(2):1507–1519. https://doi.org/10.1029/2018JB016815

Yabe S, Baba S, Tonegawa T, Nakano M, Takemura S (2021) Seismic energy radiation and along-strike heterogeneities of shallow tectonic tremors at the Nankai Trough and Japan Trench. Tectonophysics 800:228714. https://doi.org/10.1016/j.tecto.2020.228714

Yagi Y (2012) Seismic source process of the 2011 Tohoku-oki earthquake (in Japanese with English abstract and figure captions). Zisin (j Seismol Soc Jpn) 64(2):143–153. https://doi.org/10.4294/zisin.64.143

Yagi Y, Fukahata Y (2011) Rupture process of the 2011 Tohoku-Oki earthquake and absolute elastic strain release. Geophys Res Lett 38(19):L19307. https://doi.org/10.1029/2011GL048701

Yagi Y, Kikuchi M, Yoshida S, Yamanaka Y (1998) Source process of the Hyuga-nada earthquake of April 1, 1968 (M_{jma} 7.5), and its relatonship to the subsequent seismicity (in Japanese with English abstract and figure captions). Zishin (j Seismol Soc Jpn) 51:139–148

Yagi Y, Kikuchi M, Yoshida S, Sagiy T (1999) Comparison of the coseismic rupture with the aftershock distribution in the Hyuga-nada earthquakes of 1996. Geophys Res Lett 26(20):3161–3164. https://doi.org/10.1029/1999GL005340

Yagi Y, Kikuchi M, Nishimura T (2003) Co-seismic slip, post-seismic slip, and largest aftershock associated with the 1994 Sanriku-haruka-oki, Japan, earthquake. Geophys Res Lett 30(22):2177. https://doi.org/10.1029/2003GL018189

Yamamoto Y, Obana K, Takahashi T, Nakanishi A, Kodaira S, Kaneda Y (2013) Imaging of the subducted Kyushu-Palau Ridge in the Hyuga-nada region, western Nankai Trough subduction zone. Tectonophysics 589:90–102. https://doi.org/10.1016/j.tecto.2012.12.028

Yamamoto Y, Yada S, Ariyoshi K, Hori T, Takahashi N (2022) Seismicity distribution in the Tonankai and Nankai seismogenic zones and its spatiotemporal relationship with interplate coupling and slow earthquakes. Prog Earth Planet Sci 9:32. https://doi.org/10.1186/s40645-022-00493-4

Yamanaka Y, Kikuchi M (2003) Source process of the recurrent Tokachi-oki earthquake on September 26, 2003, inferred from teleseismic body waves. Earth Planet Space 55(12):e21–e24. https://doi.org/10.1186/BF03352479

Yamanaka Y, Kikuchi M (2004) Asperity map along the subduction zone in northeastern Japan inferred from regional seismic data. J Geophys Res 109(B7):B07307. https://doi.org/10.1029/2003JB002683

Yamashita Y, Yakiwara H, Asano Y, Shimizu H, Uchida K, Hirano S, Umakoshi K, Miyamachi H, Nakamoto M, Fukui M, Kamizono M, Kanehara H, Yamada T, Shinohara M, Obara K (2015) Migrating tremor off southern Kyushu as evidence for slow slip of a shallow subduction interface. Science 348(6235):676–679. https://doi.org/10.1126/science.aaa4242

Yamashita Y, Shinohara M, Yamada T (2021) Shallow tectonic tremor activities in Hyuga-nada, Nankai subduction zone, based on long-term broadband ocean bottom seismic observations. Earth Planet Space 73:196. https://doi.org/10.1186/s40623-021-01533-x

Yamaya L, Mochizuki K, Akuhara T, Takemura S, Shinohara M, Yamada T (2022) CMT inversion for small-to-moderate earthquakes applying to dense short-period OBS array at off Ibaraki region. Earth Planet Space 74:164. https://doi.org/10.1186/s40623-022-01721-3

Yanagisawa H, Goto K, Sugawara D, Kanamaru K, Iwamoto N, Takamori Y (2016) Tsunami earthquake can occur elsewhere along the Japan Trench—historical and geological evidence for the 1677 earthquake and tsunami. J Geophys Res 121(5):3504–3516. https://doi.org/10.1002/2015JB012617

Ye L, Lay T, Kanamori H (2012) The Sanriku-Oki low-seismicity region on the northern margin of the great 2011 Tohoku-Oki earthquake rupture. J Geophys Res 117(B2):B02305. https://doi.org/10.1029/2011JB008847

Yokota Y, Koketsu K (2015) A very long-term transient event preceding the 2011 Tohoku earthquake. Nat Commun 6:5934. https://doi.org/10.1038/ncomms6934

Yoshioka S, Mikumo T, Kostoglodov V, Larson KM, Lowry AR, Singh SK (2004) Interplate coupling and a recent aseismic slow slip event in the Guerrero seismic gap of the Mexican subduction zone, as deduced from GPS data inversion using a Bayesian information criterion. Phys Earth Planet Inter 146(3–4):513–530. https://doi.org/10.1016/j.pepi.2004.05.006

Zhao D, Huang Z, Umino N, Hasegawa A, Kanamori H (2011) Structural heterogeneity in the megathrust zone and mechanism of the 2011 Tohoku-oki earthquake (M_w 9.0). Geophys Res Lett 38(17):L17308. https://doi.org/10.1029/2011GL048408

Zhuang J, Ogata Y, Vere-Jones D (2002) Stochastic declustering of space-time earthquake occurrences. J Am Stat Assoc 97(458):369–380. https://doi.org/10.1198/016214502760046925

Publisher's Note